Construction Practices for Placing 48-Inch Precast, Prestressed Concrete Cylinder Piling in Deep Water

WALTER W. GRIMES, South Dakota Department of Highways

The proposal to construct a structure across more than a mile of open water up to 80 ft deep was the beginning of an extensive engineering economic analysis to determine the type and length of structure to fit the site.

A composite I-beam structure 5655.5 ft long supported on a driven pile bent was chosen. The pile bents consisted of either 8 or 12 piles, with each pile 48 in. in diameter. Each of the 276 piles would be a prestressed, precast concrete cylinder piles. Soil borings indicated the length would vary from 25 to 176 ft. To withstand handling and driving, the wall thickness would be 5 in. with spiral reinforcing, stressing tendons and 8 No. 4 bars. Each of the sixteen $^{7}/_{16}$-in. diameter prestressing cables was tensioned to stress the 7000-psi concrete to 1100 psi. Driving specifications required the piling to be seated with 50 blows per inch by a 60,000 ft-lb hammer in Niobrara chalk. The contractor elected to cast the piling at the site.

The first method of pile placement used a three-finger jet to place the piling near chalk and a hammer to drive the pile into chalk. This method proved ineffective, and subsequently a single jet was attached to the pile and the pile jetted and driven simultaneously with the final seating for bearing after removal of the jets.

After each bent was driven the piles were backfilled with sand, Class C and Class A concrete. Some of the piles were driven a total of 7000 blows.

After the bents were completed, cracks were observed in the piling in January 1964. Inspection revealed 52 piles that would require repair. The damaged piles were opened up, cleaned and backfilled with dry-pack concrete, and a steel reinforcing shell was epoxied and bolted into place.

Successful use of these piles require a knowledge of the length to cast each pile and an accurate bearing estimation. During construction, proper supervision must be exercised to insure a sound pile.

•WHEN the U.S. Corps of Engineers planned the series of dams on the Missouri River in South Dakota, direct replacement at or near the original site was provided for all the existing bridges over the river except the Wheeler or Rosebud Crossing. At this site, the Corps provided a rerouting of U.S. 18 over the dam structure and considered it had fulfilled its obligation to the state. The state did not officially accept the crossing on the Fort Randall Dam as an adequate replacement for the Wheeler Bridge. In 1960, an appropriation was secured through the Corps of Engineers for the purpose of

Paper sponsored by Committee on Construction Practices—Structures and presented at the 48th Annual Meeting.

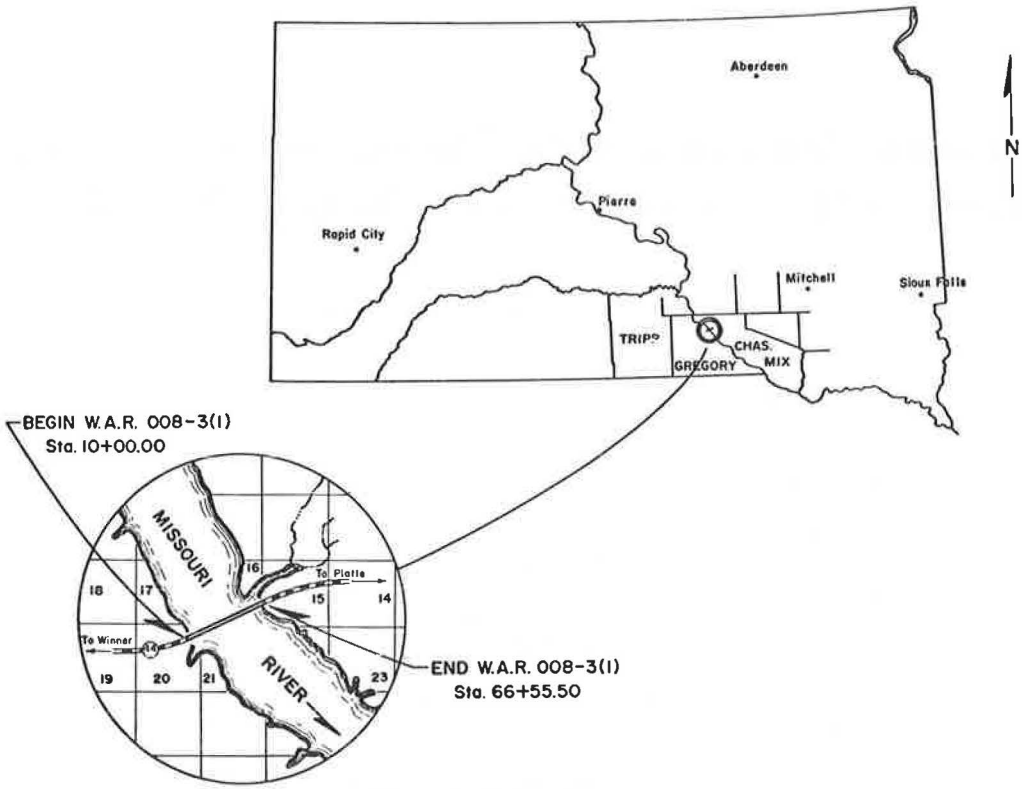

Figure 1. Project location.

constructing a bridge over Fort Randall Reservoir on a general line west of Platte. The South Dakota Highway Commission proposed that Route 44 cross Lake Francis Case west of Platte near the mouth of the Snake Creek (Figs. 1 and 2). The reservoir width at the proposed site is 5400 ft, with the water depth varying between 40 ft at the low water pool in winter and a maximum of 82 ft in spring and summer months. This water depth required a choice, based on an engineering economic analysis, between five types of construction: (a) conventional deep water construction utilizing man-excavated cofferdams; (b) use of tremie seal watertight removable forms; (c) use of precast concrete section piles filled with structural tremie-reinforced concrete without dewatering the form during placement; (d) use of steel shell forms left in place as in item c; and (e) use of prestressed pile piers driven to an anchor in the chalk.

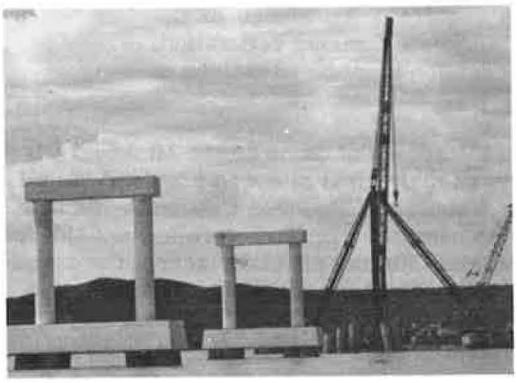

Figure 2. Stiffleg derrick working on Bent 19 with completed Bents 20 and 21 in foreground.

The state, after an intensive investigation directed toward securing the most economical structure, determined that a bridge could be build within the limits of the authorized amount. The structure would be a continuous deck plate girder bridge, founded on precast, prestressed concrete piles driven to refusal in the Niobrara chalk strata that underlie the reservoir. The structure length was 5,655.5 ft.

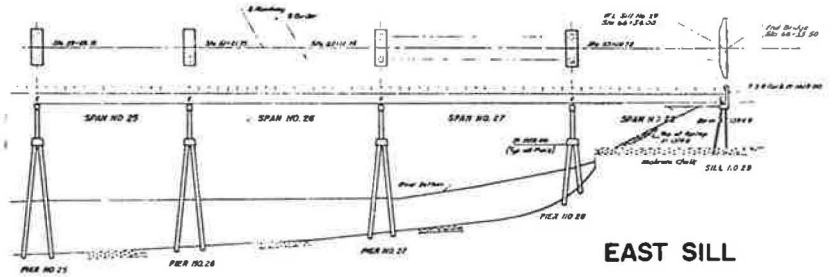

EAST SILL

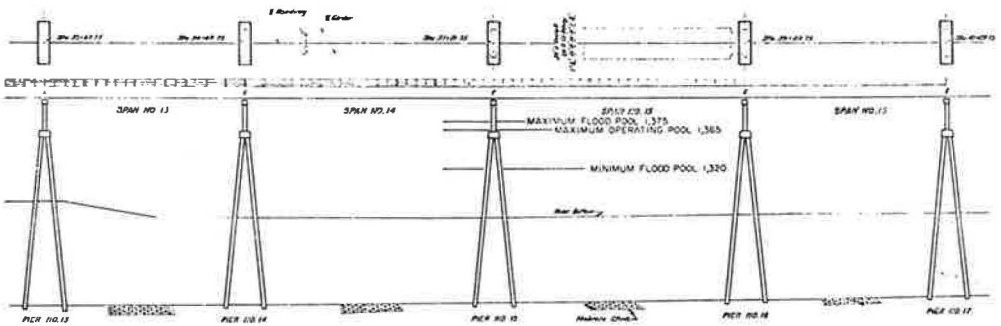

INTERMEDIATE SECTION

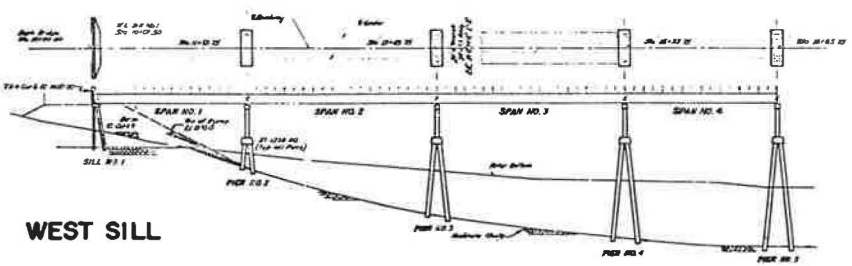

WEST SILL

Figure 3. Typical structure layout.

DESIGN CONSIDERATIONS

The following design data were assumed for this bridge (Fig. 3). The floor was to have an elevation of approximately 1411 ft and a level grade clear across the reservoir pool. The maximum operating pool given by the Corps of Engineers was 1365. Minimum operating pool in the winter was given originally at 1340, but was later lowered to 1320. The design bearing for the chalk to support the piling was 50 ton/sq ft. The major deviation from AASHO Standard Specifications was the ice load, which was set at 15,000 lb/lin ft of contact to be applied in either transversed longitudinal or quarterly in the direction with wind thrusts. This pile bent would require a stiffener cap at or near the average operating pool elevation with columns to support the plate girders for the roadway.

Driven Pile Bents

The design considerations resulted in two types of bents. The first bent has 8 piles; the second, 12 piles. The 8-pile bents (Fig. 4) were used in a combination of 5 piers with a span of 180 ft between each pier, coupled to form one continuous unit. The 12-pile bents (Fig. 5) were used in a combination of 5 piers spaced 225 ft to form a continuous unit.

On each bent, the stiffener cap was set at elevation 1358 and was 6 ft thick to form a footing for columns to support the I-beam unit of the roadway.

The unit on top of the footing would be similar to other structures of this type: the height being 26 ft; the column diameter, 4 ft; and cap, 4 ft thick. This design required a bearing capacity of 350 tons per pile. The founding material in the river was required to support this load on end bearing or distributed through the river alluvium by skin friction. The pile lengths were predicted on this bearing capacity and penetration data determined by a foundation investigation.

Pile Lengths

After establishing the bridge design criteria, the next step was to make a deep water foundation investigation. All sampling and testing operations had to be conducted from a drilling barge, as the water varied from 4 to 82 ft deep. A 25- by 100-ft barge was

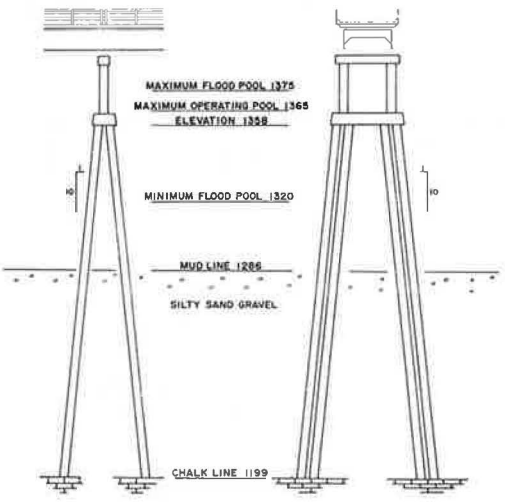

Figure 4. Typical 8-pile bent.

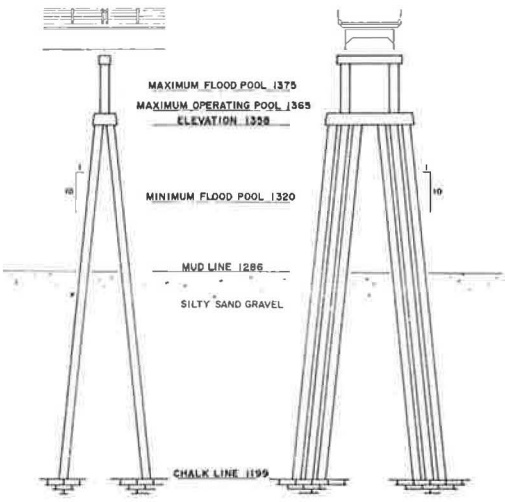

Figure 5. Typical 12-pile bent.

used as a drilling platform. A second barge was used to handle anchors, anchor cables, winch drums, marker buoys and miscellaneous equipment required to position the drilling equipment. Drive tests and wash borings were made to obtain undisturbed samples for laboratory analysis. Size analysis and unconfined compressive strength tests were performed in the laboratory and typical results were recorded on the plan and profile sheet (Fig. 6). Penetration resistance was measured as the number of blows required by 470-lb hammer dropped 30 in. to drive a 2⅞-in. retractable plug sampler 1 ft. Skin friction was measured by a dynamometer as the number of pounds pull required to start the drill stem out of the hole. A second method of testing was wash boring to the Niobrara chalk and then taking a drive core sample. Twenty-four locations were tested.

Vertical control was based on the Corps of Engineers record of pool elevations kept at the power house in Ft. Randall. Horizontal control was maintained by triangulation from base lines on each shore. With limitations on the time allotted for the preliminary investigation, no attempt was made to place the borings on the centerline of each bent; instead, a regular spacing of the holes across the reservoir was made to determine the general subsurface geology at the site.

At first, difficulty was experienced in driving the drill stem, with the attached retractable plug sampler, to the chalk. This was attributed to the extreme water depth and the resistance presented by sands in the river alluvium. Five wash borings were put down using a positive displacement pump operated at 500 psi, and no difficulty was experienced in penetrating to the chalk. From these wash borings, it was determined that when the blow count reached 250 blows per foot a core could be cut with reasonable assurance that it would be in chalk. Most chalk cores were 4 in. long, and required 250 blows to cut and a pull in excess of 33,000 lb to extract the drill stem. Based on this subsurface investigation, the pile lengths determined for each bent varied from 50 ft on the east bank and 25 ft on the west bank to a maximum of 176 ft in the middle of the channel.

Pile Design

The foundation investigation indicated a need for a total of 37,764 linear feet of piling. The structure is supported on 276 prestressed, precast concrete piles, 48-in. diameter. Each pile has a wall thickness of 5 in. and is reinforced with ¼-in. spiral steel using a 2-in. pitch 3 ft from each end and a 6-in. pitch for the remaining length of pile.

Prestressing was provided by sixteen 7/16-in. cables stressed to provide 1100 psi in the concrete section. To provide lateral stiffness 8 No. 4 rebars were added. Each pile was designed to be filled in 3 units: the L3 section, or the lower portion of the pile, was to be filled with sand; the L2, with Class C concrete; and the L1 section, 20 ft from the top of the piling, with Class A concrete. A reinforcing cage of No. 8 bars was used to tie the piling to the footing cap. All Class A concrete was required to reach 7,000 psi in 28 days. This was an unusual requirement for the Highway Department, as Class A concrete is generally 4,000 psi in 28 days. However, it was felt that the right aggregate could produce this 7,000-psi strength requirement with no difficulty to the contractor. Subsequent events forced the contractor to change from his first pit that contained some soft aggregate to another pit that consisted of sharp, angular, hard rock to meet the 7,000-psi requirement consistently.

CONSTRUCTION

In the fall of 1961, the South Dakota Highway Commission advertised for bids on the foundation for this structure. Plans and specifications called for driving 37,764 lin ft of 48-in. prestressed, precasted concrete piling and 1,008 ft of 12 BP 53-lb bearing piles in sill 1 and 29. Work was to be completed in two construction seasons.

Plans Quantities

The contractor was given the option of using a multi-unit pile, similar to the type manufactured by the Raymond Pile Corporation or a single-unit type used by Concrete Technology of Tacoma, Washington. The contractor elected to cast the piling at the site, using a single-unit pile.

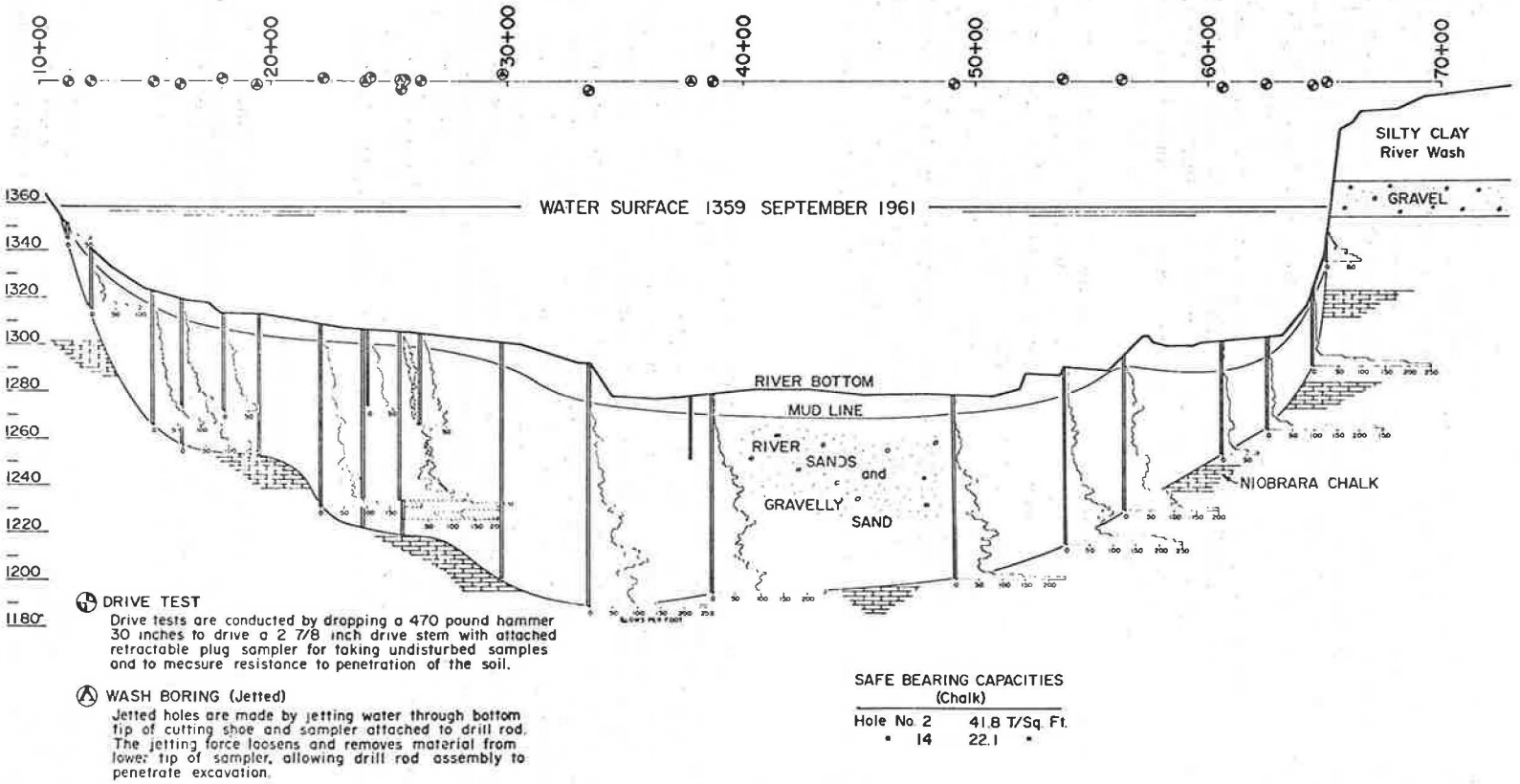

Figure 6. Subsurface profile.

Pile Construction

The contractor selected a location in Snake Creek Bay to build a casting yard (Fig. 7). The casting yard consisted of two casting beds 425 ft long. At one end was a rack containing 16 spools of prestressing cable; the other end contained a jacking frame for stressing the cable. A small overhead gantry crane was used for placing the concrete as well as extracting the piles from the forms. While the concrete was being placed in the form, a vibrating mandril was pulled through the center of the form at a speed sufficient to compact the concrete; therefore, no interior forming was necessary.

Figure 7. Casting yard: vibrating mandril, twin casting beds and gantry—pile storage at left.

In using the mandril as an internal form, a stiff no-slump concrete mix was required. Care in placing this dry mix at headers and on the ends was exercised to prevent the pile from collapsing and requiring patching. The pile was cured with a fog to maintain high humidity and kept at a temperature between 70 and 85 F.

After the concrete had cured to 5,000 psi, pick points were drilled through the pile shell and the pile extracted from the form. The pile was placed in a storage yard by the water. At this time, plugs were cast into one end of each pile. Two types of plugs were used: one was a 4-ft flush-end plug; the other was a tapered plug, having 3 ft of concrete in the end of the pile with a 45-deg 2 ft long taper (Fig. 8). Both plugs were epoxied into the pile at the time the plug was cast. At this time, the pick points were epoxied and filled with a stay-crete mixture. After the piles had cured to 7,000 psi, they were moved to the launching rail and taken to the stiffleg driving unit. For moving each pile, one end near the pick point was set on a flex float unit, and the other pick point was held by a small A-frame with a winch line attached.

Pile Placement

When the pile arrived at the driving site, two methods were used to align it on the compound 1 on 10 batter. The first method used a stay lath unit 15 ft under water with a second unit at the barge level. By setting the pile into the predetermined position, a compound 1 on 10 batter was achieved. This method was used until a storm destroyed the lower stay lath unit. The contractor then computed the distance out from the centerline to the point where the pile point would intersect the mud line. He placed the pile point at that intersection point and leaned it into the upper stay lath unit. The pile was either jetted or jetted and hammered to the final accepted bearing capacity. The original specifications required the piling to be seated with 50 blows per inch into the chalk by a 50,000 ft-lb hammer. To achieve this specification, the contractor used a three-finger jet with each nozzle set 90 degrees from the others. This three-finger jet was used to put the piling down as far as possible. Then the pile was hammered to the chalk. However, this method proved ineffective because the three-finger jet washed a hole at the wrong angle and tended to concentrate any large gravel found in the sandy zones into a nest of boulders that the pile could not penetrate.

A second method of placing the pile used a single-bar jet placed on the pile before positioning. The single-bar jet was strapped with quick snap releases to the pile so that the jet worked directly ahead of the pile tip. The hammer could be used at the same time, allowing the pile to be jetted and hammered simultaneously. This method proved quite effective. With the three-finger jets, it often required a full shift to place one pile. With the single-bar jet and simultaneous hammering, it required approximately 55 minutes to place a pile.

Several problems occurred during the placement of the piles. Slipped plugs required a change in plug type; pick points popped out. A question arose as to how many blows

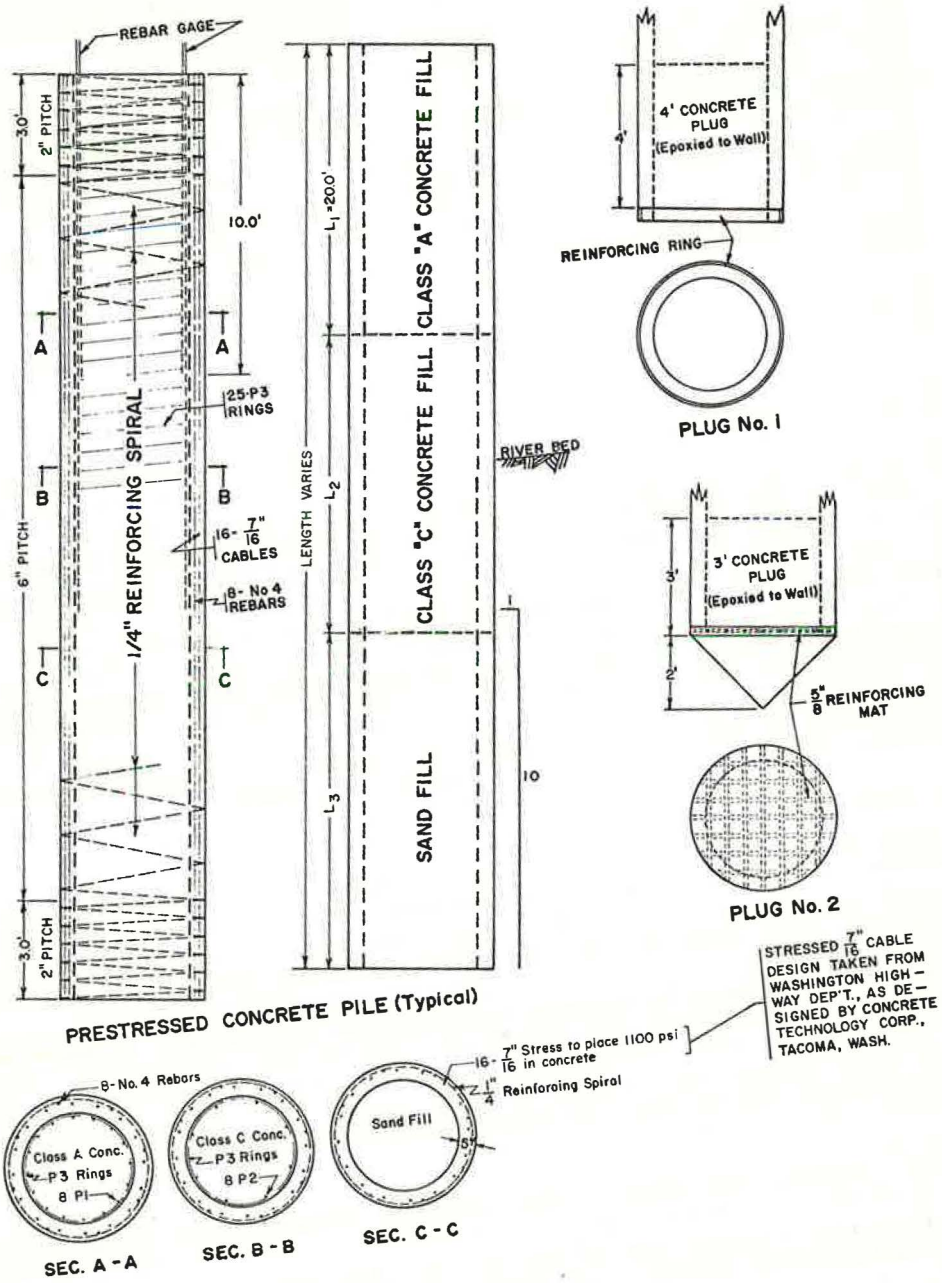

NOTE:
L_1 = Constant
L_2 = Difference between L_1 & L_2
L_3 = Normally taken as the lower $\frac{1}{3}$ of Pile

Figure 8. Prestressed concrete pile.

per inch a pile would stand without damage during the driving operation. One pile was driven as a test pile to a total of 1,792 blows for 20 in., and then pulled (Fig. 9). Inspection indicated the pile had sustained a longitudinal crack approximately 70 ft in length and that the reinforcing ring on the end had been stripped off. However, this pile would have been acceptable if it had been backfilled properly. Later studies of driven piles revealed that many piles in the various bents had been driven over 5,000 blows to get acceptable bearing. For example, in Bent 20 the pile in position 5 was driven 1,251 blows to place it. Pile 9 was driven 5,237 blows to get acceptable bearing. Both of these piles sustained no visible damage at the time of acceptance. On the other hand, in Bent 24, pile 7 was driven 327 blows and on inspection it contained 30 ft of water. Pile 8 was driven 1,710 blows in a total of 77.5 in. and contained 75 ft of water at the time of acceptance. Both of these piles were inspected by divers and had longitudinal cracks in the area where concrete had been placed into the form. These piles were pumped dry and backfilled with Class C concrete to an elevation of 1358. In Bent 16, pile 2 was reported as having water gushing out of the pile hammer helmet during the driving operation. An attempt to pump this pile dry failed. On inspection by divers, it was discovered that a pick point patch had come loose admitting the water from the jets. Since these pick points were about 6 in. square, considerable water could be admitted to a piling under pressure when one failed.

Figure 9. Test pile 2-24—113 ft long cast from 7300 psi concrete. Pile driven filled with water; seated with 1792 blows for 20-in. penetration. Pile shows plug in place, banding torn loose and a split 70 ft long in section where concrete was placed in the form.

During the fall of 1962, the piling for Bents 26, 25, and 24 (in that order) had been driven. At Bent 24 a test pile was loaded to 375 tons with little measured deformation. During the winter months examination of the pile driving records on Bent 24 disclosed 4 piles with slipped plugs (a flat-end 4-ft concrete plug epoxied into the pile). These piles and 4 piles that had broken by freezing of water which had been left in them were unacceptable to the state.

Later in the spring of 1963 when layers of cobbles and boulders were encountered between Bents 17 and 24, the contractor decided to change from a flat plug to a pointed-type plug, which was extended 2 ft beyond the end of the pile and was cast on a 45-deg angle (Fig. 8). The plug facilitated driving, but caused problems in alignment. This pointed-end piling tended to deviate from the compound 1 on 10 batter more than the flat-end type piling.

During the summer of 1962, when the contractor was assembling his equipment and testing it between Bents 17 and 24 he used three-finger jets to determine the chalk elevation at various bents. This jet moved large volumes of material at relatively low pressures and, in so doing, tended to sort the material in the river bottom. This material was described originally as a sandy gravelly alluvium river deposit. Boulders tended to concentrate at the places where piling would have to be driven later.

In 1963, when the contractor returned to place piling in these bents he encountered considerable difficulty because of this concentrated boulder zone. However, in all bents, with exception of Bent 18, the contractor was able to place the piling. At Bent 18, he had to blast and clam to remove the boulder concentration in order to place piling. In spite of popped pick points, hard driving and boulders, the contractor placed 35,882 lin ft of concrete piling. Inasmuch as the plans called for 37,765 ft, this is a computed decrease of 5.02 percent in plans quantities.

Figure 10. Bent 22 pile 4—cracks as found January 1964. Length 138 ft, 7000 psi concrete—driven a total of 6897 blows. Pile was pumped dry before filling with sand and Class C concrete.

Pile Filling

After driving each bent, the final step was filling each pile. The fill was of two types. The first type used with piling cast from 7,000-psi concrete was according to plans (Fig. 8). The other type consisted of installing a No. 8 reinforcing cage and filling the pile to the top with Class A concrete. The second type became necessary when the state permitted the contractor to use piling cast from concrete that failed to reach 7,000 psi. Approximately 41 pilings were cast with strengths between 5,500 and 6,500 psi, and these were placed in various bents during the summer of 1963. While little or no precautions were taken in placing the sand, all Class C and Class A concrete was required to be placed by tremie methods. The Highway Department felt that dropping the concrete a long distance would allow segregation and bridging to occur; this could be prevented by using tremie methods. However, in some of the piling, with popped pick points where it was impossible to dewater them, the tremie method of concrete placement was necessary for proper filling of the pile.

Broken Piling

By November 1963, the contractor had substantially completed the substructure as required by contract. However, in January 1964, inspection disclosed that numerous piles had ruptured to the extent of breaking the steel reinforcement and knocking pieces out of the pile shell. A hasty agreement

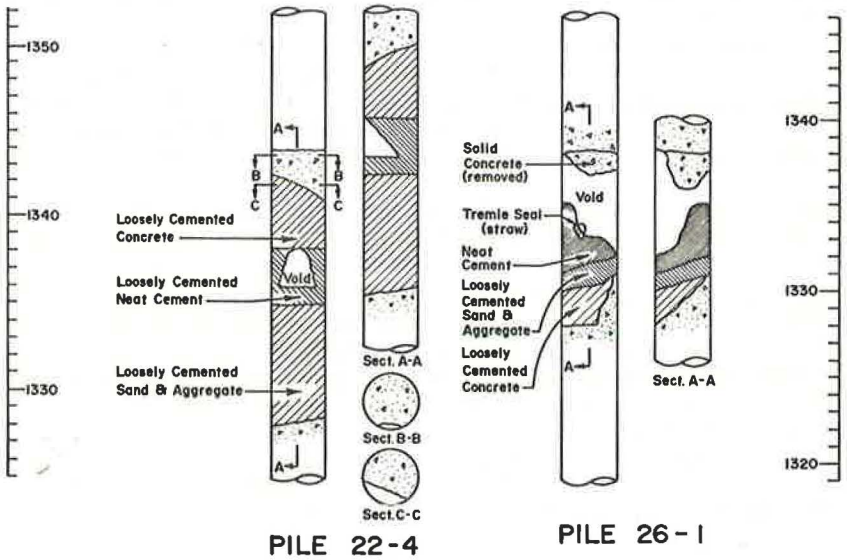

Figure 11. Repair Log Bent 22 and Bent 26.

Figure 12. Cracked piling Bent 26. Large hole and crack in Position 7; pile in Position 1 was driven a total of 308 blows; dry when filled with sand and Class C concrete.

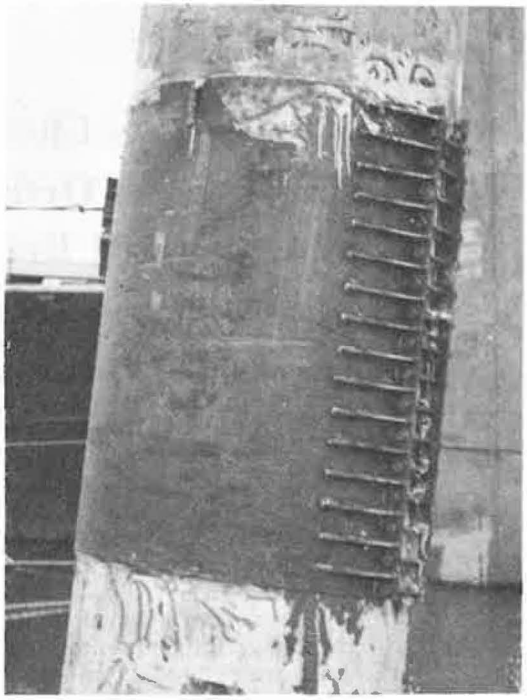

Figure 13. Steel reinforcing band as placed on pile 1 Bent 26—epoxied and bolted in place after deleterious material had been removed and replaced with dry pack concrete.

was concluded with the contractor to inspect all damaged piling using sonic methods and core drilling. This inspection determined that 52 piles were damaged to the point where repairs were necessary.

In piling that required repairs, zones up to 14 ft thick consisting of segregated concrete, silt, sand, gravel, hay and even an 8 x 8 timber were removed. Typical of the piling repaired were the following: In Bent 22 pile 4, 14 ft of loosely cemented aggregate, neat cement, low-strength concrete and a void were cleaned from the pile shell and replaced with dry-packed concrete. After cleaning the exterior shell a steel reinforcing band of $\frac{3}{8}$-in. steel was epoxied and bolted into place (Figs. 10 and 11). Bent 26 pile 1 had 6 prestressing cables exposed with a 3-ft void where the water around the pile had washed out unconsolidated material. Ten feet of loose material including a straw tremie seal was removed and replaced with dry pack. The exterior of this pile was banded with a reinforcing unit, epoxied and bolted into place (Figs. 11, 12, and 13). All piles that were repaired were reinforced by banding to replace the steel that had been cut out to gain access to the pile core.

CONCLUSIONS

Prestressed, precast concrete cylinder piling provided an economical foundation for this 5655.5-ft structure in deep water. However, successful use of this type of piling requires the ability to predict its correct length and bearing capacity. This is accomplished by performing adequate foundation studies, especially penetration tests and estimates of skin friction values. During the construction phase, proper control must be exercised to coordinate the action of jetting and the hammer for maximum placement of piling. Finally, extreme care in backfilling must be taken by requiring a full tremie backfill that has been vibrated and checked by random coring or sonic testing methods to insure a sound pile that will withstand the rigors of weather extremes and perform as a structural member.

Studies Leading to Choice of Epoxy Asphalt for Pavement on Steel Orthotropic Bridge Deck of San Mateo-Hayward Bridge

BEN BALALA, California Division of Bay Toll Crossings

Long-span bridges with orthotropic steel decks have created the need for a lightweight, durable surfacing to act as both a leveling course and pavement. The pavements used by the originators of orthotropic steel deck plate girders in Europe are not feasible for use in this country. Developments in synthetic resin pavements show promise. The problem, insofar as available materials are concerned, is related to overlays used to repair damaged portland cement concrete bridge decks.

The experiences of the California Division of Bay Toll Crossings on major toll bridges in the San Francisco Bay Area are related. These include choice of a thin epoxy coal tar overlay, $\frac{1}{8}$ in. to $\frac{3}{16}$ in. thick on the San Francisco-Oakland Bay Bridge concrete decks, and choice of an epoxy asphalt concrete pavement, $1\frac{1}{2}$ in. to $2\frac{1}{2}$ in. thick on the steel orthotropic deck of the San Mateo-Hayward Bridge. The first epoxy coal tar was experimentally applied to the San Francisco-Oakland Bay Bridge in 1958. Subsequent studies progressively testing over 20 materials are still in progress.

The author believes that when numerical criteria have been established various resins may be satisfactory if acceptable application methods can be developed. A clearinghouse for accumulation of experience on the subject is required. Experimental applications are needed. The methods for measuring adhesion in direct tension on a diamond-drill cut core and fatigue in bending are mentioned as a start on the problem of establishing numerical criteria.

•LONG-SPAN bridges with orthotropic steel decks have created the need for a lightweight, durable surfacing to act as both leveling course and pavement. A variety of solutions to this problem by the originators of this type of construction in Europe are either not feasible or not permanent enough for recently projected uses. Developments in synthetic resins show promise in solving this problem. Earlier studies for concrete bridge deck overlays gave some insight into the area of resinous pavements.

The qualitative criteria developed for the intended use were investigated for various materials and choice made for the San Mateo-Hayward Bridge. Continuing developments and the results obtained in both testing laboratories and actual installations will probably lead to innovations in the use of synthetic resins for this purpose.

The history of construction of orthotropic steel deck bridges and the history of research into pavements for orthotropic steel decks in general are well covered (4, 6, 9).

Paper sponsored by Committee on Adhesives, Bonding Agents and Their Uses and presented at the 48th Annual Meeting.

The technical data from actual tests and other relevant data appear in the references at the end of this article. The information on completed work has also been covered (1, 11).

This paper will be confined mainly to the reasons for the tests, the interpretations made from the data obtained, and the reason for the choice made for this particular installation. Of necessity, the materials were all proprietary compounds and because of their nature exact formulations are not available. This made the evaluation procedure by actual field tests unavoidable.

THE PROBLEM

The steel girder with orthotropic steel deck developed in Germany after World War II has found wide acceptance for long-span bridges primarily because of its attractive appearance. On the San Mateo-Hayward Bridge the steel box girder was chosen because of its unobtrusive silhouette as compared with a steel truss bridge. This choice led to studies which found substantially what subsequent investigations have confirmed, that the problem of paving steel plate decks is not yet completely or satisfactorily solved.

The European bridges have been paved by a number of methods which were not considered feasible under conditions prevailing in the paving industry in this country. The pavements used in Germany were mainly mastics which were subject to rutting and shoving particularly in hot weather. Stabilization of these mixtures is achieved by rolling rock into the surface and resistance to shoving by welding attachments to the steel deck to produce physical anchors. The practice in continental Europe is to use a multilayered construction; and with the long guarantees which are prevalent in the construction industry there, this type is generally acceptable.

The first and best-known pavement studies made in this country for steel orthotropic decks were made for the Poplar Street Bridge on a prototype at Troy, Illinois. This was an asphaltic concrete with various additives including neoprene, rubber, asbestos fiber and a bond or prime coat of epoxy coal tar. Shortly after the Troy experiments came the actual paving, in 1964, of the Port Mann Bridge, a steel arch with an orthotropic steel deck, with asphaltic concrete over an epoxy red lead corrosion protective coat and an epoxy coal tar bond coat containing embedded grit. The Port Mann pavement is regarded as completely successful. The Troy Bridge developed cracks in the surfacing during its 2-yr test period. These were the North American predecessors of the pavement chosen for the San Mateo-Hayward Bridge.

From a strictly rational standpoint, even neglecting the experience of others, it appeared that several criteria for a pavement could be established:

1. Satisfactory bond to steel.
2. Sufficient ductility and elasticity to expand and contract with temperature changes in the steel substrate and to accommodate flexure under load without cracking or disbonding.
3. Sufficient stability to resist shoving and rutting.
4. A construction process permitting placement at a reasonable cost over large areas to tolerances acceptable to high-speed vehicular traffic.

The actual limiting numerical values for these criteria must be determined by future experience for the various paving methods and materials used. We did compare the materials available and used 200 psi in tension for bond and a million repetitions for flexure as the numerical values for criteria to choose materials for experimental installation and study.

EARLY STUDIES

The Division of Bay Toll Crossings first became involved with resinous paving materials when the problem of surfacing the 25-year-old concrete decks of the San Francisco-Oakland Bay Bridge was encountered in 1962. This surface was a 59-ft 4-in. wide lightweight concrete deck surfaced with ordinary sand cement topping and divided into six lanes by ceramic tile markers embedded in the mortar topping. The deck was in

good condition but it was necessary to obliterate the tile markers, which were slightly raised above the surface of the concrete in order to change the traffic pattern.

Studies at this time evaluated moduli of elasticity, coefficient of expansion, and adhesion for a number of aggregate-filled resins as well as for latex modified portland cement concrete.

The subject of resins had been broached to the Division of Bay Toll Crossings in 1958 by a test application of Guardkote 140 on the San Francisco-Oakland Bay Bridge upper deck with the cooperation of the Shell Chemical Company. Guardkote 140 was an epoxy coal tar formulation derived from basic patents held by the Pittsburgh Coke and Chemical Company.

At about this same time we were approached by the California Chemical Company, Oronite Division of Standard Oil Company of California, regarding use of a polyester resin for this purpose. The possibility of a polyester performing the same function as an epoxy at about half the cost sounded attractive. A further attraction was the fact that although the epoxies were truly two component materials requiring intimate mixing and precise proportioning, the polyesters were catalyzed only and less critical mixing would still produce the required end product.

Test installations of five materials each about 20 ft long and about 12 ft wide were placed on the lower deck of the San Francisco-Oakland Bay Bridge in 1962. There were two latex-modified concretes, three polyester resins, an epoxy asphalt, and a proprietary concrete floor system without an adhesive (2). The epoxy asphalt formulation used in this application never seemed to set up, and abraded quickly under the heavy traffic. The proprietary concrete floor system and the latex-modified concretes showed under hand hammer soundings, extensive rattly areas indicating general lack of bond. The three polyester resins were excellent. The only apparent difficulty or obvious drawback to the polyester resin applications was lack of a commerical method producing an acceptable riding surface.

It became necessary to terminate the test when the lower deck paving contract was awarded in 1964. All test areas other than the polyester resins were readily cleaned down to the original concrete deck which was the new unsurfaced lightweight concrete over the former interurban trackway. It was practically impossible to remove the polyesters without removing part of the concrete substrate, and they were covered by the new surfacing.

The surfacing chosen for the upper deck paving contract in 1963 and the lower deck in 1964 on the basis of cost, commercial quality of application equipment and material, convenience to traffic, and current availability of contractors and equipment was Shell Guardkote 140 (basically a flood coat of epoxy coal tar filled with clean, hard sand passing a number 10 screen), at that time under the control of Shell Chemical Company. This was not a perfect solution but with the state of knowledge at that time it fulfilled most requirements. It obliterated the tile markers satisfactorily, renewed the surface, obliterated the difference in texture between the new and old concrete slabs on the lower deck, and provided a construction method that was compatible with the complicated lane-scheduling procedure required to switch traffic from mixed bidirectional traffic on each deck to unidirectional mixed traffic on each deck. It did not, however, provide a new screedable surface since the placing procedure is somewhat similar to that for a seal coat in that it repeats to some degree the imperfections of the underlying pavement.

In addition, we became acquainted with the capabilities of resin producers and their statements, which we have no reason to doubt, that if we could tell them the physical characteristics of the material required for our use, they could produce it. Numerical criteria developed by future tests may yet produce an opportunity for the resin producers to fulfill their promises.

Shell representatives in 1962 also described their Epon asphalt system, but the half-inch average thickness proposed for the San Francisco-Oakland Bay Bridge due to weight limitations was not considered feasible for Epon asphalt, basically a $\frac{3}{8}$-in. maximum asphalt-concrete aggregate mixture bound with an epoxy-asphalt compound.

There were countless products investigated that did not receive complete study due to lack of proper financial or technical backing by the vendor. A definite factor in deciding on a coal tar epoxy for the San Francisco-Oakland Bay Bridge was the furnishing of a bonded written guarantee for three years.

LATER STUDIES

When the problem of paving the San Mateo-Hayward Bridge was faced in 1964, it was soon apparent from studies of European pavements that the problem of paving steel plate decks needed further study.

The best pavement based on long-time use was the so-called German Gussasphalt, a job-cooked mastic that had been developed through local usage and perpetuated with patented procedures and formulations and kept acceptable by guarantees. As far as our application was concerned, there were two reasons why Gussasphalt was not considered seriously. First, as with all mastic type mixtures that retain their plasticity, we expected that the performance under heavy traffic in hot weather would be unacceptable, and second, it seemed impossible under the existing construction industry framework to import such a patented controlled process involving not only material and equipment but also very exacting and demanding labor and construction procedures.

We were also aware of the Troy prototype paving experiments and there were again two basic reasons for not following that pattern. First, we had never found confirmation in the paving industry that rubber additives would improve asphaltic mixtures to the degree that we required for paving on steel decks, and second, the epoxy coal tar bond coat increased costs to the point where solid instead of layered construction could be considered. Later cracking problems at the Troy bridge terminated our interest in that system.

The Port Mann Bridge was apparently proceeding satisfactorily with a different multilayered system: a red lead epoxy polyamide paint overlaid with epoxy coal tar with grit embedded to act as a "tooth" for the overlaying asphalt concrete. There were again several reasons for not following this method. The floor system of the Port Mann Bridge with floor beams at about 5-ft 6-in. intervals was much stiffer than that proposed for San Mateo-Hayward with a minimum floorbeam spacing of 10 ft 6 in. Also it seemed by this time that a simpler system involving only one type material should be sought.

In 1964, a series of tests was designed to investigate a one-material system—a prime or bond layer on the steel deck of the same material used to cement together the aggregates in the overlying pavement. This would eliminate investigation of additional possible reactions between a variety of materials and also eliminate the cost of additional equipment and operations required for differing materials. The type of inorganic zinc protection system required by the designers had already been chosen. The contract specified inorganic zinc as a second line of defense from corrosion in addition to the pavement. The contractor chose Enjay Chemical Company's Rust-Ban 191. This same Rust-Ban was used on all laboratory test specimens.

Two fundamental tests were used as criteria for choosing materials for a field test. Pavement specimens were prepared on ½-in. thick, 4-in. by 18-in. steel plates coated with inorganic zinc and 1½ in. of compacted paving material. Diamond drill cores (2-in. diameter) were cut through this pavement to the steel and pulled off in direct tension to measure adhesion. Other specimens were placed between supports at 15-in. centers and deflected with a 700-lb load applied repeatedly so as to produce tension on the exposed face of the paving material to establish a fatigue strength (3).

At this time we were surprised to find that we were unable to produce a satisfactory specimen with the epoxy coal tar Guardkote 140 as the resin. It has since been stated by various chemists that the curing agent in this formulation reacts with zinc and thus affects the bond between the epoxy coal tar and the zinc-coated steel. On the other hand, we are informed that epoxy asphalt employing a curing system different from epoxy coal tar has no effect on the zinc coating. This may account for some of the failures of the epoxy coal tar paving attempted on zinc-sprayed orthotropic decks. Apparently, the bond between clean bare steel and epoxy coal tar is satisfactory.

Again Shell was approached concerning the epoxy asphalt discussed earlier during the San Francisco-Oakland Bay Bridge tests. However, that company had had some discouraging experience and was not interested at first. Sometime later, after internal changes of responsibility, Shell returned to us with a revised formulation which the company was willing to subject to our test procedures. This Type III Epon asphalt had been reformulated and reevaluated on the basis of field experience especially with re-

TABLE 1

PARTIAL LIST OF MATERIALS INVESTIGATED

Binder Material	Supplier
Epon asphalt	Shell Oil Company
Guardkote 250	Shell Oil Company
Guardkote 140	Shell Chemical Company
Polyester resin	California Chemical Company, Oronite Division
Polyester resin	Reichhold Chemicals, Inc.
Polyester resin	Cook Paint and Varnish Company
Latex	B. F. Goodrich Company, Chemical Division
Latex	Dewey and Almy Chemical Corporation
Epoxy asphalt	Protex-A-Cote, Inc.
Asphalt concrete	California Highway Specifications
Miradon	Humble Oil and Refining Company
Humbleweld 7502	Humble Oil and Refining Company
Resiweld R7122	H. B. Fuller Company
Resiweld 7122M	H. B. Fuller Company
Resiweld 7121	H. B. Fuller Company
Resiweld R7123	H. B. Fuller Company
Concresive 1112	Adhesive Engineering
Concresive 1113	Adhesive Engineering
Ductron	Standard Oil Company of Ohio
Epoxy IR413A	California Division of Highways, Materials and Research Department Formulation
CDC	Mitchell, Pianta and Pfenning, Inc., San Antonio

gard to curing time and flexibility or ductility of the resultant pavement.

TEST RESULTS

As a result of laboratory tests (5, 8), two field applications were made with five materials in each test in the fall of 1965. One test area was made available by the State Division of Highways at the Ulatis Creek Bridge near Vacaville on an Interstate Highway in one of the eastbound lanes. This bridge is an orthotropic steel deck that is structurally stiff but, due to its short span, very light. The second area was a prototype section of the San Mateo-Hayward Bridge orthotropic section erected over an abandoned scale pit on the site of the former toll plaza at the west end of the San Mateo-Hayward Bridge. The five materials (Table 1) were as follows:

1. Ordinary asphaltic concrete, $\frac{3}{8}$-in. maximum aggregate;
2. Shell's Epon asphalt, Type III, graded aggregate $\frac{3}{8}$-in. maximum;
3. Fuller's Resiweld R7122, sand resin mortar;
4. Shell's Guardkote 250, sand resin mortar; and
5. Adhesive Engineering's Concresive 1113, sand resin mortar.

The immediate and early result of these field applications was a prompt failure of the asphalt concrete at Ulatis Creek by slipping. This was repaired by the State Highway Maintenance Department. The repaired section performed much better than the original installation. All of the resin pavements were applied according to the recommendations and with the assistance of their sponsors although the actual work was done under contract. At the San Mateo-Hayward Bridge even the ordinary asphaltic concrete remained intact through the entire test period. The Ulatis Creek materials are still in place. The test area over the scale pit had to be removed to complete the San Mateo Bridge for public traffic.

Traffic is unusually heavy and fast at Ulatis Creek, whereas at the scale pit location it was light by comparison and of limited duration due to construction exigencies.

In spite of the fact that the resin pavements, with the exception of the epoxy asphalt, were very rough and despite the fact that all of the joints between the various materials were square, whereas the pavement continued across the skewed joints in the steel on the Ulatis Creek Bridge, the Ulatis Creek resin pavements are all in good condition. The pavements have cracked over the skewed joints but only minor spalling is evident. The roughness produced violent impacts and vibration without producing visible damage. This roughness was overcome later—not to diminish abuse of the pavement but for the relief of the traffic which tended to avoid the rough area. An abrasive grinding operation was used for corrective work such as is used on portland cement concrete pavement that is out of specification for roughness.

At Ulatis Creek all materials except the ordinary asphaltic concrete performed very well, although the riding surface of the three light-colored epoxies was very rough because of construction procedures.

At the scale pit installation, there was no surface evidence of unsatisfactory performance in any of the materials. The most interesting results were observed during removal of the pavement from the steel bridge deck prototype.

Various methods of removal were tried including a demolition ball and a bulldozer. The asphaltic concrete came off rather readily as expected, and at the fracture faces, it separated from the aggregate particles and also cleanly from the inorganic zinc covering the deck.

The epoxy asphalt at fractures broke cleanly through the aggregate particles and in places came up with the inorganic zinc film attached. The three light-colored epoxies also brought up inorganic zinc. They did not include any aggregate particles larger than sand in the mixture.

A 200-ft length of steel bridge one lane in width was paved in the summer of 1968 just before the paving contract to observe and study the effect of the construction procedure on the transverse and longitudinal bolted splice plates and the two-course construction in general. Results were good.

THE CHOICE

The choice of the Epon asphalt (7) was based on four factors:

1. Cost is between ordinary asphaltic concrete and the light-colored epoxies. The final contract cost was about one dollar per square foot in place including the deck preparation but not the inorganic zinc coating.
2. Surface tolerance and riding characteristics are as good as asphaltic concrete and better than the light-colored epoxies.
3. Construction procedure was feasible by modification of existing construction equipment.
4. Physical characteristics were far superior to ordinary asphaltic concrete and approached those of the more expensive epoxies.

CONSTRUCTION

The contractor engineered and purchased the special equipment required to mix and proportion the epoxy asphalt components and installed it at a paving plant rented for the duration of the work which took about three weeks. The spreading equipment had a detention tank to hold the mixed components at an elevated temperature to speed the curing.

Epoxy asphalt has an extended curing time which varies with the ambient temperature. This can be accelerated by holding at an elevated temperature. The problem in the field is to keep it at an elevated temperature long enough so that it does not take unduly long for the material to reach its ultimate properties but not so long that workability and compressibility are affected to a degree that is detrimental to the construction procedure (11). In contrast to earlier formulations, the present Type III epoxy asphalt formulation is not critically sensitive in this regard.

The pavement has a typical Marshall stability of 14,400 lb at 140 F and 4,200 lb at 400 F. By contrast, ordinary asphalt concrete has a Marshall stability of 2,600 lb at 140 F and has virtually no stability at 400 F.

THE FUTURE

Following completion of work leading to the choice of material for this project, other material suitable for use were submitted to us. We have continued laboratory tests, and at least two additional materials should be considered in future investigations. One of these is Cybond produced by American Cyanamid Company, a polyester resin mortar primed with polyester resin and the other CDC, a polyester resin (10) primed and bonded with epoxy resin. These should be field tested and appraised for determination of the cost of installation.

It is encouraging that the American Iron and Steel Institute has retained the Battelle Institute and, under the direction of Fred Fondriest, has published several reports on the state of the art. This could turn out to be a necessary clearinghouse for findings on orthotropic paving procedures. However, field tests are required for a variety of materials and procedures to ascertain whether laboratory criteria can be established to determine probable field performance.

Additional work should be done on commercial applications of resin materials to bridge decks with surface tolerances meeting the riding requirements of high-speed traffic. It is believed that costs can be clearly assessed when the procedure and choice of material have been determined. The science of resin formulation has been developed so that with sufficient flexibility a number of resins should be acceptable and costs would then be the determining variable.

REFERENCES

1. Bay Bridge Modernization. Western Construction, Nov. 1963.
2. Final Inspection Report of the Lower Deck Overlay Test Patches. Division of Bay Toll Crossings, April 1964.
3. Laboratory Tests for Steel Deck Overlay, San Mateo-Hayward Bridge. California Division of Highways, Materials and Research Dept., Sept. 1964.
4. Battelle Memorial Institute. Current Paving Practices on Orthotropic Bridge Decks. American Iron and Steel Inst., Bull. 1, Oct. 1965.
5. San Mateo-Hayward Bridge Improvements, Test Overlays-Steel Deck. Contract No. 5026, Resident Engineer's Report, Dec. 1965.
6. Battelle Memorial Institute. Research on and Paving Practices for Wearing Surfaces on Orthotropic Steel Bridge Decks. American Iron and Steel Inst., Bull. 3, Aug. 1966.
7. Results of Studies of Materials for Steel Orthotropic Deck Pavement, San Mateo-Hayward Bridge. Division of Bay Toll Crossings, Dec. 1966.
8. Metcalf, C. T. Flexural Tests of Paving Materials for Orthotropic Steel Plate Bridges. Highway Research Record 155, p. 61-81, 1967.
9. Battelle Memorial Institute. Paving Practices for Wearing Surfaces on Orthotropic Steel Bridge Decks. American Iron and Steel Inst., Bull. 6, Jan. 1968.
10. Estrada, N. S. Polyester Overlays for Road and Bridge Protection and Repairs. Highway Research Record 242, p. 36-40, 1968.
11. First Orthotropic Bridge Deck Paved with Epoxy Asphalt. Civil Engineering, April 1968.

Polyester Concrete: Load Rate Variance

LAWRENCE I. KNAB, U.S. Army Corps of Engineers

The effect of the variance of load rate on the engineering properties of a plain polyester concrete system was investigated. Both the tensile and compressive phases of the system were evaluated. In the tensile phase, the load rates ranged from slow static through the dynamic range; whereas in the compressive phase, the load rates varied from very slow static through very high static. Tests were conducted using one type of a polyester resin combined with a feasible gradation of a standard reproducible aggregate. Wherever possible, standard ASTM tests for portland cement concrete were used with each load rate held constant throughout the testing time of each specimen.

Ultimate stress, modulus of elasticity, and the strain at ultimate stress were the basic engineering properties considered. Significant variation of these three properties in both the tensile and compressive phases was obtained by varying the load rate. This investigation conclusively showed that the polyester concrete system studied will withstand both slow and fast static loading conditions in both tension and compression.

•CONCRETE can be defined as an artificial conglomerate rock consisting of aggregate and a binder. In portland cement concrete, the binder is a paste composed of cement and water. In synthetic concretes, a synthetic resin such as a polyester or epoxy constitutes the binder. The aggregate used in synthetic concrete is similar to that of portland cement concrete.

The innovation of synthetic concretes for civil engineering applications has created considerable interest. Synthetic concrete systems are being used for surfacing and/or patching materials for concrete bridge decks, highways, and airfield pavements. Presently, the structural potential of the synthetic systems is also being investigated. Synthetic concretes exhibit distinct advantages over standard portland cement concrete.

1. Very high tensile, compressive and flexural strengths—two to three times that of standard portland cement concrete;
2. Rapid rate of cure—many synthetic systems achieve near full strength in several days or less;
3. Excellent impact and abrasion resistance;
4. Very high resistance to freeze-thaw and general weathering action;
5. Excellent chemical, solvent, water and salt spray resistance; and
6. High-strength bonding characteristics with respect to most materials.

There are also several disadvantages of synthetic systems:

1. Some synthetic systems are limited to dry conditions; and
2. High cost of the synthetic systems—four times, or more, that of portland cement concrete.

Paper sponsored by Committee on Adhesives, Bonding Agents and Their Uses and presented at the 48th Annual Meeting.

The synthetic resin used as a binder in this study is a polyester resin. Since the system's binder is an organic plastic, the effect of varying the load rate on the system's properties poses a significant question.

TEST MATERIALS

Due to the very high strength (22,000 to 24,000 psi unconfined compression) and excellent reproducibility, trap rock was chosen for use as both coarse and fine aggregate.

Table 1 gives the aggregate properties and gradations. The polyester resin chosen was a rigid, low viscosity, room temperature curing material. Table 2 gives the description and properties of the resin as stated by the producer. The catalyst necessary for the reaction to occur was methyl ethyl ketone peroxide. The physical properties of the cured system for both aggregate gradations used are given in Table 3.

MIXING PROCEDURE AND CURING

The aggregate was surface dried, weighed in the proper proportions (fine/coarse aggregate ratio 1:1 by weight), and mixed thoroughly by hand or with a small mechanical mixer. The required amount of catalyzed resin was added to the mixed aggregate. Table 4 gives the aggregate gradations and the resin percentage for all tests performed. For approximately thirty minutes after adding the catalyst, the system's consistency resembled thick molasses. The system progressively thickened for an additional thirty minutes until gelling began. The components were thoroughly mixed and rodded (where applicable) into the test molds. The test molds were then vibrated externally to minimize air entrainment. The specimens were then placed in a 100 F curing room.

TABLE 1

AGGREGATE GRADATIONS, MIX PROPORTIONS AND PHYSICAL PROPERTIES OF NEW HAVEN CRUSHED TRAP ROCK

(a) Aggregate Gradation

U. S. Standard Sieve Size	Cumulative (% retained by weight)		
	Coarse Aggregate		Fine Aggregate Screenings
	3/4-In. Max.	3/8-In. Max.	
3/4 In.	7.4		
1/2 In.	72.6		
3/8 In.	93.2		
No. 4	99.5	87.0	0.6
No. 8			22.6
No. 16			48.8
No. 30			64.2
No. 50			74.5
No. 100			83.7
No. 200			85.1
Pan	100.0	100.0	100.0

Fineness Modulus = 2.94

(b) Mix Proportions

Sieve Size	3/4-In. Max. Size Aggregate (% by total weight)	3/8-In. Max. Size Aggregate (% by total weight)
3/4 In.	32.6	—
3/8 In.	10.4	40.3
Screening	43.0	40.3
Resin	14.0	19.4
	100.0	100.0

31% resin by total volume
Catalyst—1% (wt. of Resin)

(c) Physical Properties

Unconfined compressive strength = 22,000 - 24,000 psi
Specific gravity = 2.93

TABLE 2

SELECTRON 5119

Room Temperature Curing Polyester Resin

Description:

SELECTRON 5119 is a low viscosity, room temperature curing resin which performs well under varied conditions in many types of applications. It has been used successfully as a surface coating for wooden structures; it has been reinforced with fiber glass in many types of laminating applications; and it has been filled with mineral fillers and used for all kinds of applications from electrical potting to synthetic marble foor tile.

Outstanding Characteristics Include:

Gel time versatitility to meet variations in size of parts and environmental temperatures.

Low viscosity for rapid glass fiber wet-out.

Rapid cure to a tack-free surface.

Properties of Liquid SELECTRON 5119 at 77° F.	Typical Values
Color	Purple
Specific gravity	1.13
Weight per gallon, lb	9.4
Viscosity, Brookfield, cps	650
Stability (in the dark)	>4 mos.
Monomer content (Styrene), %	35

Catalyst Recommendations:

SELECTRON 5119 is prepromoted, thus only the addition of methyl ethyl ketone peroxide catalyst is required before use.

Approximate Gel Time in Minutes

% MEK Peroxide	60 F	77 F	90 F
0.5	—	70	48
1.0	96	26	19
1.5	57	18	12
2.0	40	12	8
2.5	27	—	—

Typical Properties of Cured SELECTRON 5119

	Casting	Mat. Laminate
Reinforcement	none	3 plies 2 oz mat
Catalyst	1% benzeyl peroxide	2% MEK peroxide
Cure	1 hr at 170 F 1 hr at 250 F	72 hr at 77 F
Glass content, %	none	32
Barcol hardness	45-50	50-55
Flexural strength, psi	14,800	28,200
Flexural modulus, x 10^6 psi	0.66	1.5
Tensile strength, psi	8,500	22,000
Tensile modulus, x 10^6 psi	0.58	1.3
Elongation in tension, %	1.49	1.5
Compressive strength	23,500	25,500
Izod impact strength, ft. lb./in. notch	0.32	7.4
Water absorption, 24 hr. immersion, %	0.097	
Heat distortion, 264 psi, F.	142	

TABLE 3

AVERAGE PHYSICAL PROPERTIES OF A PLAIN POLYESTER CONCRETE SYSTEM

Type Mix	Specific Gravity	Mass Density (slugs/ft³)	Seismic Velocity (ft/sec)	Thermal Coefficient of Expansion (in./in./° F)	Shrinkage (total)	Dynamic Modulus, Sonic (psi)
3/8-in. max. size agg.	2.02	3.92	10700	0.89×10^{-5}	1.14%	2.89×10^6
3/4-in. max. size agg.	2.43	4.71	10880	—	—	3.87×10^6

TABLE 4

OVERALL COMPARISON OF TENSION AND COMPRESSION: MATERIALS, MIXING, CURING, EQUIPMENT, TECHNIQUE

Type of Test and Range	Dimensions of Test Specimen	Agg. Gradation and Percent Resin (by total weight)	Strain Recording Mechanism	Equipment Data Readout	Equipment Load Application	Cure (days)
Tensile split, static (low, med, high)	6-in. dia. × 12-in. high cylinder	3/4-in. max. size agg. mix, 14% resin	SR-4 Type A-1 strain gage on end of cylinder	Type 564 storage oscilloscope strain-load trace	Baldwin 400,000-lb testing machine	4 to 15 at 100 F
Tensile, dynamic impact	2-in. dia. × 35-in. long cylinder	3/8-in. max. size agg. mix, 19.4% resin	2 Type EA-13-250BB-120 strain gages placed on periphery of cylinders	Tektronix 555 oscilloscope strain-time trace	Dynamic impact loading device using 0.55-lb projectile	44
Unconfined compression, static (low)	6-in. dia. × 12-in. high cylinder	3/4-in. max. size agg. mix, 14% resin	Compressometer Model PC-6M	Wiedemann strain-load recorder assembled on Baldwin	Baldwin 400,000-lb testing machine	3 at 100 F
Unconfined compression, static (very low)	6-in. dia. × 12-in. high cylinder	3/4-in. max. size agg. mix, 14% resin	3 vertical 1-in. BLH strain gages, Type FAH-100-12-SX centered vertically and spaced at 120 deg around specimen	Hamilton strain gage readout boxes	Baldwin 400,000-lb testing machine	4-6 at 100 F
Unconfined compression (low, med.)	6-in. dia. × 12-ir.. high cylinder	3/4-in. max. size agg. mix, 14% resin	3 vertical potentiometers spaced at 120 deg around specimen	Type 564 storage oscilloscope load-deformation trace	Baldwin 400,000-lb testing machine	2½ at 100 F + ½ at 70 F to 4 at 100 F
Unconfined compression (high)	6-in. dia. × 12-in. high cylinder	3/4-in. max. size agg. mix, 14% resin	3 vertical 1-in. strain gages spaced at 120 deg around specimen	Type 564 storage oscilloscope load-strain trace	Baldwin 400,000-lb testing machine	6 to 15

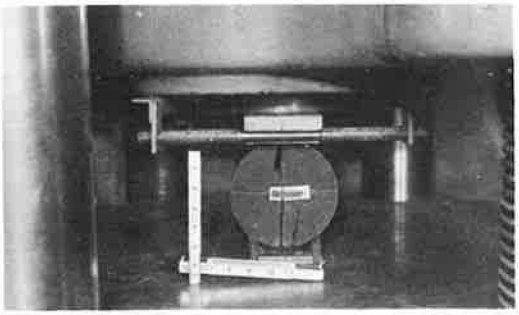

Figure 1. Tensile split specimen (6-in. diameter by 12-in. length cylinder) in Baldwin testing machine just after failure. Horizontal 1-in. strain gage on specimen.

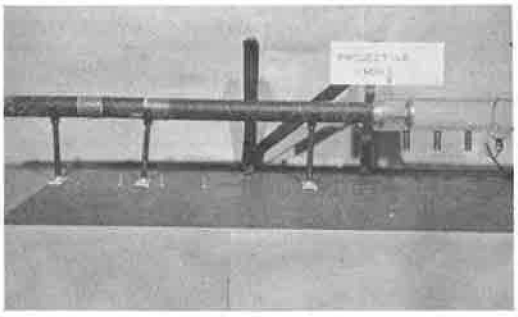

Figure 2. Dynamic impact specimen (2-in. diameter by 35-in. length) in testing position. Tape on specimen covers strain gages. Projectile used is indicated.

The required setting (gelling) and curing time of the system is dependent on the amount of catalyst added and the temperature of the system. Both larger percentages of catalyst and higher temperatures accelerate gelling time. Higher temperatures also yield faster curing rates. Approximately 50 percent of the system's ultimate strength is developed in 6 to 8 hr at 70 F and 95 percent developed in about 3 days at 70 F. Table 4 gives the conditions of cure for all specimens tested.

TEST PROGRAM AND RESULTS

Variance of Tensile Load Rate

Static tensile load rates were conducted varying the load rate from 4000 lb/min (31-min rise time) to 5,000,000 lb/min (2-sec rise time) on the Baldwin testing machine. Rise time is defined as the time required to load a specimen from zero to ultimate load. The tensile split test (ASTM C496) was performed by loading a 6- by 12-in. cylinder on its side, with a 1-in. Type A-1, SR-4 strain gage mounted in the center on one end of the cylinder to measure the tensile strain. Figure 1 shows a tensile split specimen in the testing machine just after failing. Data recording equipment for static tensile split tests consisted of a Tektronix, Type 564 storage oscilloscope which yielded load-strain plot.

In the dynamic tensile range, an impact loading device was used producing rise times from 60 to 80 μ-sec. The dynamic impact test consisted of an induced, transient strain pulse which was built up suddenly under impact and confined within the specimen. The

TABLE 5

SUMMARY OF STATIC TENSILE PROPERTIES
TENSILE SPLIT TEST

Load Rate (kips/min)	Rise Time[a] (min)	Avg. Ultimate Stress (psi)	Avg. Dev. From Mean Stress (psi)	Avg. Init. Modulus E (psi x 10^6)	Avg. Dev. From Mean E (psi x 10^6)	Avg. Strain at Ult. Stress (μ-in./in.)	Avg. Dev. From Mean Strain (μ-in./in.)	No. of Specimens Tested
4	31.0	1150	97(8.4%)[b]	2.10	0.46(21.8%)[b]	513	96(18.7%)[a]	3
48	2.7	1160	89(7.7%)	2.28	0.44(19.3%)	500	53(10.6%)	3
95	1.3	1110	56(5.0%)	2.32	0.93(40%)	543	142(26.2%)	3
190	0.70	1170	82(8.2%)	2.51	0.43(17.1%)	417	56(13.4%)	3
285	0.49	1150	141(12.2%)	2.33	0.33(14.2%)	493	96(19.5%)	3
400	0.38	1310	177(13.5%)	2.44	0.31(12.7%)	560	80(14.3%)	3
750	0.20	1350	168(12.4%)	2.84	0.66(23.2%)	507	149(29.3%)	3
5000	0.033	1470	80(5.4%)	1.72	0.03(1.7%)	685	70(10.2%)	4

[a] Time required to load from zero to ultimate load.
[b] Average percent deviation from mean = (avg. dev. from mean)/(mean) x 100.

TABLE 6

DYNAMIC TENSILE PROPERTIES, DYNAMIC IMPACT TEST

Specimen No.	Rise Time (μ-sec)	Mass Density (slugs/ft³)	Seismic Velocity (ft/sec)	Critical Fracture Strain (μ-in./in.)	Dev. From Mean Fracture Strains (μ-in./in.)	Fracture Stress (psi)	Dev. From Mean (psi)	Dynamic Modulus (psi x 10^6)	Dev. From Mean (psi x 10^6)
1	60	4.33	9680	—[a]	—	—	—	3.90	1.01
2	80	3.48	9350	1100	50	2320	520	2.11	0.78
3	80	3.88	9540	1250	200	3060	220	2.45	0.44
4	—	3.86	9440	—	—	—	—	2.38	0.51
5	80	3.92	9710	1100	50	2830	10	2.56	0.33
6	60	3.94	10930	950	100	3100	260	3.28	0.39
7	60	4.03	11260	800	250	2850	10	3.55	0.66
8	—	4.31	9320	1000	50	2870	30	2.60	0.29
9	80	3.49	11400	—[b]				3.15	0.26
Avg.				1050[c]	117(11%)[d]	2840[c]	175(6.2%)[d]	2.89(18%)[d]	0.52

[a]Specimen sustained 1200 μ-in./in. strain with no fracture.
[b]Specimen fractured at impact end.
[c]Average of six only.
[d]Average percent deviation from mean (avg. dev. from mean)/(mean) x 100.

transient strain pulse reflected off the free end of the specimen and caused a tensile spall failure. Specimens, 2-in. diameter by 35 in. long, were prepared and cured, and the fundamental frequency of the specimens was determined. One-quarter inch gage length strain gages, two per specimen, were mounted on each specimen. Figure 2 shows a view of the impact projectile and specimen in the testing position; Table 4 gives the details of each tensile test performed.

In the static range, the results are summarized in Table 5. Graphs of ultimate stress, initial modulus of elasticity, and strain at ultimate stress, each versus load rate, are shown in Figures 3 through 5. The dynamic tensile results are given in Table 6.

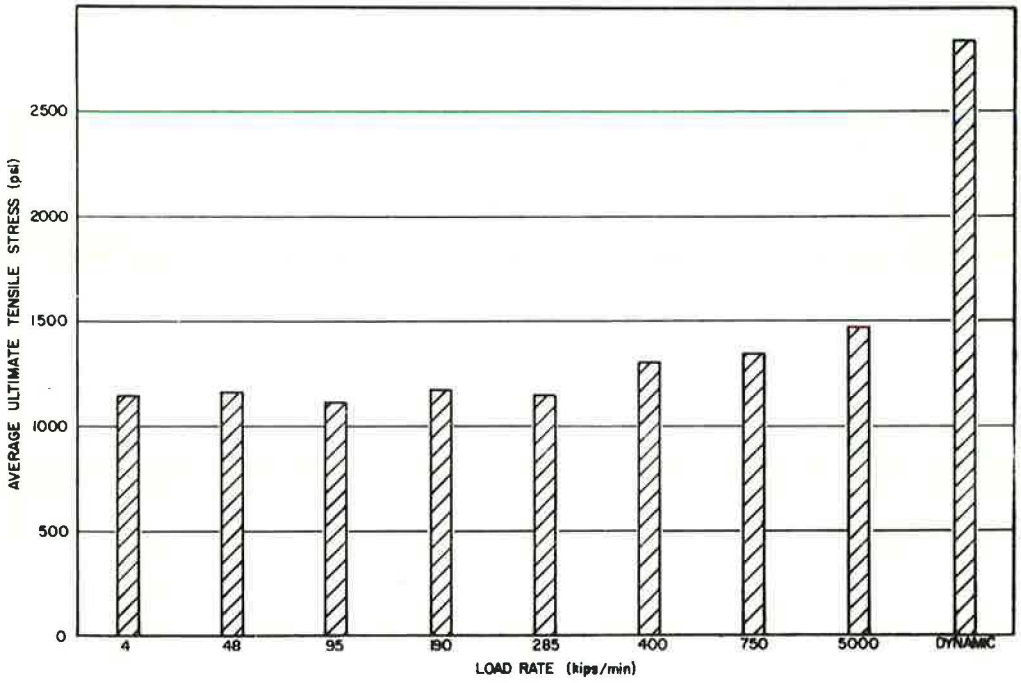

Figure 3. Average ultimate tensile stress vs load rate.

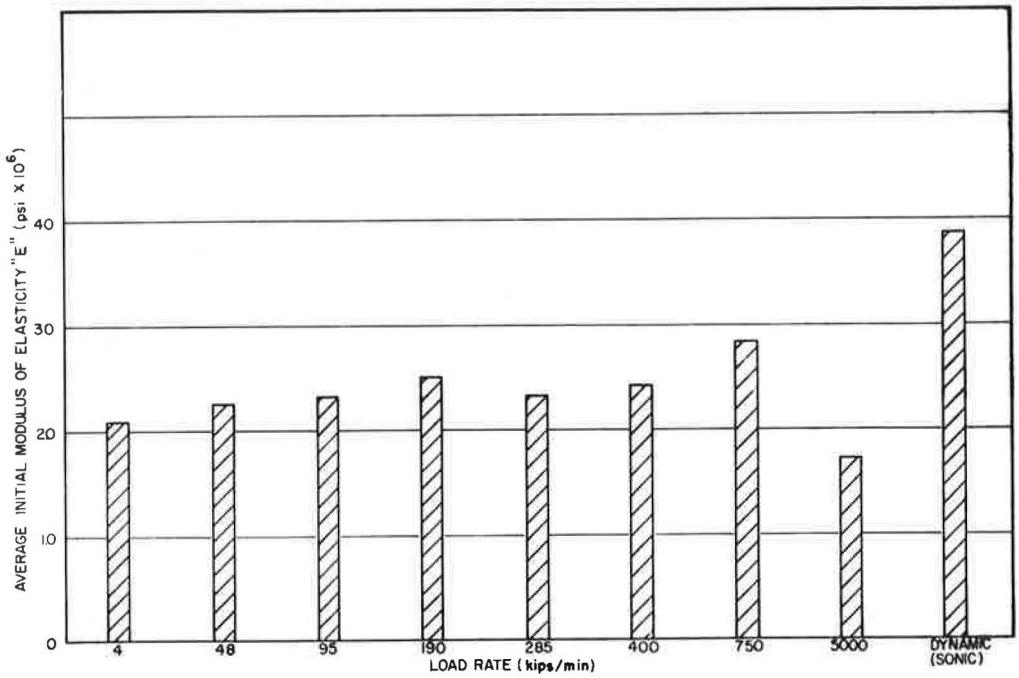

Figure 4. Average initial tensile modulus of elasticity vs load rate.

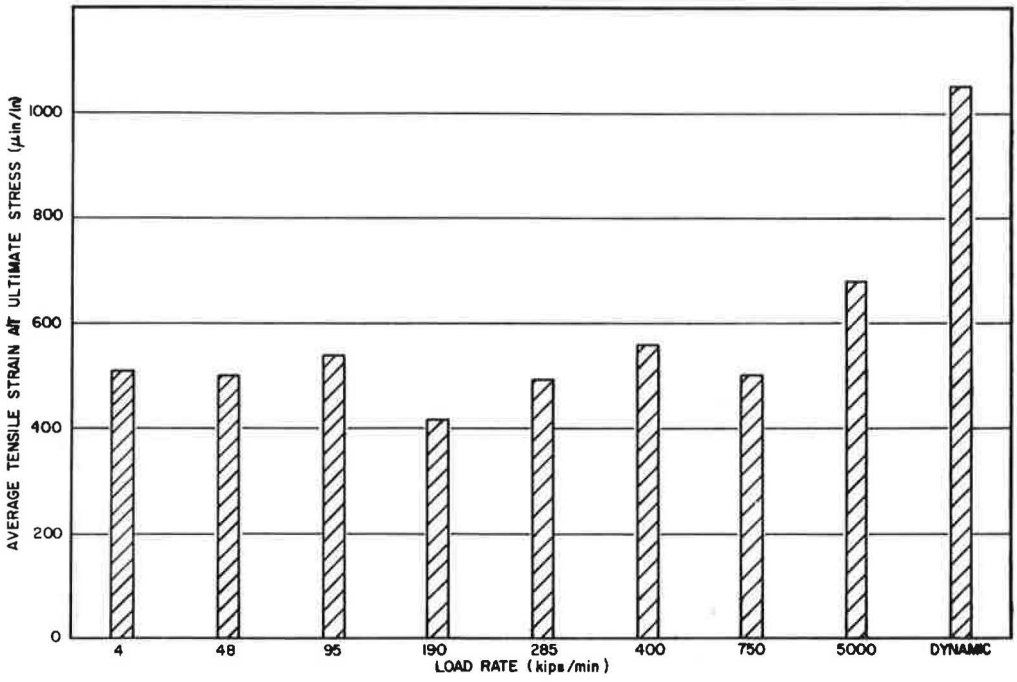

Figure 5. Average tensile strain at ultimate stress vs load rate.

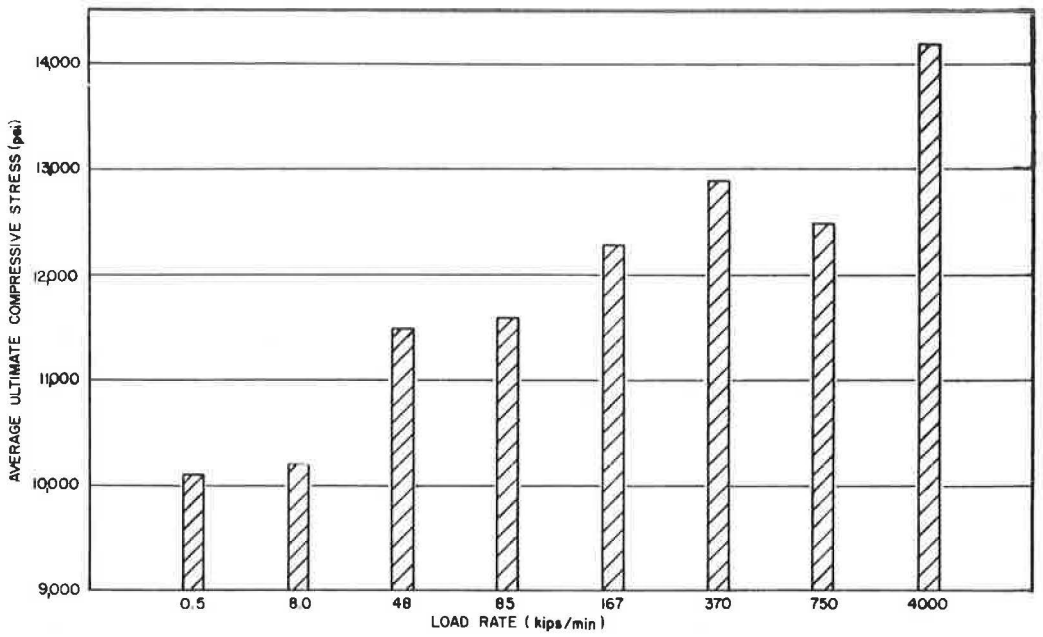

Figure 6. Average ultimate compressive stress vs load rate unconfined compression (6- × 12-in. cylinder).

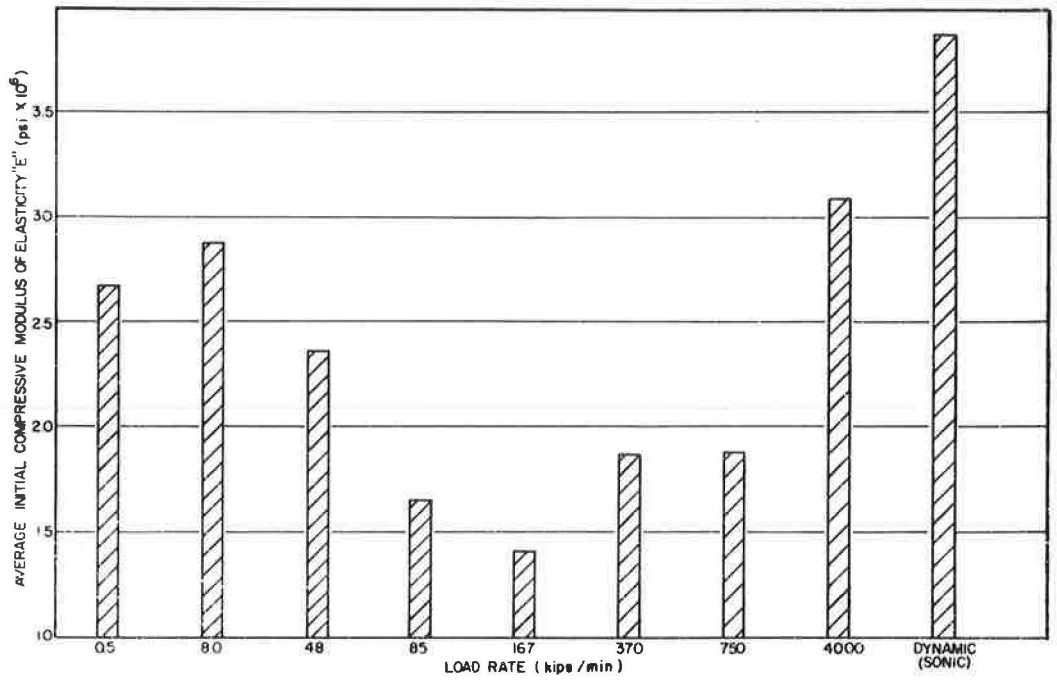

Figure 7. Average initial compressive modulus of elasticity vs load rate unconfined compression (6- × 12-in cylinder).

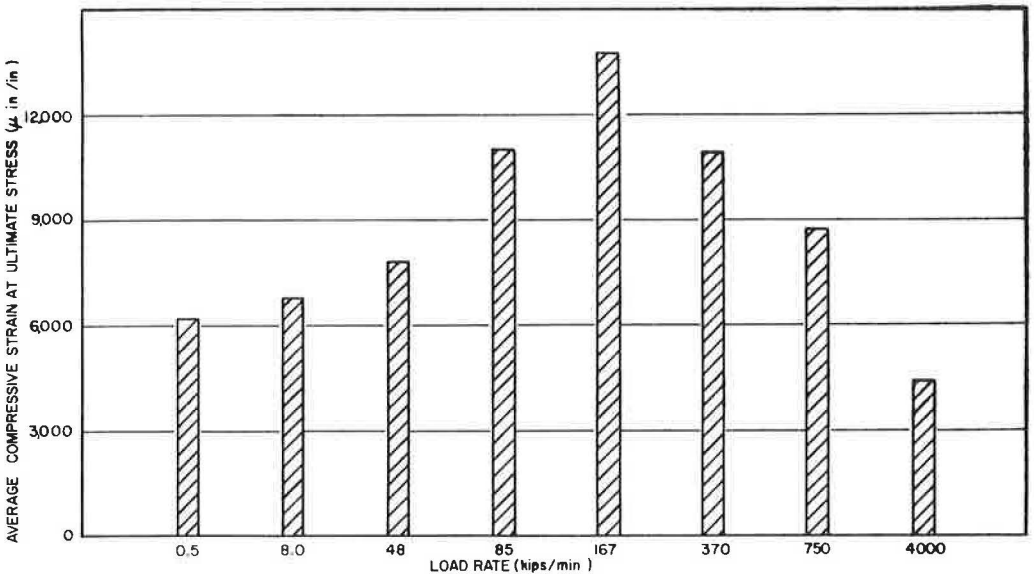

Figure 8. Average compressive strain at ultimate stress vs load rate unconfined compression (6- × 12-cylinder).

Variance of Compressive Load Rate

Static compressive load rates were conducted varying the load rate from 500 lb/min (600-min rise time) to 4,000,000 lb/min (6-sec rise time) on the Baldwin testing machine. The standard, unconfined compression test (ASTM C470) was performed on 6- by 12-in. cylinders. The cylinders were cured and capped with a standard sulfur compound. Data output for the static unconfined compression tests are given in Table 4.

The static compressive test results are summarized in Table 7. Graphs of ultimate stress, initial modulus of elasticity, and strain at ultimate stress, each versus load rate, are shown in Figures 6 to 8.

DISCUSSION

Variance of Tensile Load Rate

A library search was conducted to determine the most feasible method of obtaining the static tensile properties of the system under varying load rate. After careful consideration, the tensile split test (indirect tension test) was chosen because it is easy to perform, yields the most uniform values, and is closer to the true tensile strength than the flexure test. In general, the low to medium static tensile tests indicated little change in the three properties considered. The overall comparison of the static tensile tests did indicate increasing ultimate stress and strain at ultimate stress values with increasing load rate. A decrease in the initial modulus of elasticity was observed with the high static load rate. The high static load rate data were more consistent within the individual load rate group than both the low and medium static load rate data. The overall maximum percent variations for the static tensile properties were 25 percent for the ultimate stress, 40 percent for the initial modulus of elasticity, and 39 percent for the strain at ultimate stress (Table 5). (Overall maximum variation is defined as the difference between the highest value (a) and the lowest value (b) of a particular property for an entire static load range: maximum percent variation = $(a - b \times 100)/a$.)

Since a dynamic impact loader was available and sufficient data had been compiled using portland cement concrete ($\frac{3}{8}$-in. maximum size aggregate) with the loader, it was decided to use the loader to obtain dynamic tensile data for the polyester concrete.

TABLE 7

SUMMARY OF STATIC COMPRESSIVE PROPERTIES UNCONFINED COMPRESSION TEST

Ultimate Stress Index (0.500 kips/min = 1)	Load Rate (kips/min.)	Rise Time (min)	Average Ultimate Stress (psi)	Average Deviation From Mean Stress (psi)	Average Initial Modulus "E" (psi x 10^6)	Average Deviation From Mean "E" (psi x 10^6)	Average Strain at Ultimate Stress (μ-in./in.)	Average Deviation From Mean Strain (μ-in./in.)	No. of Specimens Tested
1	0.5	620	10100	399(3.9%)[a]	2.68	0.23(8.6%)[a]	6260	400(6.4%)[a]	3
1.01	8	36.0	10200	71(0.7%)	2.87	0.08(2.8%)	6860	270(3.9%)	3
1.14	48	6.8	11500	210(1.8%)	2.37	0.07(3.0%)	7920	390(4.9%)	3
1.15	85	3.9	11600	140(1.2%)	1.66	0.16(9.6%)	11000	980(8.8%)	3
1.22	167	2.1	12300	250(2.0%)	1.41	0.00(0.0%)	13750	1250(9.1%)	2
1.28	370	1.0	12900	140(1.1%)	1.87	0.17(9.1%)	10970	1640(15.0%)	3
1.24	750	0.48	12500	530(4.2%)	1.89	0.10(5.3%)	8750	0(0.0%)	3-ult. stress 2-E, strain[b]
1.41	4000	0.10	14200	—[c]	3.10	0.10(3.2%)	4400	300(6.8%)	7-ult. stress 4-E, strain[d]

[a] Average percent deviation from mean = (avg. dev. from mean)/(mean) x 100.
[b] Three specimens used from ultimate stress but only 2 recorded E, strain.
[c] Specimens failed at or near limit of testing machine.
[d] Seven specimens used for ultimate stress but only 4 recorded E, strain.

TABLE 8

TENSILE VARIATION OF LOAD RATE OVERALL COMPARISON OF STATIC AND DYNAMIC PROPERTIES

Type Test	Rise Time (min)	Ultimate Stress Avg. Values (psi)	Ultimate Stress Deviation From Mean, Avg. (psi)	Initial Modulus of Elasticity Avg. Values (psi x 10^6)	Initial Modulus Deviation From Mean, Avg. (psi x 10^6)	Strain at Ultimate Stress Avg. Values (μ-in./in.)	Strain at Ultimate Stress Deviation From Mean, Avg. (μ-in./in.)
Static: Low	31.0	1150	97(8.4%)[a]	2.10	0.46(21.8%)[a]	513	96(18.7%)[a]
Static: Medium	2.7 to 0.20	1110 1350	(5%) (13.5%)	2.28 2.84	(12.7%) (40.0%)	417 560	(10.6%) (29.3%)
Static: High	0.033	1470	80(5.4%)	1.72	0.03(1.7%)	685	70(10.2%)
Dynamic:	1×10^{-6} to 1.33×10^{-8}	2840	175(6.2%)	Dynamic modulus $^3/_8$-in. max. agg. 2.89 ($^3/_4$-in. max. agg. 3.87)[b]	0.52(18%) (0.6%)[c]	1050	117(11%)

[a] Average percent deviation from mean = (avg. dev. from mean)/(mean) x 100.
[b] The $^3/_4$-in. max. agg. specimens (6- x 12-in. cyl.) were not tested in dynamic impact.
[c] The 0.6 percent indicates the average percent deviation for the fundamental frequency of the 6- x 12-in. cylinder.

The results of the dynamic tensile impact test indicated, with reasonable certainty, values of approximately twice the ultimate stress and strain at ultimate stress of the static tensile figures. The average percent deviation from the mean for both the dynamic and static tensile tests were of the same magnitude (Table 8), illustrating the significant scatter of data in the tensile phase of the system. (The average deviation from the mean was obtained by summing the absolute values of the differences between the individual test values and the average for that particular load rate group and then dividing by the number of specimens tested. The average percent deviation from the mean equals the average deviation from the mean divided by the mean, the quantity times 100.)

Inasmuch as eight specimens were tested at the one dynamic load, the dynamic data may be considered as more conclusive than data for any of the individual static load rate groups, which had only three of four specimens per group.

When comparing the overall static and dynamic tensile properties, several pertinent variances were observed. Increasing load rate caused increasing ultimate stress and strain values. As anticipated, the dynamic modulus (sonic value) $^3/_4$-in. maximum size aggregate was larger than any of the static initial moduli.

In this comparison, it should be realized that for portland cement concrete, the tensile split strength is about 1.3 to 1.5 times the true axial tensile strength. It should also be noted that the dynamic impact test is not monotonic, i.e., uniformly increasing load rate until failure. The test consists of a transient pulse which is built up suddenly under impact and is confined within the specimen until failure occurs. Since the impact specimen's test section (length where fracture can occur) is relatively short compared to the total specimen length, the dynamic strength values will probably be greater than the true dynamic values. Thus, the longer is the test section, the more likely there will be a material flaw, and hence, failure will occur. Another consideration in comparing the static to the dynamic results is that two different mixes were used. It is felt that the $^3/_8$-in. maximum size aggregate mix used in the dynamic tests was stronger than the $^3/_4$-in. mix used in the static tests. With the larger aggregate, there was less homogeneity, allowing greater chance for stress concentration around the larger aggregate.

With the preceding discussion in mind, the dynamic impact ultimate stresses and strains are probably closer to a 3:1 ratio than to the true axial static values. Table 8 summarizes the static and dynamic tensile properties.

Variance of Compressive Load Rate

The standard static unconfined compression test (6- by 12-in. cylinder) was chosen since it was easy to perform and widely accepted. In general, the properties of the compressive phase were significantly affected by variance of load rate; the most evident being that increasing load rate meant increasing ultimate stress. Little deviation from the mean was noticed within each individual load rate group (Table 7).

The comprarison of the very low static load rate of 500 lb/min with the low static rate of 8000 lb/min showed little variation in properties. Overall increasing load rate caused a significant increase in ultimate stress. In general, higher initial moduli were associated with lower ultimate strain, with the low and high load rates showing the larger initial moduli. As the load rate was increased, the values of the static initial moduli approached the value of the dynamic (sonic) modulus.

The overall maximum percent variation for the static compressive properties was 29 percent for the ultimate stress, 55 percent for the initial modulus of elasticity and 68 percent for the strain at ultimate stress.

Comparison of Tensile and Compressive Properties

Comparing the overall maximum percent variation of the static properties revealed greater variation in compression than in tension.

1. Ultimate stress—the tensile variation was slightly less than the compressive variation;

TABLE 9

OVERALL COMPARISON OF TENSILE AND COMPRESSIVE PROPERTIES

Type Test	Phase	Rise Time (min)	Ult. Stress Avg. Values (psi)	Strain at Ult. Stress (μ-in./in.)	Initial Mod. of Elasticity x 10^6 (psi)
Static, tensile split—low	1	31.0	1150	513	2.10
Static, tensile split—medium	1	2.7 to 0.20	≥1110 ≤1350	≥417 ≤560	≥2.28 ≤2.84
Static, tensile split—high	1	0.033	1470	685	1.72
Dynamic impact test	1	1×10^{-6} to 1.33×10^{-6}	2840	1050	$\frac{3}{8}$-in. max. size agg. -2.89 $\frac{3}{4}$-in. max. size agg. -3.87
Static unconfined compression—low	2	600 to 36.0	≥10100 ≤10200	≥6260 ≤6860	2.68 2.87
Static unconfined compression—medium	2	6.8 to 0.48	≥11500 ≤12500	≥7920 ≤13750	≥1.41 ≤2.37
Static unconfined compression—high	2	0.10	14200	4400	3.10

2. Initial modulus—the tensile variation was approximately three-fourths the compressive variation; and
3. Strain at ultimate stress—the tensile variation was slightly greater than one-half the compressive variation.

The system had a significantly larger scatter of data in tension (within each individual load rate group) than in compression. The average percent deviation from the mean figures for tension and compression in Tables 7 and 8 indicates that the tensile scatter is larger. The dynamic tensile scatter approximates the static tensile scatter (Table 8), thus supporting the higher scatter of data of the system in tension. Hence, the argument that the larger scatter of tensile data was due to test difference (tensile split versus unconfined compression) is probably not valid.

In both tension and compression, increasing load rate indicated higher ultimate strengths in about the same proportions. The static ultimate compressive strength values were about 9 to 10.5 times the static tensile split ultimate strength values, using comparable load rates (Table 9). It should be noted, however, that for standard portland cement concrete the tensile split values are about 1.3 to 1.5 times the true axial values. Hence the ultimate static compressive strengths are about 12.5 to 14.5 times the true, static, axial, ultimate tensile strengths.

CONCLUSIONS

1. Variance of load rate significantly affected the three engineering properties in both tension and compression.
2. Increasing load rate indicated increasing strength of the system in both tension and compression.
3. The system's properties within individual load rate groups were not as consistent in tension as in compression.
4. The overall maximum percent variation for the three individual static properties considered was greater in compression than in tension.
5. Increasing load rate indicated higher ultimate tensile strains.
6. Little change of the properties was observed in the low to medium static tensile range.

7. Low static compressive strengths were approximately 10,000 psi with no decrease in ultimate strength or strain when changing the rate of loading from 8000 lb/min to 500 lb/min.

These conclusions indicate the feasibility of the polyester concrete system in applications requiring a very high tensile and compressive strength, quick setting and curing time, and excellent freeze-thaw weathering and chemical resistance. The system will withstand both slow and fast static loading conditions in tension and compression.

RECOMMENDATIONS

1. The polyester concrete system exhibited compressive strengths of at least 10,000 psi. This strength indicates the potential of the system for use as a high-strength structural concrete. Many structural concrete applications require a resistance to slow permanent deformation under constant long-term static loading (creep). It is therefore recommended that this system be evaluated with respect to creep. The system could be statically loaded in compression to some percentage of its ultimate load capacity and the deformation of the system observed with time.
2. Although the tensile split test values do serve as an indication of the flexural strength of the system, it is felt that the effect of load rate variance on the flexural properties of the system should be investigated.
3. If the system is to be subjected to repeated loading, the effect of cyclic loading should be investigated.
4. The high-strength bonding characteristics of the system indicate excellent compatibility with both conventional and fibrous reinforcement. The characteristics of such composite systems, including effect of load rate variance, should be investigated.
5. Optimization of the desired properties of the plain or composite systems should be investigated. These should include: type of binder; aggregate type, shape, and gradation; binder-aggregate ratio; and reduction of rigidity mismatch between aggregate and binder slurry.

ACKNOWLEDGMENTS

The author wishes to acknowledge the U.S. Army, Corps of Engineers, Ohio River Division Laboratories, Mariemont, Ohio, for their complete sponsorship of this paper. All original testing, analysis, and publication were performed at the ORD Laboratories.

REFERENCES

1. Timms, Albert G. Concrete Strength. Modern Concrete, Jan. 1957.
2. Mitchell, Neil B., Jr. The Indirect Tension Test for Concrete. Materials Research and Standards, ASTM, Vol. 1, No. 10, Oct. 1961.
3. Thaulow, Sven. Tensile Splitting Test and High-Strength Concrete Test. Jour. ACI, Jan. 1957.
4. Mellinger, F. M., and Birkimer, D. L. Measurements of Stress and Strain on Cylindrical Test Specimens of Rock and Concrete Under Impact Loading. Tech. Report No. 4-46, Department of the Army, Ohio River Division Laboratories, Corps of Engineers, April 1966.
5. Knab, Lawrence I. The Effect of Load Rate Variance on the Engineering Properties of a Plain Polyester Concrete System. B.S. thesis, University of Cincinnati, May 1968.

Atmospheric Corrosion Tests of Unpainted Steels for Use in Construction of Highway Bridges

BRUCE COSABOOM and GEORGE S. KOZLOV,
New Jersey Department of Transportation; and
JAMES ZOCCOLA, Bethlehem Steel Corporation

A 1967 paper on atmospheric corrosion tests of low-alloy steels and the applicability of the test results to highway bridges concluded that further testing and research were necessary in order to clarify certain concepts. Since then, the New Jersey Department of Transportation and the Bethlehem Steel Corporation have jointly undertaken the development and implementation of corrosion tests of unpainted steels. This paper is a preliminary report on the corrosion tests and includes no data results, and therefore no formal conclusions, as yet. These tests, conducted in the industrial atmosphere of Newark, New Jersey, are intended to provide data that will aid in determining the effect of road salt spray and local corrosion factors, as well as in establishing time-corrosion curves. Rust-staining of adjacent materials (i.e., concrete bridge abutments and columns) is also accounted for in the test program.

Because of the many difficulties encountered in the procedure originally proposed, the program does not account for such concepts as stress corrosion effects, cyclic load on corrosion rate, reduction in fatigue strength, and loss of tensile strength due to corrosion. Details of the complete test program in progress are given.

•AN earlier study (1) led the New Jersey Department of Transportation to the conclusion that an atmospheric corrosion test program should be undertaken in order to study certain factors that may influence the corrosion rates of unprotected steels. Since then, this test program has been developed and undertaken jointly by the Department and Bethlehem Steel Corporation.

The purpose of the program is essentially twofold: to provide information about corrosion effects on steels for use on unpainted highway bridges, and to afford a means of correlation between the current ASTM method of atmospheric corrosion testing and the corrosion tests discussed in this paper.

In the previous report many concepts involving the corrosion of metals were studied. It was concluded that further research was necessary on the following factors:

1. t_x = the number of years of exposure required for the time corrosion curve to become essentially linear;
2. The depth of corrosion penetration into an exposed surface after t_x years;
3. The corrosion rate after t_x years;
4. The "exposure factor", a design factor that would account for the relative severity of various steel exposure conditions;

Paper sponsored by Committee on Metals in Highway Structures and presented at the 48th Annual Meeting.

5. The "pitting factor", a design factor that would account for the effect of pitting on the strength of construction steels;
6. The degree of reproducibility of results;
7. The effect of static loads on the corrosion rate;
8. The effect of cyclic loads on the corrosion rate;
9. The effect of prior corrosion on static and dynamic strength;
10. The possible effect of corrosion-fatigue and stress corrosion;
11. The effect of "other factors", i.e., different environments, submersion in water, effects of welding;
12. The appearance of rusted steel; and
13. The rust-staining of adjacent surfaces.

Many difficulties were encountered in developing the proposed testing procedures. It is for this reason that the program adopted had to be limited in scope and that it will not account for such factors as effects of stress corrosion, cyclic load on corrosion rate, and reduction in fatigue and tensile strength due to corrosion and pitting (pitting factor).

The actual program adopted jointly by the New Jersey Department of Transportation and Bethlehem Steel Corporation consists of the following:

1. Corrosion tests for sample panels of steel exposed in different locations and positions;
2. Periodical and occasional visual inspections of the bridge members of an experimental unpainted bridge; and
3. A visual survey and/or photographic record of the bridge steel and concrete supports, and a visual survey of other unpainted and painted bridges.

The experimental unpainted bridge referred to is constructed of Mayari-R low-alloy steel, which is produced by the Bethlehem Steel Corporation.

PHOTOGRAPHIC RECORDS OF BRIDGE STEEL AND CONCRETE SUPPORTS

Photographs of the experimental bridge with sample panels for corrosion tests mounted on the bridge beams are shown in Figures 1, 2, and 3. The photographs were

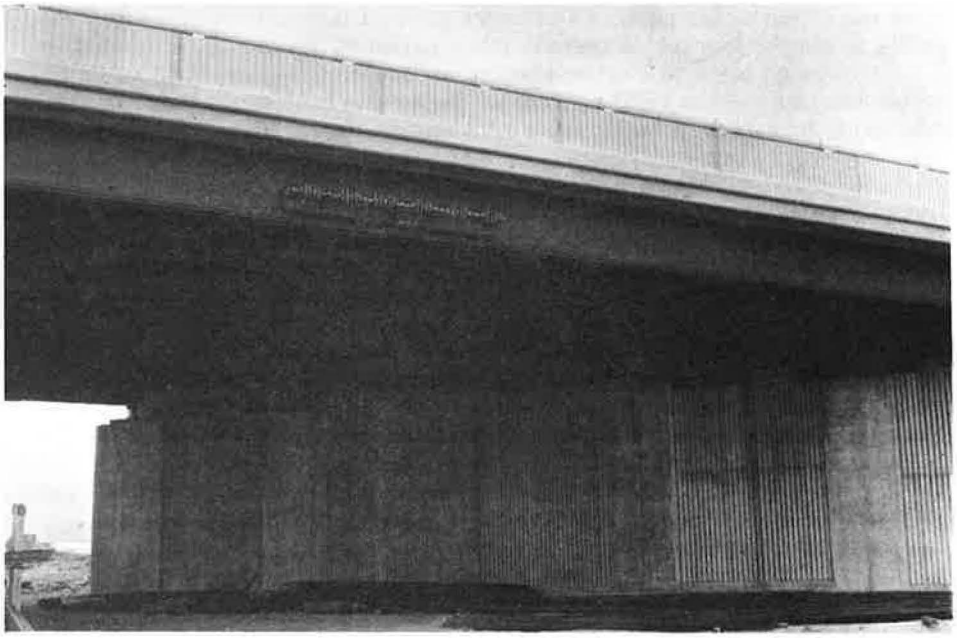

Figure 1. Bridge 9 showing location of test specimens.

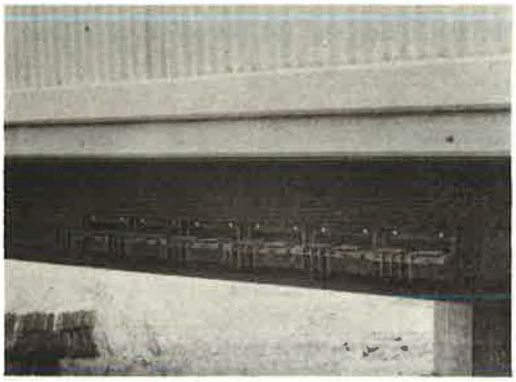

Figure 2. Sample panels mounted on bridge beam.

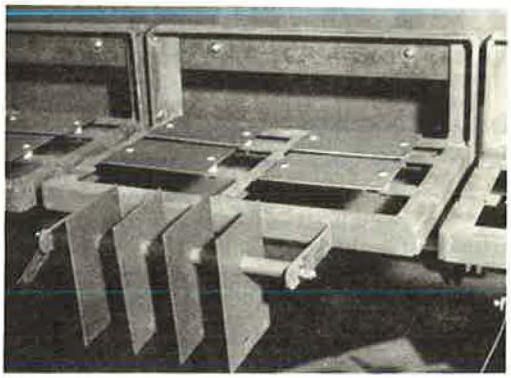

Figure 3. Mounting rack with specimens.

taken approximately 1 year after the bridge steel erection; some rust staining of the concrete abutments has appeared. The concrete had already received one chemical treatment to remove rust stains in June 1967, just after the bridge steel erection (April 1967); however, no stain-preventing measures had originally been undertaken on any parts of the bridge; i. e., the concrete had been unprotected. Additional chemical treatment of the same type is planned for the concrete abutments. The cleaning product used is a blended inhibited acidic cleaner with a penetrant. It consists of a number of compounds including sodium thiosulfate. It should be noted that this chemical treatment is a cleaning process and not a protective device for the concrete. The rust staining at the bridge is expected to diminish with time of exposure. Eventually it may reach a point at which rust staining of the concrete is no longer a problem and cleaning maintenance can be eliminated.

CORROSION TESTS

Purpose

Exposed metal sample panels are mounted at two sites and in various positions. The exposure sites were chosen for purposes of correlation of the various corrosion results with the results of similar corrosion tests in other areas of the nation. It is also intended that the corrosion tests will allow a better estimate of the time-corrosion curve of the unpainted steel and of the local "corrosion factors". Both exposure sites are in the area of Newark, New Jersey, which has an industrial atmosphere.

Scope

At the time of mounting, the surface conditions were the same for all sample panels, i.e., clean and free of all foreign matter. This was accomplished through gritblasting and a degreasing treatment. The specimens of steel are being exposed for specific periods of 1 to 16 years, and were first mounted on specific dates in May 1968. Upon removal of specimens, the weight loss due to corrosion will be evaluated and this value will be used to determine the time-corrosion curve of the unpainted steel and local corrosion conditions. The weight loss will be transformed into an average thickness loss, which is, of course, actually a loss in cross-sectional area of the specimens.

Comparison of corrosion results on these specimens will provide information on local exposure conditions. If there is nonuniform corrosion on the specimen surfaces—that is, if pitting occurs to a significant extent—then the degree of pitting and perhaps the pit depth should be recorded and evaluated.

Materials

The specimens are rolled sheet metals made of five different materials as follows: rolled zinc, plain carbon steel, Mayari-R (ASTM A-242), Mayari R-50 (ASTM A-588-Grade B), and copper-bearing steel. A percent-composition analysis is given in Table 1.

TABLE 1

TEST MATERIALS WITH CHEMICAL ANALYSIS AND CODE NUMBERS

Code Number	Material	Analysis, Percent									
		C	Mn	P	S	Si	Ni	Cr	Cu	V	Mo
503	Copper-bearing steel	0.020 0.023	0.34 0.35	0.003 0.006	0.011 0.014	0.01	0.02	0.02	0.21	–	–
504	Mayari R-50 steel	0.13	1.02	0.008	0.018	0.22	0.27	0.64	0.21	0.062	–
506	Mayari-R steel	0.09	0.65	0.11	0.032	0.29	0.66	0.52	0.27	–	0.010
507	Plain carbon steel	0.07	0.35	0.009	0.020	<0.001	0.01	0.02	0.021	–	–
N1747	Rolled zinc	–	–	–	–	–	–	–	–	–	–

Specimen Preparation

The sample panels measure 4 by 6 by $^1/_{10}$ in. with the exception of a few experimental formed-box sections. The specimens were cut from rolled sheets and mounting holes were drilled, after which all edges were machined to remove imperfections from cold-working. The surfaces were thoroughly cleaned by gritblasting and a degreasing treatment to remove all dirt, oil, grease, and other foreign matter. The specimens were identified by code numbers stamped on one surface. After cleaning, the specimens were weighed in grams with an accuracy of four places. The weights were permanently recorded. The Bethlehem Steel Corporation performed the preparation of specimens for mounting.

Specimen Mounting

The specimens were generally mounted in three different positions on the racks. A number of specimens were mounted in the horizontal plane to duplicate the position of the flanges of bridge beams. Similarly, a number of specimens were mounted in the vertical plane to duplicate the position of the webs of bridge beams. A third mounting position was also selected, at 30 deg from the horizontal plane, to conform with the standard ASTM atmospheric corrosion testing procedure.

Although the idea of vertical and horizontal boldly exposed samples was developed jointly, the actual design and manufacturing of the racks was accomplished by Bethlehem Steel research personnel. All materials for racks and specimens were supplied by that company. The installation of the racks and specimens was carried out jointly by Bethlehem Steel and the New Jersey Department of Transportation. During the process of mounting, all specimens were handled with clean white gloves. Thus, the cleanliness of the specimen surfaces at the start was ensured.

As stated previously, two different sites were selected for mounting the specimens. For the sake of clarity, details for mounting the specimens will be handled separately for each site.

Experimental Bridge Installation

The experimental bridge at Newark was constructed as part of the contract for Interstate Route 78; it is not expected to be in operation until 1972. The superstructure consists of Mayari-R steel beams supporting a reinforced concrete deck slab. The steel work was erected April 26 and 27, 1967.

Specimens of Mayari-R and plain carbon steel were mounted on three deck supports made of Mayari-R steel on May 10, 1968. Each rack is in a different location on the bridge beams, as shown in Figure 4. Figures 2 and 3 show the specimens as mounted on the racks. (Note the specimen identification numbers in Figure 3). A total of 144 specimens were mounted: 72 panels are vertical, the other 72 horizontal. Half of the panels in each position are plain carbon steel, the other half are Mayari-R steel. Care

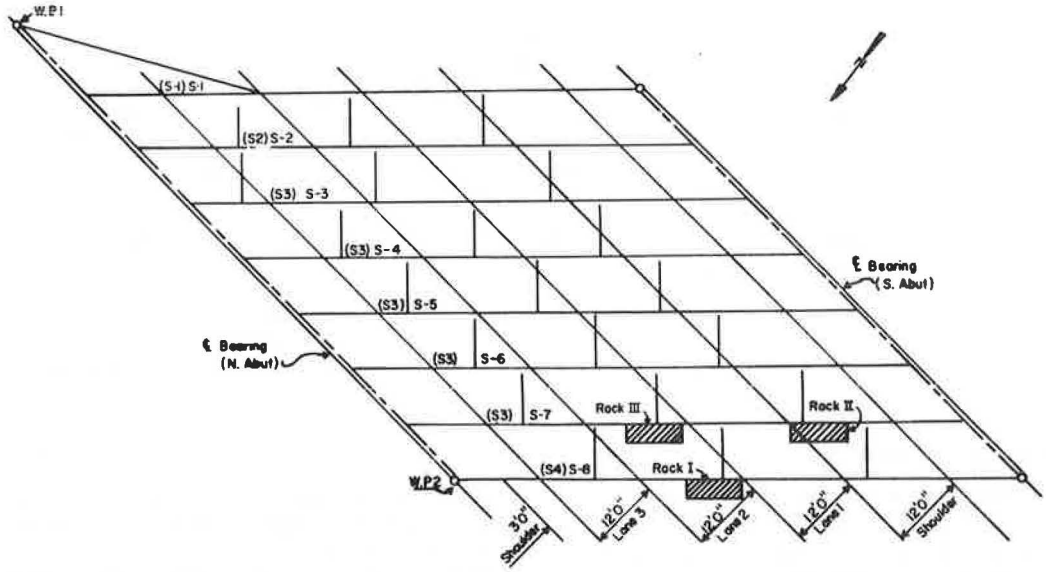

Figure 4. Location of test racks with respect to the bridge stringers.

was taken to ensure that the supports were mounted horizontally, so as to ensure horizontal and vertical positioning of the sample panels, as desired.

As shown in Figures 1 and 4, the group of specimens of Rack I is located on fascia beam (S4) S-8, directly over the central area of the roadway. These specimens are boldly exposed to receive the full effects of rainfall and direct sunlight.

Rack holder II is located on beam (S3) S-7, over the shoulder area of the roadway. This interior position, sheltered from the cleansing effect of rain and slower to dry, will duplicate conditions that have led to increased corrosion of low-alloy steels in other applications. Rack holder II should receive maximum amounts of road salt spray, dirt, fumes, etc., from vehicles passing under the bridge.

Rack holder III is also located on beam (S3) S-7. It is placed over the central area of the roadway and should experience the effects anticipated from a sheltered location. However, it should not receive the maximum amounts of spray from passing vehicles.

Through the selection of these specimen locations on the bridge, the salt-spray effect is designed into the corrosion tests. The test specimens are not specifically located to allow exposure to salt water running off the bridge, as would be experienced at an expansion joint. Due to practical limitations, this specific test is not thought to be feasible.

It is worth noting at this point that these specimens, because of their horizontal and vertical positioning, do not permit direct correlation with standard atmospheric corrosion tests in the literature. To facilitate such correlation, standard specimen orientation was provided at a second installation on the roof of a nearby building. The horizontal and vertical specimen positioning at the bridge site was chosen, as stated before, to duplicate the orientation of the flanges and webs of bridge beams.

Roof Installation

The test rack for the roof installation is located on the roof of a New Jersey Department of Transportation maintenance garage in Newark, very close to the experimental bridge site. The test rack is shown with specimens in Figure 5. Notice that the rack allows for mounting of specimens in vertical and horizontal directions, as well as a position at 30 deg from the horizontal. This is important since most ASTM atmospheric corrosion tests use an incline of 30 deg-from-horizontal as a standard exposure position

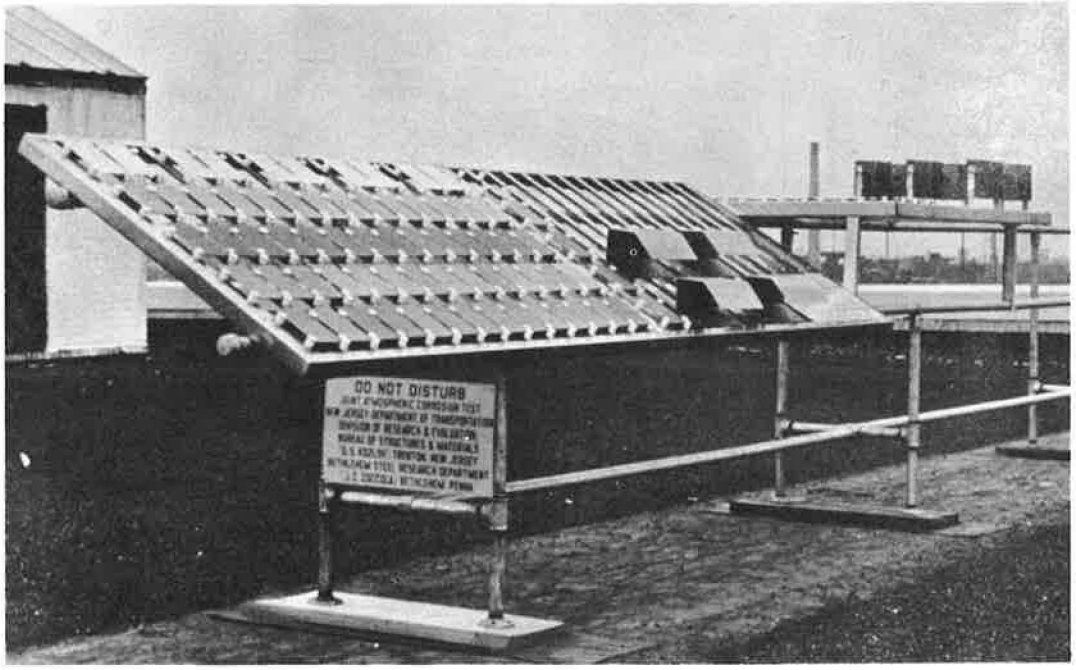

Figure 5. Roof installation of specimens.

for sheet products. The test rack was purposely constructed longer than necessary, to accommodate any possible additional specimens for installation at a later date. The specimens shown in Figure 5 were installed on May 15, 1968.

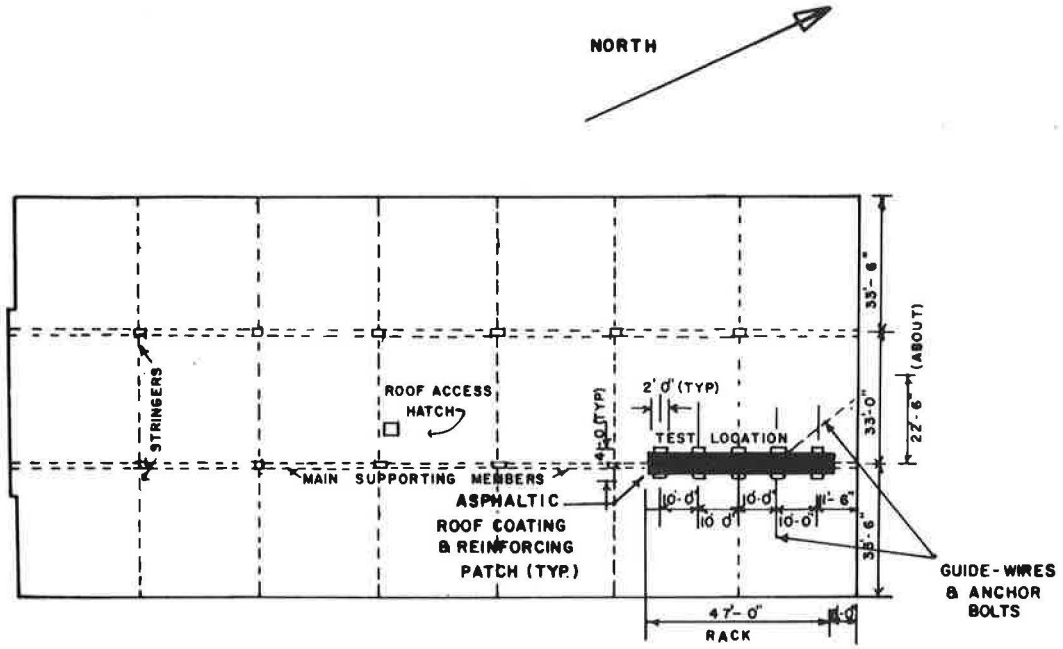

Figure 6. Roof framing plan showing location of test rack.

TABLE 2

SCHEDULE OF INSTALLATION AND REMOVAL OF TEST SPECIMENS

Exposure Site	Material	Specimen Orientation	Installations (Years After Init. Date)[a]	Removals (Years After Init. Date)[a]	No. of Specimens						Total No. of Specimens
					Installed			Removed			
					Hor.	Vert.	30 deg	Hor.	Vert.	30 deg	
Bridge 9 over Route 1-78, Newark, New Jersey	Mayari-R and plain carbon	Vertical and horizontal	Initial date	-	72	72	-	-	-	-	240
			x	-	48	48	-	-	-	-	
				1	-	-	-	12	12	-	
				2	-	-	-	12	12	-	
				4	-	-	-	12	12	-	
				x	-	-	-	12	12	-	
				x + 1	-	-	-	12	12	-	
				x + 2	-	-	-	12	12	-	
				8	-	-	-	12	12	-	
				x + 4	-	-	-	12	12	-	
				x + 8	-	-	-	12	12	-	
				16	-	-	-	12	12	-	
Dept. of Transportation garage roof, Newark, New Jersey	Mayari-R and plain carbon	Vertical and horizontal	Initial date	-	24	24	-	-	-	-	80
			x	-	16	16	-	-	-	-	
				1	-	-	-	4	4	-	
				2	-	-	-	4	4	-	
				4	-	-	-	4	4	-	
				x	-	-	-	4	4	-	
				x + 1	-	-	-	4	4	-	
				x + 2	-	-	-	4	4	-	
				8	-	-	-	4	4	-	
				x + 4	-	-	-	4	4	-	
				x + 8	-	-	-	4	4	-	
				16	-	-	-	4	4	-	
	Mayari-R, plain carbon, Mayari-R-50, Cu-bearing, rolled Zn	30 deg from horizontal	Initial date	-	-	-	70[b]	-	-	-	70[c]
				1	-	-	-	-	-	14	
				2	-	-	-	-	-	14	
				4	-	-	-	-	-	14	
				8	-	-	-	-	-	14	
				16	-	-	-	-	-	14	

[a] The "x" installation and removal will occur after the bridge and highway below the bridge are opened to traffic.
[b] In addition to these panels, small formed box sections are being exposed for appearance of each type of metal.
[c] One of these panels will be held for possible display.

The location of the test rack on the roof (Fig. 6) was dictated by two factors. First, the structural features of the garage require that the rack be aligned over a main supporting member to minimize the effect of the increased load. Second, the location was selected to be as far as possible from any vents or stacks that might emit fumes that would abnormally influence the corrosion rates on any of the specimens. The rack has a northeast-southwest orientation, the specimens facing 10 deg east of south. This deviates slightly from the standard ASTM exposure tests, in which the specimens face due south.

With the mounting of these specimens, two direct correlations will be obtained. First, corrosion rates of the specimens with a 30-deg slope may be correlated with rates of specimens tested elsewhere in the nation according to ASTM methods. Second, corrosion rates of horizontal and vertical specimens may be correlated with rates of specimens on a 30-deg slope. An indirect correlation may then be obtained between horizontal and vertical tests in Newark and standard ASTM corrosion tests anywhere in the nation.

Number and Type of Specimens

The position, type, and number of specimens on each rack at each location have been permanently recorded. The following is a summary of all the specimens to be installed during the 16-year test period:

1. 240 test specimens of Mayari-R and plain carbon steel, arranged vertically and horizontally in sets of 8 specimens, shall be located on the bridge.
2. 80 specimens of Mayari-R and plain carbon steel, arranged vertically and horizontally, shall be located on the garage roof.
3. 70 specimens of Mayari-R, plain carbon, Mayari R-50, copper-bearing, and rolled-zinc materials placed at 30 deg from horizontal, shall be located on the garage roof.

The future placement of additional specimens on the garage roof test area will be a joint decision of the participating organizations.

The foregoing description of test specimens includes the total number of specimens for the 16-year test period. Not all of the specimens have been installed initially. Remaining specimens will be installed at predetermined intervals. A schedule of installations and removal of specimens is given in Table 2. Note that a number of specimens are to be installed when the experimental bridge and the highway below the bridge are opened to traffic. This is to test the salt spray effect on the unpainted steel.

CONCLUDING COMMENTS

At the time of the preparation of this paper, the test program has only been initiated. A few points are, however, worth noting:

1. Cleaning maintenance has been necessary on the concrete bridge abutments because of rust-staining. And, to date, further cleaning will be required although it is not known for how long. On the basis of future results, it may or may not be wise to consider application of a protective covering to adjacent surfaces. Of course, to begin with, the run-off water should be kept away from the piers and abutments, thus preventing staining.
2. Although the specimens were mounted approximately 1 year after the bridge steel erection, and they have only been mounted for a few months, they have already blended very well in color with the bridge steel, which is rustic in appearance.
3. The test program began very well and no special problems are anticipated.

Later progress reports will include test results and data with details of the handling, cleaning, weighing, and examination of the specimens and any other pertinent information.

REFERENCE

1. Division of Research and Evaluation, Bureau of Structures and Materials, State of New Jersey, Department of Transportation. An Analysis of Atmospheric Cor-

rosion Tests on Low-Alloy Steels—Applicability of Test Results to Highway Bridges. Highway Research Record 204, pp. 22-45, 1967.

Discussion

JOHN R. DAESEN, The Galvanizing Institute—We believe the test of unpainted steels by the New Jersey Department of Transportation and Bethlehem Steel Corporation misses its objective, because of the form of test material chosen.

Because the need for evaluation of effect of corrosion on dynamic strength, corrosion fatigue, and stress corrosion is recognized by the present authors, as well as in the 1967 paper, the choice of $\frac{1}{10}$-in. thick rolled sheet to predict performance of structural steel shapes for bridges can hardly be approved. It is well known that surface soundness, structure, and homogeneity strongly influence the effects of corrosion, with or without stress, and these surface conditions are by no means equivalent in $\frac{1}{10}$-in. thick rolled sheet and structural shapes with up to $\frac{3}{4}$-in. thickness of section.

The effect of these differences on pitting effects, if not on general corrosion rate, cannot be disregarded, because local centers of accelerated corrosion are potential stress raisers.

Results of corrosion tests on sheets of comparable compositions in many environments have already been published and compared. The only new values to be obtained in this test are the effect of shading from the sun and rain, and the effect of contaminated spray from the roadway. It is just these conditions that should intensify the effect of surface inhomogeneity or variable structure. The "pitting factor" found in sheet cannot be expected to be representative of the surface of bridge structural members.

We feel, therefore, that the test should have used material from commercial beams for bridges. To meet the needs of weighing, the test samples should be planed down to $\frac{1}{10}$-in. thickness, leaving intact one original commercial surface, as received. The edges and reverse surface could be masked off. After exposure, the simplest of dynamic or fatigue tests on specimens so prepared would be invaluable in demonstrating the advisability of more elaborate tests.

Of less importance, but in the same vein, we suggest that the so-called A 36 plain carbon steel, with 0.07 and carbon, 0.35 manganese, less than 0.001 silicon, and 0.021 percent copper, is not a composition that would develop the strength of the other steels tested, and may well be not representative of the corrosion resistance of plain carbon steel bridge beams.

Similarly, the use of rolled zinc, obviously intended to represent the performance of galvanized steel, is an error that can only mislead. More than half of the thickness of the galvanized coating on such steel as is used for bridges is zinc-iron alloy, with corrosion resistance in unshielded industrial exposure superior (by some 30 to 40 percent) to that of zinc (as reported by me in "Corrosion Resistance of Galvanized Coatings," Second International Congress on Metallic Corrosion, page 699).

Demonstrating the nature and extent of variability of surface structure and corrosion in rolled structural sections, Figures 7, 8, and 9 show irregular attack on a 2 by $\frac{1}{4}$-in. low-alloy steel angle, exposed 10 years in an industrial atmosphere. The steel analyzed 0.08 carbon, 0.39 manganese, 0.125 phosphorus, 0.39 silicon, 0.59 chromium, 0.22 nickel, and 0.33 percent copper. This is typical of the "slow rusting" steels. The bevel at a sawed edge, Figure 7, filed at 30 deg to the corroded surface, indicates the irregularity of attack. The complex nature of the rust layer shown in the "as polished" cross sections, Figures 8 and 9, indicates the importance of structure at the surface in setting up stress-raising pits.

Figures 10, 11, and 12 show massive slabs of "rust" up to $\frac{1}{4}$-in. thick formed on a railway station column built of 6 by 6-in. steel angles "protected" by aluminum paint. The hydrated oxide material is magnetic, but is seen to be entirely nonmetallic, and the structure of the "as polished" cross sections suggests how the progress of corrosion has varied with local differences in structure of the steel, even well below the immediate

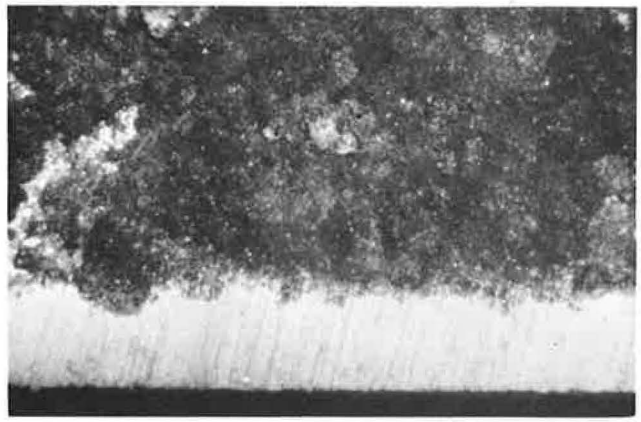

Figure 7. Low-alloy angle, surface, 15X.

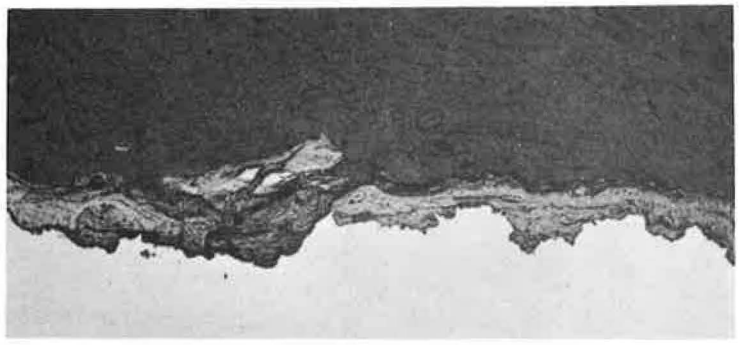

Figure 8. Low-alloy angle, cross section, 100X.

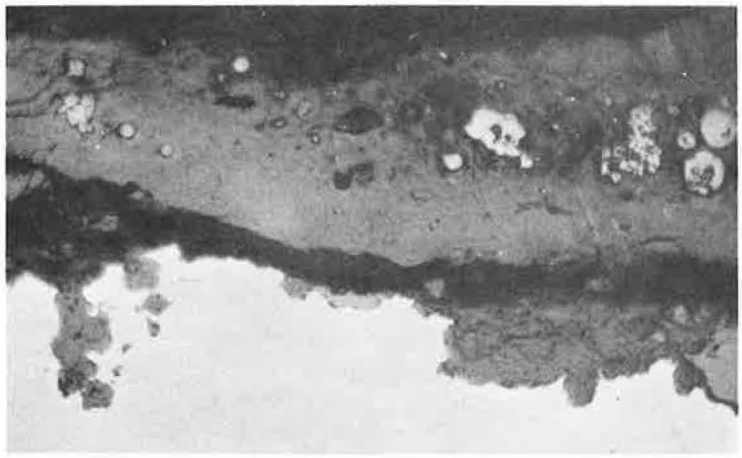

Figure 9. Low-alloy angle, cross section, 500X.

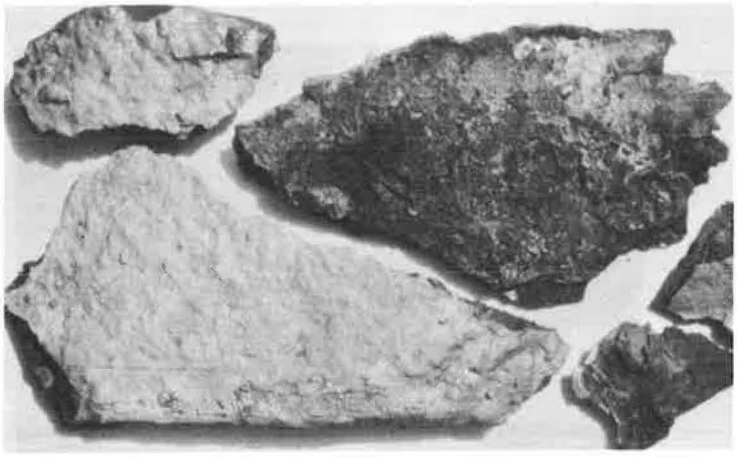

Figure 10. Massive rust buildup; $^{4}/_{5}$ natural size.

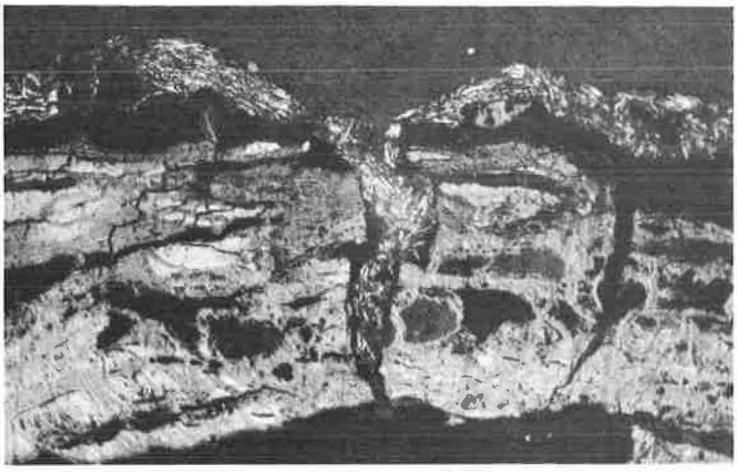

Figure 11. Rusted section at surface, 100X.

Figure 12. Rusted interior section, 100X.

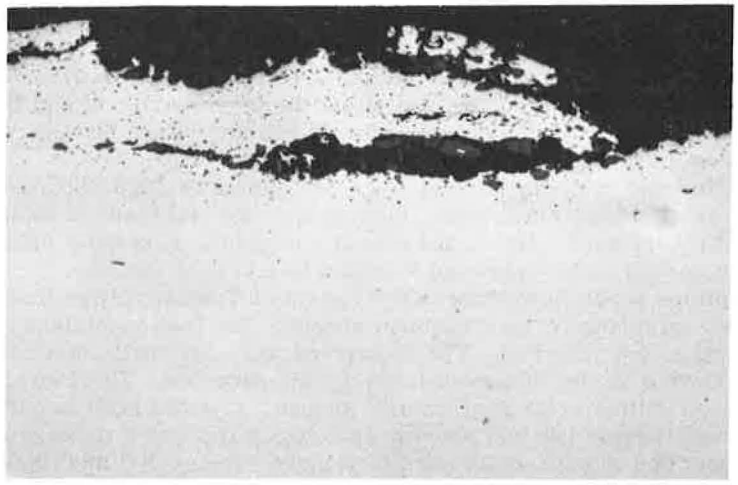

Figure 13. Sliver of 8-in. beam as received, 100X.

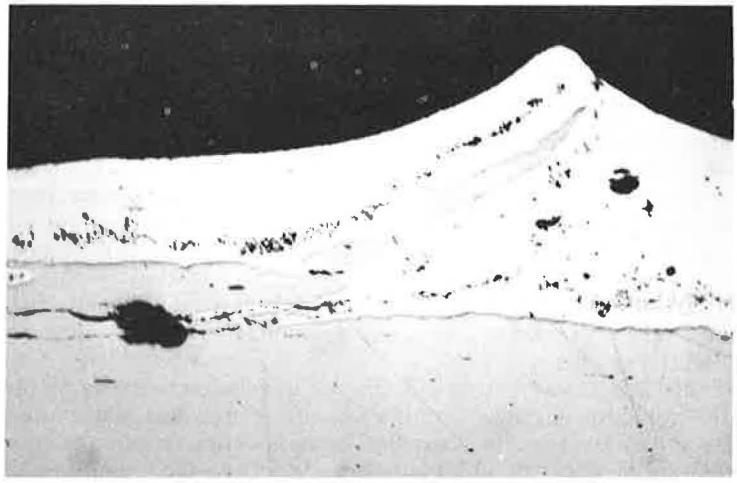

Figure 14. Sliver after galvanizing, 100X.

surface. Such massive rust is not uncommon under paint. This demonstrates that an intact coating of hydrated magnetic oxide can permit continued corrosion to complete destruction.

Finally, Figure 13 shows in cross section a small sliver from the surface of an 8-in. wide flange beam of A 36 plain carbon steel, illustrative of surface defects found in massive sections, and less prevalent in $^{1}/_{16}$-in. thick rolled sheet. Figure 14 shows how molten zinc, in galvanizing, searches out (as corrodents do) these defects, lifting the overlapping steel.

This discussion is offered to suggest the need for more realistic planning of tests that are designed to indicate performance of exposed structures against corrosion, and to urge the New Jersey Department of Transportation to amend their corrosion tests on material under consideration for highway bridges.

BRUCE COSABOOM and GEORGE S. KOZLOV, Closure—It is our opinion that the discussion is, in part, not pertinent, and is generally incorrect.

The discussion directly attacks the material that is being tested as well as the research that is presently being conducted jointly by the Department and Bethlehem Steel. It is our intent to refute certain points of the discussion, while leaving other points to be refuted by Bethlehem Steel.

Daesen states that a $^{1}/_{10}$-in. thick rolled sheet cannot be used to predict performance of structural steel shapes for bridges, making specific reference to factors such as dynamic strength, corrosion fatigue, and stress corrosion. It is quite clearly stated in the paper that the corrosion tests are not intended to test such factors.

It is the opinion of the New Jersey Department of Transportation that the material in these tests is representative of structural shapes. The test specimens actually came from structural shape material. The specimens were originally much thicker, but they were rolled down to $^{1}/_{10}$-in. thickness for weighing purposes. Therefore, the material chosen is indeed the material of structural shapes. In addition, it is our opinion that the surface conditions of the test specimens actually represent those of structural shapes: the specimens were gritblasted to remove surface dirt and imperfections. The low-alloy structural shapes were also gritblasted on the New Jersey experimental bridge, and Bethlehem Steel similarly recommends this process for all low-alloy steel to be used on bridges.

Therefore, it is our opinion that the tests by the Department and Bethlehem Steel do not miss their objective (as the objective is stated in the paper), because of the form of test material chosen. It is our opinion that the information gained concerning the extent of corrosion and pitting for a zero-stress condition will be valuable, accurate, and pertinent.

The Department is interested in low-alloy steel from the user's point of view. We feel that the severe industrial location, in addition to the salt spray and sheltering, as mentioned in the paper, is quite pertinent to our purposes. We also feel that these effects are important to other users of low-alloy steel. Daesen contradicts himself when in one sentence he discredits our research and the next sentence spells out the importance of certain factors; indeed, factors which in our opinion will be accounted for in our tests.

Again, we feel that the surface of our test specimens could hardly be more representative of the surface of bridge structural members. However, this point should be discussed by Bethlehem Steel.

Daesen attacked the use of rolled zinc in our corrosion tests as an obvious intention to represent the performance of galvanized steel. There was and is absolutely no such intention. If we did entertain this idea, then zinc specimens most certainly would have been installed on other racks in other positions, i. e., on the experimental bridge racks. Rather, it should be noted that very few zinc specimens were used; they were installed only at the roof location, and only in the 30-deg slanted position. These specimens are to serve only as a method of correlating the roof site with other ASTM corrosion-test sites.

Daesen refers to the thick rust coating that existed on steel angles "protected" by aluminum paint. He demonstrates that rust commonly exists under paint. We are sure that this piece of information is well known. (We are equally certain that it has nothing to do with our corrosion tests!) Daesen also concluded "that an intact coating of hydrated magnetic oxide can permit continued corrosion to complete destruction"—on regular steel. He has given no information on low-alloy steels. Bethlehem Steel claims that the rust coating on low-alloy steels will protect the underlying steel to a large extent—enough to warrant the unpainted use of such steels. We are aware that severe rusting will continue on regular steel, if allowed. However, Daesen has not shown evidence of such continued deep rusting on the low-alloy steels. He has not given negative or positive evidence concerning the claim of Bethlehem Steel on low-alloy steel. And this is exactly one area in which we believe that our joint corrosion tests will yield valuable information. Where Daesen has used the results of one material to imply something of another

material, we intend to imply nothing, and cautiously obtain results on the material in question.

Daesen demonstrates how molten zinc searches out defects in surfaces of structural steel members. This can hardly be regarded as pertinent to the subject matter.

In summary, we believe that our existing joint corrosion tests are indeed realistic and will yield valuable information. We believe that Daesen's discussion is not pertinent on a few points, and is incorrect on others. We realize that our tests do not account for certain important factors. Unfortunately, we are limited through one cause or another in our ability to carry out additional and extensive research beyond that which exists. However, this does not discredit the existing research, and it is our belief that no amendments are necessary in the material being tested.

JAMES ZOCCOLA, Closure—I concur with the comments made by Kozlov and Cosaboom in rebuttal to Daesen's discussion. The following are some additional aspects that should be mentioned.

The composition, surface, and structure of the weathering steels exposed as $^{1}/_{10}$-in. sheet should be well representative of plate and structurals in regard to their corrosion performance. It is not necessary nor practical in this test to machine down structural plate, mask the edges, or reverse surface. The surface was typical (gritblasted), as were the bridge members, as recommended in order to obtain a uniform, pleasing, weathered appearance.

Daesen's discussion of surface conditions such as laps is not relevant since this type of defect is rather rare and its significance in weathering behavior is questionable. Also, special racks were designed and fabricated to openly expose both top and bottom surfaces. We realize the carbon content is slightly lower than normal in the plain carbon and copper-bearing steels. But it is well known that the carbon content, in the small amounts we are discussing, has no effect on the atmospheric corrosion resistance of the steels.

The pitting behavior will not be disregarded and is to be evaluated, as stated in the paper. However, from our long-term atmospheric studies of the corrosion performance of weathering steels, we do not believe pitting will be significant.

Ultrasonic Testing of Structural Welds

DEXTER A. OLSSON, Bethlehem Steel Corporation

During the past five years Bethlehem Steel Corporation has developed and applied techniques for the ultrasonic testing of butt welds which provides an assurance of weld quality similar to that achieved with radiography. Although there are no revolutionary breakthroughs involved, a number of significant innovations permit a more repeatable weld test than has previously been achieved with ultrasonics. The Bureau of Public Roads has cooperated with Bethlehem Steel Corporation for several years in these developments. They have recently published a training text and have permitted the use of the method in a recent circular memorandum.

•THE ULTRASONIC testing of welds is a much discussed but little used inspection technique, which, in theory, offers significant advantages to both customer and fabricator. Bethlehem Steel Corporation has been using this inspection technique as a production tool for the last five years. Production work has provided the basis for a number of innovations in technique, equipment and inspection philosophy.

In general, this work has been limited to the inspection of full penetration butt welds in plate thicknesses from $^{5}/_{16}$ in. to 5 in.

Since the various innovations are interrelated in a complex manner, we shall arbitrarily discuss them in the order in the test in which they actually occur. Following this we will discuss auxiliary areas, namely calibration devices and defect location aids. For reference purposes the basic ultrasonic weld testing scheme is described in Figure 1.

Conventional pulse echo instrumentation is used. Pulse length controls are set at near maximum values. Transducers of 2.25-mc frequency either $^{1}/_{2}$ by 1 in. or $^{1}/_{2}$ in. square are generally used. Quartz has not been used as a transducer material. All of the common "ceramic" types are utilized.

A search unit wedge design of the type shown in Figure 1 was chosen for two reasons. First, this design permits extremely close approach to the weld bead reinforcement. Second, internal wedge reflections are minimized, permitting interpretation of near defects when testing at high sensitivity. Figure 2 compares internal reflection noise for various angle search unit designs with information on the relative closeness of approach to weld bead reinforcements.

All of the common couplants have been evaluated. Glycerine appears to be the best according to our production experience. Theoretical considerations reinforce this observation. The close acoustical match between lucite and glycerine minimizes spurious propagation caused by surface roughness. The overall efficiency of glycerine as a couplant minimizes transmission efficiency variations caused by surface roughness. It should be emphasized that surface roughness variations have a much greater effect on longitudinal beam testing than on shear wave testing for the same reasons of coupling efficiency. Therefore, angle beam tests of greater reliability can be conducted on rougher surfaces. These couplant effects are a result of transmission efficiencies (Table 1).

Having introduced the sound pulse into the plate adjacent to the weld, the next matter to be considered is the angle at which the sound is propagated through the plate and into

Paper sponsored by Committee on Metals in Highway Structures and presented at the 48th Annual Meeting.

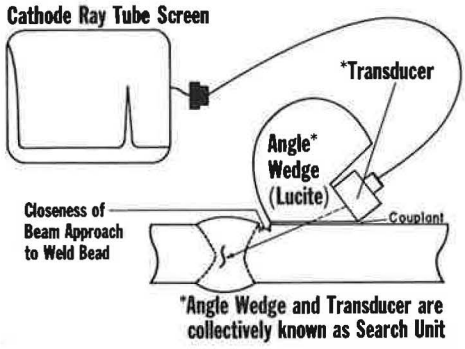

Figure 1. Basic ultrasonic weld testing scheme.

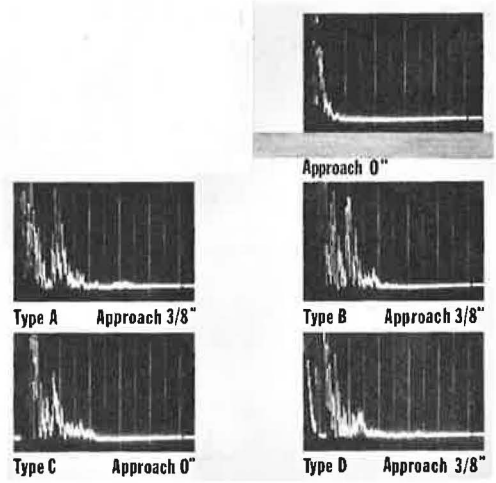

Figure 2. Wedge noise and weld bead approach.

the weld. It is believed that the flattest possible testing angle should be used. The basic reason for this choice is the fact that typical production defects tend to be perpendicular to the plate surface or are associated with weld preparation surfaces. The choice of flatter angles offers several other advantages. First, flatter angles result in more beam spread in the plate thickness. Second, flatter angles permit more of the weld volume to be inspected without resorting to bouncing the sound from the opposite plate surface. This is advantageous since bouncing causes definite errors in defect location (1).

The flattest angle we consider practical for weld inspection is 75 deg. Most tests are limited to 70 deg. Higher angles contain surface wave components which make interpretation difficult or impossible. The angles generally used for particular thicknesses are as follows:

Thickness (in.)	Angle (deg)
1/4 to 2	70
2 to 3	70 or 60
3 to 5	60 or 45
Over 5	45

Steeper angles are used in heavier material for two reasons. The long sound path needed for flatter angles introduces more attenuation into the test than can be easily compensated. Beam spread associated with flatter angles in heavy sections becomes a disadvantage, reducing defect detection reliability.

The phenomenon of mode conversion is quite often discussed with regard to angle choice. Mode conversion is not related specifically to any testing angle but only to the angle of sound incidence upon a reflecting surface. The critical angle of incidence is 30 deg. Therefore, detection of vertical reflectors using a 60-deg angle is questionable. In practice, the only real precaution necessary when using 60 deg is the strict avoidance of plate edges or vertically drilled holes as calibration standards. Actually, 60 deg is a good testing angle because many weld preparations involve 30-deg surfaces, which, as a lack of fusion, are ideally de-

TABLE 1

Transmissivity (single interface)	
Lucite - glycerine	85.85%
Lucite - water	63.05%
Lucite - oil	53.87%
Angle beam testing transmissivity	
(1) Lucite glycerine steel	15.24%
(2) Lucite water steel	7.10%
(3) Lucite oil steel	4.91%
Overall transmission variation with surface variation (a 2% variation from a 10% direct lucite steel coupling condition)	
(4) Lucite glycerine steel (shear)	0.96%
(5) Lucite water steel (shear)	3.65%
(6) Lucite oil steel (shear)	5.39%
(7) Quartz glycerine steel (longitudinal)	12.63%

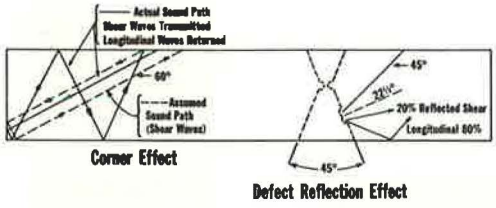

Figure 3. Mode conversion effects.

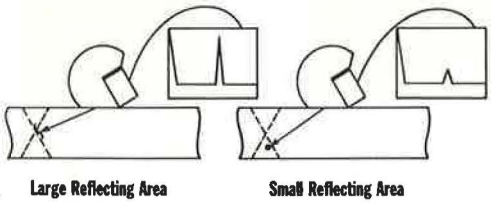

Figure 4. Signal amplitude is a measure of defect reflecting area.

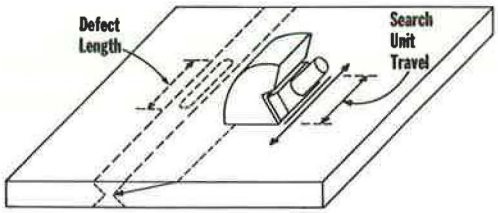

Figure 5. Search unit travel is a measure of defect length.

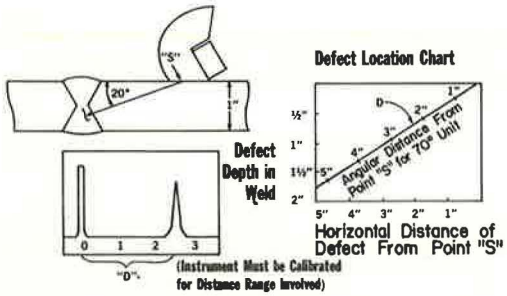

Figure 6. Defect location can be accurately done.

TABLE 2

Defect No.	Angle (deg)	Amplitude (db)	Plate Thickness (in.)	Defect Length (in.)
		(a) Defect Type Porosity		
53	70	7	⅜	2
	60	9		
56	70	7	2	½
	60	6		
	45	Not detected		
		(b) Defect Type Slag		
60	70	8	½	½
	60	10		
61	70	8	½	½
	60	10		
66	70	8	½	1
	60	11		
67	70	8	½	1¼
	60	7		
68	70	7	½	1
	60	8		
85	70	16	1¼	3
	45	10		
49	70	13	⅜	2
	60	15		
50	70	8	⅜	¼
	60	10		
51	70	12	⅜	¾
	60	14		
52	70	19	⅜	2
	60	17		
99	70	8	3	½
	60	13		
	45	Not detected		
100	70	11	3	½
	60	11		
	45	15		
101	70	13	3	½
	60	11		
	45	14		
103	70	8	3	¼
	60	12		
	45	11		
105	70	13	3	1½
	60	18		
	45	8		
		(c) Defect Type Lack of Penetration		
54	70	31	1	5¼
	60	28		
58	70	19	2	12
	60	18		
	45	12		
		(d) Defect Type Cracking		
42	70	18	4½	1⅛
	45	26		
		(e) Defect Type Lack of Fusion		
57	70	19	2	1½
	60	24		
	45	18		
59	70	13	2	2
	60	15		
	45	15		
69	70	28	2	6
	60	16		
	45	26		
70	70	20	1½	4
	60	16		
	45	21		
102	70	21	3	2½
	60	20		
	45	21		
104	70	13	3	3½
	60	17		
	45	13		

tected with 60 deg. By the same token, 45 deg is a poor angle for the detection of lack of fusion for the same reasons. These effects are shown in Figure 3. Some data relating testing angle to defect detection reliability for actual defects are given in Table 2.

When the pulse has traveled to the defect, been reflected and returned through the transducer, it must be interpreted. There are six basic types of information which can

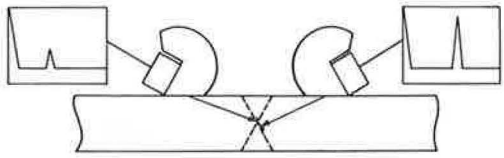

Figure 7. Testing from both sides of weld reveals defect orientation.

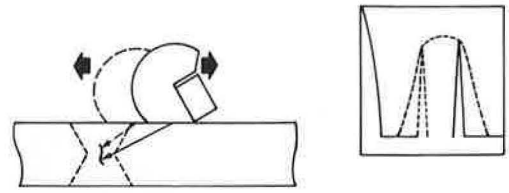

Figure 8. Travel to and from the weld reveals defect height.

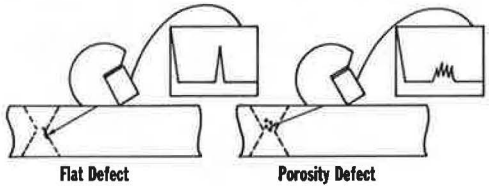

Figure 9. Pulse shape indicates nature of defect.

be extracted. Figures 4 through 9 depict these information types. We feel that the first three types of information are of primary importance in determining defect severity and pinpointing defect location for excavation. The other three types deal with parameters not easily quantified and should not be used as a basis for acceptance or rejection. However, these types of information are of great value to the welding engineer or supervisor who must intelligently correct defective welding conditions.

In order to establish a basis for amplitude rejection, it is necessary to develop data on a great many defects. It was found that conventional methods of test standardization and amplitude read out were not sufficiently accurate. Rather than attempt to judge the height of signals on the screen, an attenuator (or calibrated gain control) was used. The instrument is calibrated on an arbitrary nondirectional reference reflector such as the 1.5-mm hole in the IIW block. Defect amplitude is related to this reference by equating all signal heights to that of the reference using an attenuator. The difference (in db) is now amplitude information. CRT presentation, vertical linearity deviations, and visual error are largely eliminated.

Since CRT linearity limitations are eliminated, the clipping or reject control can now be used, not "to clean up the screen" but to decrease the vertical dynamic range presented on the CRT. This increases the accuracy of amplitude measurement using an attenuator still further.

Using this approach, a great many welding defects were measured, as shown in Figure 10. The attenuation within the material has been corrected by adding 2 db/in. after the first inch of sound travel to all readings. This value was obtained by making a great many readings on various steel thicknesses and reflector types. Figure 11 shows the

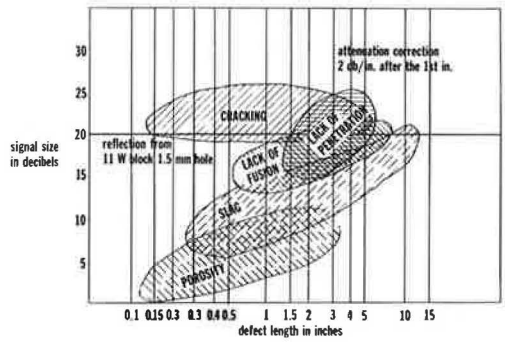

Figure 10. Weld tests at 70 deg: 120 defects—plate thickness $^{5}/_{16}$ in. to 5 in.

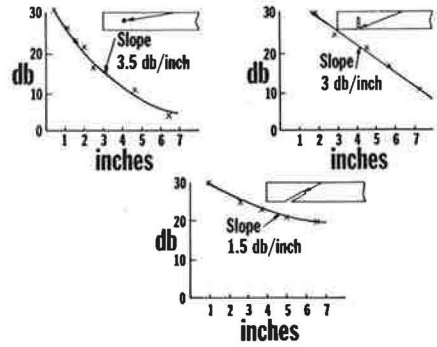

Figure 11. Results of some attenuation tests.

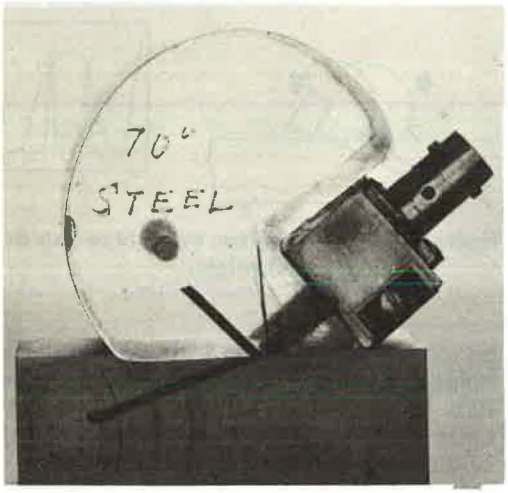

Figure 12. Sensitivity standard.

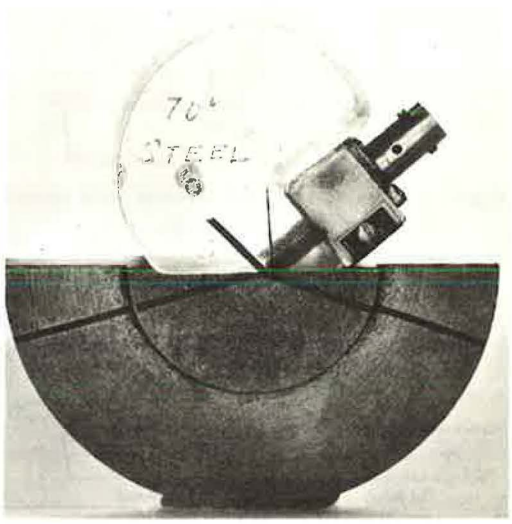

Figure 13. Distance calibration standard for angle beam testing.

results of some of these tests. Increased attenuation is noted close to the search unit for reflectors incorporating the cylindrical surfaces of drilled holes, as compared with flat-bottomed holes drilled at the testing angle. These geometrical effects apply only to cylindrical surfaces and care should be taken not to use such standards for attenuation measurements. In all cases, the attenuation is the slope of the curve.

As was previously stated, the IIW block 1.5-mm hole has been used as a sensitivity standard. Since different angles and resulting different path lengths introduce the geometrical effects, a simple standard, in which the distance to the reflector is 1 in. for 70 deg, 60 deg and 45 deg, has been developed (Fig. 12).

Defect length is measured conventionally based on the point at which a 5-db drop in signal is encountered.

Defect location in cross section is accomplished using conventional geometrical methods. IIW block distance calibration surfaces may be used. We have developed a simple calibration standard for distance which gives calibration pulses at even-inch increments. This standard is shown in Figure 13. We prefer to calibrate for actual sound path length. We feel that the weld inspector is thus made more aware of the geometrics with which he is working. Having thus calibrated, a chart such as Figure 14 can be used for defect location. To further simplify this procedure, we have developed a simple retractable tape (Fig. 15) for each angle

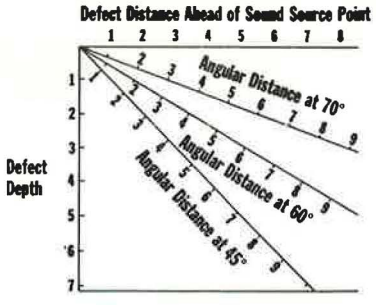

Figure 14. Defect location chart.

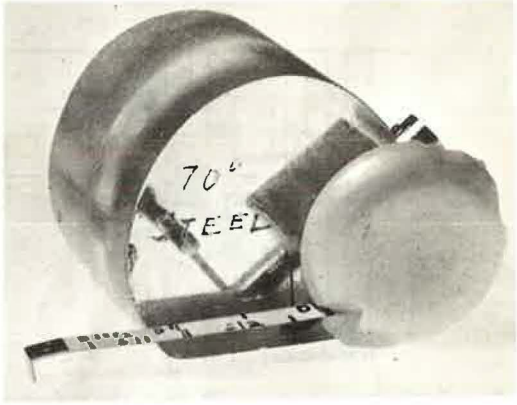

Figure 15. Retractable tape for defect location.

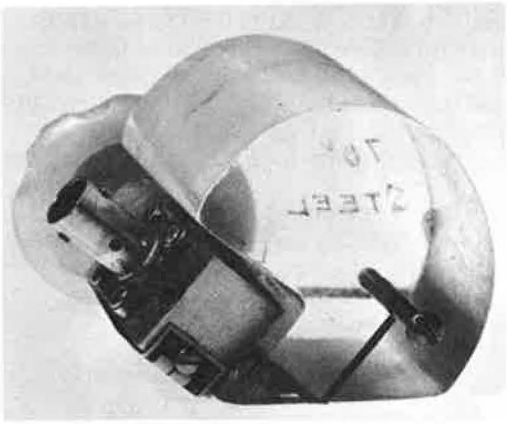

Figure 16. Internally calibrated search unit.

which becomes part of the search unit. The tape is pulled out to the equivalent path length. At this point the defect is directly under the tape end and the defect depth is read from a secondary scale opposite the observed path length dimension.

As mentioned earlier, it is necessary to correct for defect location errors when a bounce from the opposite plate surface is used. For angles greater than 45 deg, a small Δ value must be subtracted from the apparent horizontal dimension (sound emission point to defect). There is no correction at 45 deg. At 60 deg, the correction is about $\frac{1}{8}$ in.; at 70 deg, about $\frac{1}{4}$ in.

One of the pitfalls of ultrasonic weld testing is the fact that the test is not self-calibrating. There is no back reflection or other continual reminder of testing uniformity. Normal shop line voltages and battery-powered unit voltage variations near the end of battery life can cause gradual sensitivity changes which go unnoticed. We use constant voltage transformers and voltage drop alarms to protect us from these effects. In addition, we have developed an internally calibrated search unit (Fig. 16) which provides a continual simple check of amplitude and horizontal calibration stability. A hole is drilled in the wedge so that a small amount of sound reflected from the contact surface will be in turn reflected from the hole. This results in a small discrete signal on the screen which can be used to monitor testing uniformity. The reflector hole is threaded and a screw inserted. Moving the screw changes reflector characteristics slightly. The screw is used to compensate for slight wedge wear.

The nature of the data recorded in Figure 10 makes possible an ultrasonic weld inspection standard based on amplitude and length. Most present weld quality requirements can be interpreted in terms of amplitude and length using such information. The data clearly indicate the factors which lend to ultrasonic weld inspection reliability in detecting the more serious defect types. Radiography has forced on us the necessity of accurate defect identification since generally the most serious defects are most poorly detected. By its nature, ultrasonic testing reflects defect severity directly. Therefore defect identification becomes much less important:

Defect Type	Defect Severity	Radiographic Sensitivity	Ultrasonic Sensitivity
Crack	↑	↓	↑
Lack of fusion			
Lack of penetration			
Slag			
Porosity			

The most important part of the weld testing system is the inspector. Use of amplitude and length rejection criteria has removed from him the onus of defect decisions based purely on subjective observations. However, he must still have a detailed knowledge of ultrasonics and must be capable of working easily with complicated situations in three-dimensional geometry.

We give each of our weld inspectors a four- to five-week classroom course to this end. We have generally drawn on groups of radiographers qualified to 250-1500 or on experienced draftsmen for our personnel.

Our work in the area of ultrasonic weld testing over the past year has been in cooperation with the Bureau of Public Roads. We are developing a specification and a training manual for the inspection of bridge weldments. The publication and implementation of this work should expand the use of ultrasonics as a weld testing tool.

Generally, this work has been limited to full penetration butt welds in thicknesses from $^{5}/_{16}$ in. to 5 in. We have also applied it to full penetration T-welds in the same thickness range. It would be dangerous to attempt to apply the results of this work to other weld configurations or thicknesses. Partial penetration welds and backing strip welds can be thus inspected but spurious reflections caused by these configurations must be taken into account. We are extremely dubious as to the direct application of this information to fillet welds.

We hope that the result of our work will be greater use of ultrasonic weld testing. The use of amplitude and length rejection criteria will simplify interpretation. Eventually we may be able to treat particular areas in large welds more critically than others, depending upon the excellent defect location ability of ultrasonics to tell us whether or not defects are in more highly stressed weld areas.

REFERENCE

1. Niklas, L. In Materials Testing, Aug. 1965.

Installation of Preformed Neoprene Compression Joint Seals

STEWART C. WATSON, Acme Highway Products Corporation

ABRIDGMENT

•THE effectiveness of in-service performance of a compression joint seal is dependent to some degree upon proper installation.

SEAL POSITION IN JOINT SHAPE—CONTRACTION JOINTS

Generally, the following principles of positioning in contraction jointing apply (see Fig. 1):

1. The seal configuration should be positioned in the joint shape with its vertical axis reasonably parallel to the joint interfaces.
2. The inner and outer webs of the seal configuration should be juxtaposed in their true congruence rather than being intussuscepted or telescoped with a resultant potential for "popping" as the joints begin to open in contraction.
3. The top corners of the seal should be in reasonable contact with the joint interfaces.
4. The top of the seal, at the time of installation preferably, should not be higher than ¼ in. below the riding surface of the pavement for contraction joint seals $^{13}/_{16}$ in. (uncompressed width) and smaller. For larger seals, such as 1¼-in. contraction seals (uncompressed width) and down to but not including $^{13}/_{16}$-in. sizes, the top surface should be positioned at approximately ½ in. below the riding surface of the pavement at the time of installation. While this might appear to be somewhat low in the joint, long-term experience has shown that typical attrition to the top edges of joints, as well as the inevitable minor edge raveling from joint sawing, justifies these setting heights as being practical. To obtain their full life, these rubber seals should never under any condition of slab movement be touched by traffic, studded tires, snowplow, etc., since attrition will take its toll. The top portions can actually sustain wear not unlike the heels of shoes.

SEAL POSITION IN JOINT SHAPE—EXPANSION JOINTS

Pavement expansion joints are normally wider, usually anywhere from ¾ to 1½ in. wide, and since they exist to relieve compressive stress, they require different construction practices to reflect movement phenomena peculiar to their specific application. When used in a line of contraction joints or as bridge approach joints, expansion joints, in addition to reflecting normal thermal volume change, can and usually do progressively close. The construction practice recommendations shown in Figure 2 are simply obtained in the field and preclude the possibility of seal extrusion. Generally, the same four positioning rules used in contraction jointing will apply to expansion joints as well. Due to the complete absence of control of joint geometry, plus a tendency toward durability loss from the old hand-edging process, a recent strong trend is in evidence toward the sawing of expansion joints. Ideal control of expansion joint geometry, including the relief steps in Figure 2, is now being achieved by tandem blade sawing over the joint filler material.

Paper sponsored by Committee on Sealants and Fillers for Joints and Cracks in Pavements and presented at the 48th Annual Meeting.

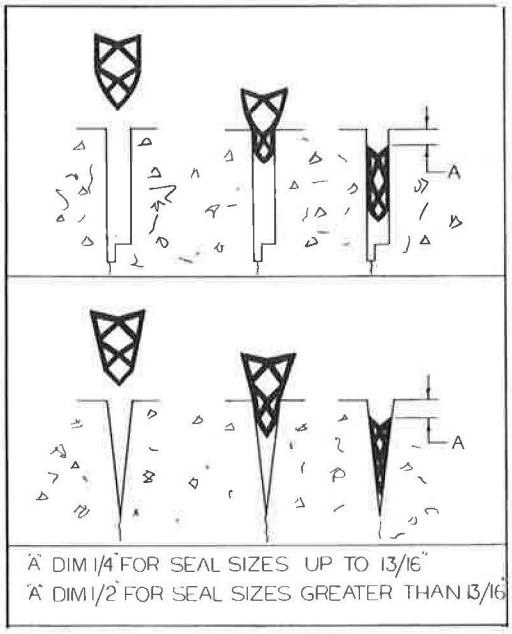

Figure 1. Seal position in joint shape—contraction joint.

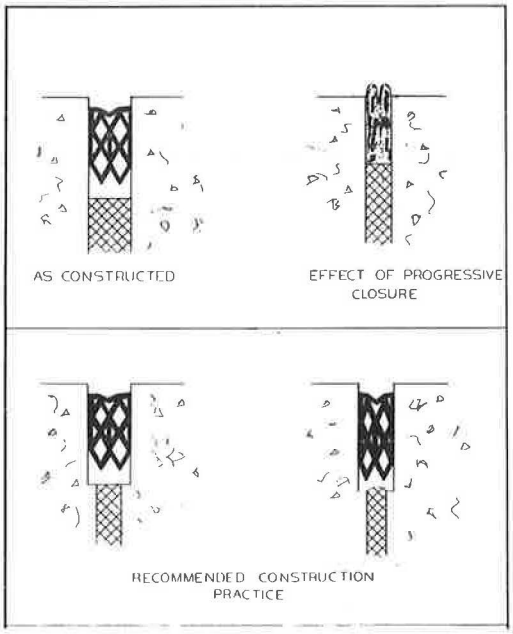

Figure 2. Seal position in joint shape—expansion joint.

SEAL POSITION IN JOINT SHAPE—LONGITUDINAL JOINTS

Since most longitudinal joints are tied together with a variety of devices, keys, etc., it is logical to assume that a zero movement condition prevails. Based on wide-spread photographic evidence from thousands of miles of concrete pavements now in service throughout North America and abroad, it is suggested that there may well be a number of categories of movement phenomena that can and actually do occur at longitudinal joints which would permit the entry of free water, solids and chemicals deleterious not only to concrete, but the highly corrodible metals used in tie bars and hook bolts and the hydraulically vulnerable subbase as well.

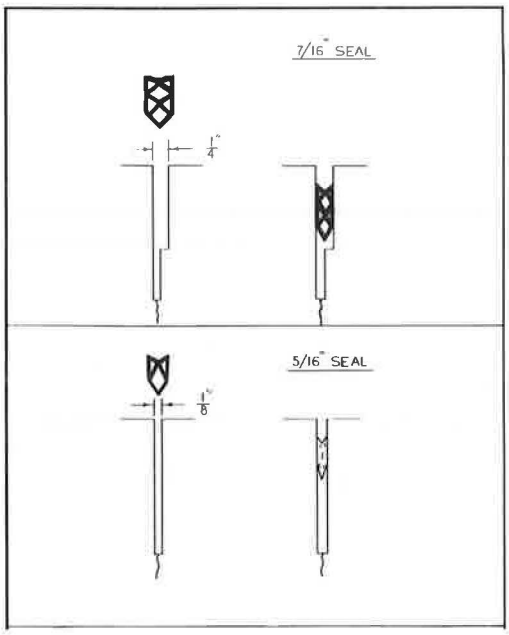

Figure 3. Seal position in joint shape—longitudinal joint.

The rules for positioning transverse joints similarly apply to longitudinal joints. Since the stroke of movement is not nearly so dynamic as with transverse joints, smaller seal, and in non-freeze-thaw areas, narrower joint widths have appeared to offer successful sealing solutions.

Figure 3 illustrates $\frac{1}{8}$-in. saw cuts and small $\frac{5}{16}$-in. seals currently in wide use on Texas Highway Department longitudinal joints in continuously reinforced pavements. The $\frac{1}{4}$-in. saw cut with a $\frac{7}{16}$-in. seal is used on longitudinal joints in New York, Maryland, Ontario, and Quebec, and freeze-thaw areas in general.

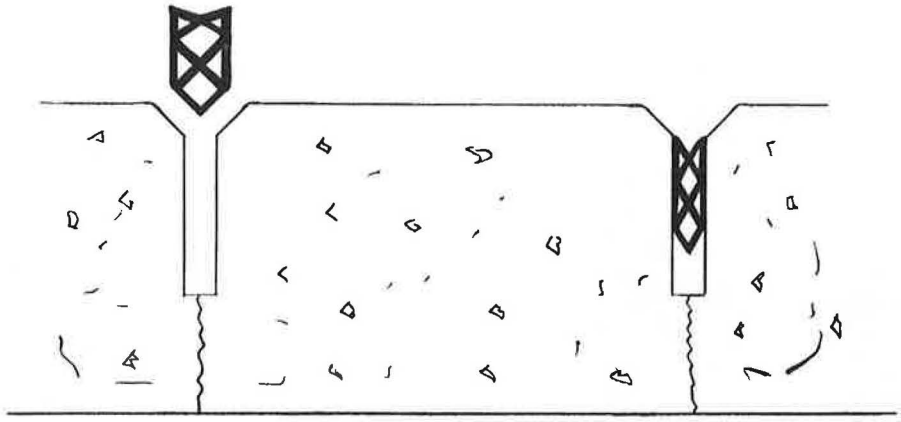

Figure 4. Detail of beveled saw cuts showing position of compression seal (Swiss-German system, slab length 7.8 meters).

LUBRICANT-ADHESIVE

It would be extremely difficult, if not impossible, to insert a compression seal into most joint openings without lubricating the joint interfaces. In addition to this, a priming agent is required to establish continuity of the seal with the joint interfaces. Further, it would be desirable to bond compression seals in place and so a lubricant that is also an adhesive with an approximate 3- to 5-min pot life is used. Insufficient as well as excessive lubricity can be troublesome in the installation practice. A sufficient amount of the lubricant-adhesive should be used to negate the forces of frictional refusal as differentiated from mechanical refusal.

EDGE BEVELING

The practice of beveling the edges of saw cuts and setting the compression seals near the bottom of the bevel began in Switzerland and is now spreading throughout Europe. Figure 4 illustrates the principle involved, and long-term comparisons of performance in the field of both conventional saw cuts and beveled edge saw cuts have proved the latter markedly superior. New York State, with its wide comparison seal experience, and a number of other states are now requiring beveled edges.

Post-construction condition surveys of many millions of feet of both compression seals and field-molded sealants have left no question in the writer's mind that this is the direction to go in jointing and sealing practice.

Figure 5. Fully automatic compress-eject machine with edge ramp for transverse joints.

GROWTH—STRETCH

Realizing that a resulting condition of over-compression could be equally as detrimental as over-elongation, limits of somewhere between 5 and 8 percent elongation in properly constructed contraction joints appear to be desirable.

MACHINE INSTALLATION METHODS

Automatic and semiautomatic methods of machine installation are presently in

Figure 6. Self-operating vacuumatic longitudinal installing machine preceded by upcutting wire brush cleaning operation.

various stages of development and use, both in North America and in Europe (Fig. 5 and 6). They currently may be categorized in principle as follows: (a) mechanical compress-eject, (b) vacuum compress-eject, (c) two-phase pull down, (d) combination vacuum compress-two-phase pull down, (e) progressive set of rolling wheels, and (f) compress-eject hand roller.

The development of reliable automatic or semiautomatic machines has been relatively costly and slow, primarily because no two paving projects appear to have exactly the same joint geometry, thermal movement, seal configuration, construction personnel, etc. The causes of seal refusal are many and any abrupt change in the joint geometry, whether it is due to small spalls, excessive cavitation of interfaces, differential raveling, etc., will still cause the most sophisticated installing machine to balk. Small stones or debris on the pavement can operate to change the desired setting height.

PAVEMENT EDGE SEALING

As jointed concrete pavements proceed through and respond to the normal conditions of service life, evidence of overstressing from entry of shoulder materials into the sides of pavement slabs at the joints is often apparent. Snowplows and graders can also produce corner breaks, the result of which is to rule out the effectiveness of any sealing system at this location of the slab

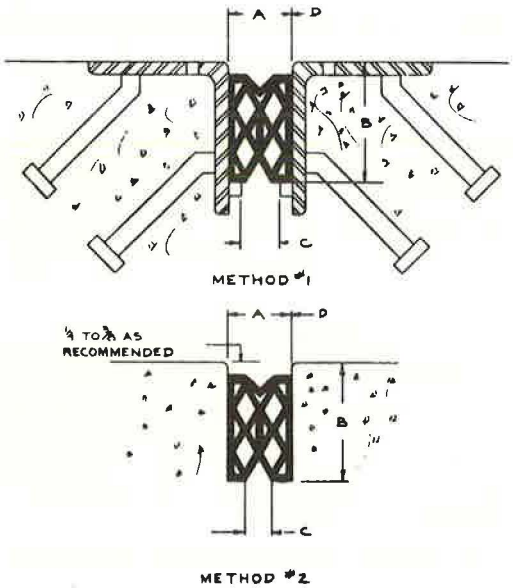

GROOVE SIZE				SEAL SIZE		SLAB LENGTH MAX.							
A	B	C	D	WIDTH	HEIGHT	60	80	90	100	120	140	160	200
1	2 3/8	5/8	5/64	1 3/4	2	■							
1 3/16	2 3/4	3/4	1/16	2	2 1/16	■							
1 3/8	3 1/2	1	5/64	2 1/4	2 5/8		■						
1 1/2	3 1/2	1	5/64	2 1/2	2 3/4			■					
1 3/4	4 1/4	1 1/4	3/32	3	3 1/32				■				
2	4 1/2	1 1/2	7/64	3 1/2	3 1/2					■			
2 3/8	5 3/4	1 1/2	1/8	4	4 2 3/32						■		
2 3/4	6 1/2	1 1/2	5/32	5	5 5/16							■	■

NOTE:
A Dim. is measured at 70 F
D Dim. is minus for every 10 F increase in temp.
D Dim. is plus for every 10 F decrease in temp.

Figure 7. Seal sizing for joints in bridges and structures.

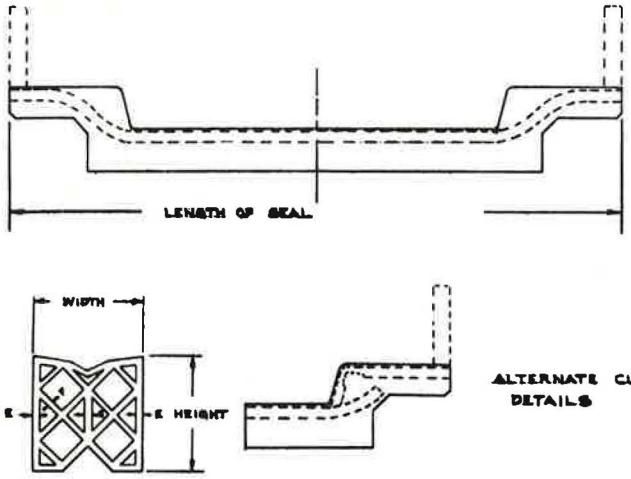

WIDTH	HEIGHT	THICKNESS E	THICKNESS F
$\frac{1}{4}$ $^{+1/8}_{-0}$	$1\frac{5}{16}\pm\frac{1}{16}$	.062±.015	.062±.015
$\frac{5}{8}$ $^{+1/8}_{-0}$	$1\frac{5}{8}$ $^{+1/8}_{-0}$	.078±.015	.078±.015
$1\frac{3}{4}$ $^{+1/16}_{-0}$	$2\pm\frac{1}{8}$	$\frac{1}{8}$ +1/32 -1/64	$\frac{3}{32}$ +1/32 -1/64
2 $^{+3/16}_{-0}$	$2\frac{1}{16}\pm\frac{1}{8}$	$\frac{1}{8}$ +1/32 -1/64	$\frac{3}{32}$ +1/32 -1/64
2 $^{+1/8}_{-0}$	$2\frac{1}{16}\pm\frac{1}{8}$	.078±.015	.078±.015
$2\frac{1}{4}$ $^{+3/16}_{-0}$	$2\frac{5}{8}\pm\frac{1}{8}$	$\frac{3}{16}$ +3/64 -1/64	$\frac{3}{32}$ +1/32 -1/64
$2\frac{1}{2}$ $^{+1/4}_{-0}$	$2\frac{5}{4}\pm\frac{1}{8}$	$\frac{3}{16}$ +3/64 -1/64	$\frac{3}{32}$ +1/32 -1/64
3 $^{+1/4}_{-0}$	$3\frac{1}{32}$ $^{+3}_{-16}$	$\frac{3}{16}$ +3/64 -1/64	$\frac{1}{8}$ +3/64 -1/64
$3\frac{1}{2}$ $^{+1/4}_{-0}$	$3\frac{1}{2}\pm\frac{3}{16}$	$\frac{3}{16}$ +3/64 -1/64	$\frac{1}{8}$ +3/64 -1/64
4 $^{+5/16}_{-0}$	$4\frac{21}{32}\pm\frac{1}{4}$	$\frac{1}{4}$ +3/64 -1/32	$\frac{3}{16}$ +3/64 -1/64
5 $^{+5/16}_{-0}$	$5\frac{5}{16}\pm\frac{1}{4}$	$\frac{1}{4}$ +3/64 -1/32	$\frac{3}{16}$ +3/64 -1/64
6 $^{+3/8}_{-0}$	$5\frac{3}{4}$ $^{+5}_{-16}$	$\frac{5}{16}$ +3/64 -1/32	$\frac{1}{4}$ +3/64 -1/64

Figure 8. Seal positioning for joints in bridges and structures.

ends and to leave the extreme ends of seals uncompressed with freedom to migrate at will. It is therefore desirable, if practical, to seal the joints at the sides of pavement slabs. Forming edge grooves also tends to minimize the runaway cracks that migrate away from the desired location.

DURABILITY OF JOINT INTERFACES

Since it is not practical to recommend a joint forming or sawing practice that would work well for all pavement designs and environments, attention should be given to producing the most durable interfaces practical for whatever method is utilized.

The sharp edges of contraction joints should be taken off by dragging a form pin across or running a wire brush machine through the joint, the latter of the two being the most effective and consistent (Fig. 6).

The tendency of a seal to refuse installation can be markedly reduced if this practice is observed. The action of the wire brush against the joint interfaces tends to expose

Figure 9. "Pogo Stick" inserter for bridge seals.

Figure 10. Roller (250 lb) for inserting bridge seals.

any potential spalls and remove sawing residue, or loose concrete, as well as to produce an interface that is ideal for bonding of the compression seal to the concrete.

BRIDGE APPROACH JOINTS

Bridge approach joints have as their primary mission the provision for relief of compressive stress between a pavement and a bridge. When used in conjunction with contraction joint pavements, in addition to normal volume changes, they will tend to progressively close. They should therefore be designed in accordance with Figure 2 or 7.

JOINTS IN STRUCTURES

Marked differences in sealing practices are called for in the design of a compression sealing system for bridges. It must have the capability to respond successfully to the many different types of movement that might occur on a specific bridge, whether straight distance change between the joint interfaces; racking distortion from the many variations of skews; horizontal, angular, vertical and articulating motion patterns; differential vibrations of slab ends; impact, warping and rotation effects; permanent changes in deck length; creep; plastic flow; etc.

Figures 7 and 8 illustrate seal configurations and construction practice recommendations currently in wide use by state and provincial highway departments throughout North America. Optional curb treatments are included.

Figure 9 shows the use of a "pogo stick" inserter tool that is an effective, low-cost inserting tool when used in conjunction with the seal configurations and construction practice recommendations shown in Figure 7.

Figure 10 depicts a heavy steel roller inserter consisting of an inner wheel and two large outer wheels of 2-in. plate steel.

Preformed Elastomeric Bridge Joint Sealers: Evaluation of the Material

GEORGE S. KOZLOV, New Jersey Department of Transportation,
Division of Research and Evaluation

This paper, the second in a series, presents up-to-date knowledge on sealer material. It includes the best available tentative qualification and identification specifications, and furnishes producers and users with practical ways to develop and/or identify a reasonably adequate product. These specifications are as realistic and as closely related to field application as present-day knowledge of the subject permits. To this end, simulated service tests were given extended coverage and a section on quality control of materials was included. The correlation between the specifications and the functional applications of the product is assured by an ongoing research program.

•A PAPER on the subject of the design and construction of bridge joints sealed by preformed elastomeric sealers was presented previously (1). Since then, new knowledge of the material has been acquired and its application was further explored. A research program was developed with the following specific aims in mind:

1. To test and improve suggested methods of design and construction of bridge joint systems and to establish relationships between deck and air temperatures and joint movements; and
2. To develop realistic material specifications, closely related to the actual field applications of the products.

As a result of the research program, a sequence of four papers was planned. The first paper, on design and construction, was published earlier (1). The present paper is the second one and its subject is the material in the preformed elastomeric sealers. The third paper is intended to cover temperature and joint movements and the fourth the results and conclusions.

The first paper barely touched the subject of the sealer's material; since then, the need for more knowledge about it has become apparent. The previous paper presented to the engineer a basic understanding of the material. This one will concern itself mainly with the qualification and identification of the material. But first it is appropriate to introduce an amendment to clarify a misunderstanding.

AMENDMENT TO THE SEALER DESIGN PRACTICES

One of the criteria for a "functional" sealer, as defined in the previous paper (1), is its ability to remain functional within certain limits of the sealer's compressibility. "Efficiency coefficients" X, Y, and Z were introduced and tables were offered as guidelines for the design of sealers. Other tables showed that the sealers presently available are not meeting the requirements. In spite of this demonstration, the factor of functional limitation somehow remained concealed.

Later in this paper, the producers and users of sealers will be offered practical ways for the development and/or identification of a reasonably good product. This section

Paper sponsored by Committee on Sealants and Fillers for Joints and Cracks in Pavements and presented at the 48th Annual Meeting.

TABLE 1

GUIDE TO THE DESIGN OF SEALERS

W_n (in.)	At 100 F		Δ at Δt = 70 F	At 30 to 90 F		Δ at Δt = 90 F	At 0 F		Limits of Span
	W_{jmin}	Z		W_j (in.)	Y		W_{jmax}	X	
1½	0.875 0.735	0.58 0.49	0.00 0.14	⅞	0.58	0.00 0.18	0.875 1.055	0.58 0.70	Up to 30 ft
1¾	0.86 0.84	0.49 0.48	0.14 0.16	1	0.57	0.18 0.21	1.18 1.21	0.67 0.69	30 to 35 ft
2	0.965 0.915	0.48 0.46	0.16 0.21	1⅛	0.56	0.21 0.27	1.335 1.395	0.67 0.70	35 to 45 ft
2½	1.165 1.145	0.47 0.46	0.21 0.23	1⅜	0.55	0.27 0.30	1.645 1.675	0.66 0.67	45 to 50 ft
3	1.52 1.47	0.51 0.49	0.23 0.28	1¾	0.58	0.30 0.36	2.05 2.11	0.68 0.70	50 to 60 ft
4	1.97 1.83	0.49 0.46	0.28 0.42	2¼	0.56	0.36 0.53	2.61 2.78	0.65 0.695	60 to 90 ft
5*	2.455 2.345	0.49 0.47	0.42 0.53	2⅞	0.58	0.53 0.68	3.405 3.555	0.68 0.71	90 to 115 ft
6*	2.97 2.90	0.50 0.48	0.53 0.60	3½	0.58	0.68 0.77	4.18 4.27	0.70 0.71	115 to 130 ft

Temperature Range: 0 to 100 F
Construction Temperature: 30 to 90 F
Installation Temperature: 30 to 90 F
Degrees of Efficiency: $Z_{min} = \pm 0.50\ W_n$; $Y_{avg} = \pm 0.60\ W_n$; $X_{max} = \pm 0.70\ W_n$

NOTE: All the above temperatures are those of the concrete. Since these temperatures cannot readily be measured, the daily average temperature of the air with a tolerance of +5 to +10 F would be presently acceptable.

*Because of the lack of experience with these two largest sizes, it is preferable not to use the sealer widths W_n = 5 in. and 6 in. until further data are available.

TABLE 2

GUIDE TO THE DESIGN OF SEALERS

W_n (in.)	At 100 F		Δ at Δt = 70 F	At 30 to 90 F		Δ at Δt = 90 F	At 0 F		Limits of Span
	W_{jmin}	Z		W_j (in.)	Y		W_{jmax}	X	
1½	0.875 0.695	0.58 0.46	0.00 0.18	⅞	0.58	0.00 0.24	0.875 1.115	0.00 0.74	Up to 40 ft
1¾	0.945 0.915	0.54 0.52	0.18 0.21	1⅛	0.64	0.24 0.27	1.365 1.395	0.78 0.80	40 to 45 ft
2	1.04 1.00	0.52 0.50	0.21 0.25	1¼	0.625	0.27 0.33	1.52 1.58	0.76 0.79	45 to 55 ft
2½	1.25 1.18	0.50 0.47	0.25 0.32	1½	0.60	0.33 0.42	1.83 1.92	0.73 0.77	55 to 70 ft
3	1.555 1.455	0.52 0.485	0.32 0.42	1⅞	0.625	0.42 0.53	2.295 2.405	0.765 0.80	70 to 90 ft
4	2.08 1.95	0.52 0.49	0.42 0.55	2½	0.625	0.53 0.71	3.03 3.21	0.76 0.80	90 to 120 ft
5*	2.575 2.435	0.515 0.49	0.55 0.69	3⅛	0.625	0.71 0.89	3.835 4.015	0.77 0.80	120 to 150 ft
6*	3.06 2.92	0.51 0.49	0.69 0.83	3¾	0.625	0.89 1.07	4.64 4.82	0.77 0.80	150 to 180 ft

Temperature Range: 0 to 100 F
Construction Temperature: 30 to 90 F
Installation Temperature: 30 to 90 F
Degrees of Efficiency: $Z_{min} = \pm 0.50\ W_n$; $Y_{avg} = \pm$ 0.60 to 0.65 W_n; $X_{max} = \pm 0.80\ W_n$

NOTE: All the above temperatures are those of the concrete. Since these temperatures cannot readily be measured, the daily average temperature of the air with a tolerance of +5 to +10 F would be presently acceptable.

*Because of the lack of experience with these two largest sizes, it is preferable not to use the sealer widths W_n = 5 in. and 6 in. until further data are available.

presents an amendment to the previous paper in the form of Tables 1 and 2. The meaning of Tables 1 and 2 is illustrated by the following example:

Span	At 20 Percent Range		At 30 Percent Range		At 40 Percent Range	
	W_n	Estimated Material Price, $/ft	W_n	Estimated Material Price, $/ft	W_n	Estimated Material Price, $/ft
90 ft	5 in.	16.00	4 in.	11.00	3 in.	6.00
130 ft	Composite sealer design (larger than 6 in.)	above 27.00	5 in. or 6 in.	16.00 26.00	4 in.	11.00

The prices mentioned are only for purposes of comparison, but it is apparent that the cost of this type of sealer application is influenced considerably by the sealer's efficiency. Often the initial cost of the product is increased, but sometimes the design and installation costs also are adversely affected.

The problem of the temperature of installation is frequently raised. This is a complex question. Practically it has been answered in the previous paper in the section, "Design of Preformed Elastomeric Joint Sealer Application". We hope to substantiate this more completely in the future.

QUALIFICATION AND IDENTIFICATION OF THE MATERIAL

As already stated elsewhere, the use of elastomeric materials in the construction field is recent and unexplored. The structural designers and builders have relatively less clear understanding of elastomers than they have of the more common construction materials. On the other hand, most specialists in the field of elastomers seem to be more concerned with material properties than with the functional requirements of application. Thus, it appears that at the present time nobody seems really to know which properties best express the actual performance of the material when it is used as preformed elastomeric joint sealers.

As a result, specifications presently available have very little basis in fact, because on the one hand there is hardly any correlation between them and the actual sealer application, and on the other hand, not enough testing has been done on actual seals.

An effort was already made to improve the understanding of the material by the engineer and of the functional criteria by all concerned. Now, mainly for the benefit of the engineer, the material specifications are discussed and presented on the basis of the best information available.

DISCUSSION OF THE TENTATIVE SPECIFICATION

I have indicated that the use of the elastomeric material in the construction field is new, and that this material and its use are poorly understood. In other words, nobody seems really to know which properties best express the actual performance of the material when it is used as a preformed elastomeric joint sealer. The tentative specification, therefore, can only be intended as an interim action, after which all concerned will have an opportunity to take steps to correct, amend, or otherwise improve it.

This specification, which is reproduced in the Appendix to this paper, covers the material and its manufacture, physical requirements and test procedures, and sampling, certification, and acceptance requirements. The section on quality control of material, mainly in the form of simulated service tests, is the most notable development.

For an easier understanding of the specification, let us start with a discussion of the tests for identification and qualification requirements (Tables A1 and A2 in the Appendix)

and clarify some possible misunderstandings. For simplicity of identification the tests are grouped and numbered. Their discussion was developed with the assistance of E. I. du Pont de Nemours and Company.

Group I, Tests 1 to 4

The tests of tensile strength, elongation, hardness, and permanent set at break are widely used to characterize rubber products. They give very little useful information themselves, since they only describe "original" properties measured right after vulcanization. But they do tend to establish the broad quality classification of the product.

The rubber industry uses the word "quality" in a specific context. When applied to a particular compound, quality refers to the degree to which the maximum properties available from the polymer have been developed. In most elastomers, polychloroprene included, there must be other ingredients in the compound, as already indicated, to develop optimal properties. Therefore, even the highest quality compound will not contain more than 60 to 65 percent of elastomer by weight. Since the elastomer is the most expensive major ingredient in a rubber compound, the higher the percentage of elastomer, the more expensive the compound will be.

Tensile strength and elongation—in a given hardness range—give an immediate indication of the quality level, because these properties reflect the degree to which the compound has been diluted. Permanent set indicates whether or not the compound has reached its optimum state of vulcanization and is reflected in stress relaxation or creep. The hardness test gives only an approximate value; it is therefore not an adequate measure of load-carrying capacity (stiffness). As stated before, however, the product must be further defined by other tests in order to determine its usefulness in a given service.

Group II, Tests 5 to 7

The oven aging, ozone resistance, and oil swell tests serve a twofold purpose:

1. To measure the effects of various environments on the rubber product, and
2. To identify the elastomer used.

It should be noted that the degree to which these tests measure the resistance to aging in different environments depends on how well each test is related to actual exposure. Precise correlation is difficult, if not impossible, to obtain without intensive study over long periods of time.

Oven aging is a rough indication of how well a rubber product will resist age deterioration (which includes oxidation effects), as well as other deteriorating factors such as heat.

The ozone test, on the other hand, measures resistance to a specific deteriorating influence. Many types of rubber are susceptible to severe attack from ozone. Since ozone is present in the atmosphere, resistance to ozone attack is necessary for a material to withstand prolonged weathering. While oxygen affects the entire unit of the material, ozone attacks the surface, causing cracks that open under loading, exposing it to further ozone damage and possibly rupture under stress.

Volume increase of the product in oil is not a true indication of the resistance of an elastomer to deterioration. If one were testing for deterioration, then one should determine retention of physical properties after oil aging. Although polychloroprene is a medium-swell elastomer, it retains physical properties better than the so-called low-swell elastomer. In this specification, the oil test (combined with the ozone requirement) serves mainly to help assure that the elastomer is polychloroprene.

The Group I and II properties must be viewed as a composite. No elastomer compound can be designed to have the maximum desirable levels of all properties. What is done to improve one property may hurt another. Therefore, each compound is a composite. The compound must have a balance of good levels of the properties most necessary to good service.

Group III, Tests 8 to 10

While one could not quite think of the recovery tests as simulated service tests, they bear more resemblance to service conditions than the others.

The high-temperature recovery test is an indication of how completely the seal is vulcanized. Poorly vulcanized seals would tend to take too high a set after being compressed in a highway joint. The field data available at this time are not sufficient to allow anyone to attempt to correlate a given recovery value with some specific useful life in a joint.

The low-temperature recovery tests have a different purpose. A seal will not pass these two tests unless it has been compounded to resist both crystallization and thermal stiffening. The recovery requirement at +14 F is designed to ensure that a crystallization-resistant neoprene polymer is used. The -20 F test will assure specifically that the compound has a good level of low-temperature flexibility and that the brittleness characteristics will be controlled. The plasticizers improve flexibility and depress the brittle point of materials at low temperatures. The -20 F temperature appears to be adequate for the area of the State of New Jersey.

The function of the material specification is to set practical limits on the important properties from a production standpoint, as well as to ensure the procurement of serviceable material. Irrelevant tests should be avoided.

There are also other basic rubber material tests such as tear, compression set, and low-temperature stiffening. These tests are omitted from the proposed specifications because they are irrelevant and could even be misleading for sealer service purposes.

The recovery tests are used to take the place of the low-temperature stiffening and compression set tests. The tear test, although valid, cannot be performed properly by methods presently available.

Both the recovery and compression set tests indicate the state of cure. Curing is executed on an already extruded product. A balance must be maintained between compression set and tear—an undercured material will cause excessive set, an overcured one will result in cracking. Obviously, neither is permissible.

The compression set on the preformed sealer, designed as a structural unit, is best represented by recovery tests, since the compression set test is preformed on the solid sample of material, whereas the recovery tests are conducted on a sample of a sealer unit. The sealers are specifically designed always to act as a structural unit within certain limits. Compression beyond these limits might result in failure. Therefore, a compression set test on solid material is not entirely representative and may even be misleading.

Both tear and compression set tests are generally good when run exactly as prescribed by ASTM. When performed on samples obtained from finished seals they can be clouded by error.

As indicated, the balance between the tests is essential regarding the state of cure. This is why it appears desirable in the future to include the tear test in the specifications, as soon as satisfactory methods of testing are developed.

Suggested Changes

In the foregoing I have suggested some changes from accepted practice in the physical properties and requirements to be specified and tested. These suggestions can now be reviewed.

The round-robin tests performed for ASTM Committee D-4, Subcommittee 3e, have indicated the increase as well as the loss of tensile strength after oven aging. Since the increase of tensile strength in this test indicates somewhat undercured material, it seems advisable to limit both.

A segment of the manufacturing industry claims that to ensure the adequacy of the degree of precision in the process of extrusion of sealers larger than 4 in. the "minimum tensile strength" property requirement of 1800 psi is essential. As indicated before, in a given hardness range this means dilution of the compound and lower "quality" level of the material. Because the properties that best express the actual performance of the material when used as a subject sealer are unknown, such relaxation of the subject requirement, I suppose, could be tolerated until it becomes apparent that it will not also lead to a lower quality product (a sealer). Under these circumstances any increase in hardness requirements becomes ill-advised.

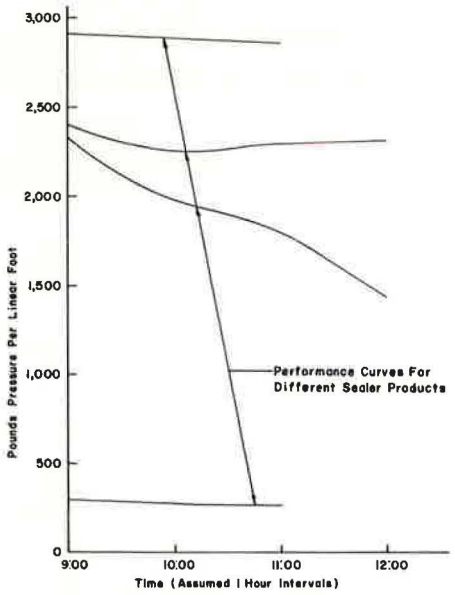

Figure 1. Pressure-decay curves (averages) for nominal sealer size $2\frac{1}{2}$ $(W_n) \times 2\frac{3}{4}$.

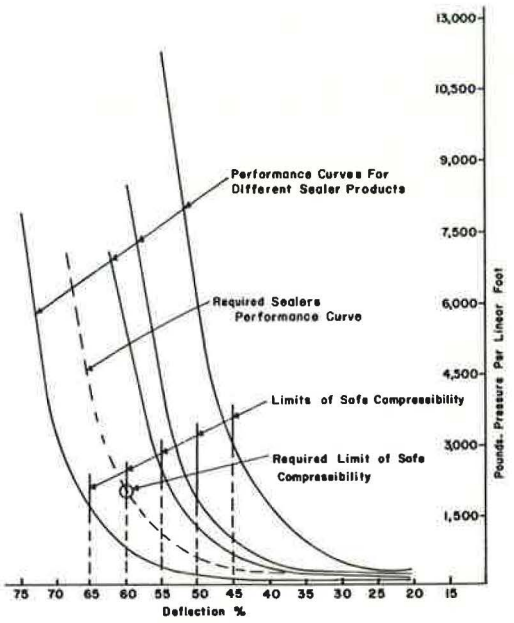

Figure 2. Pressure-deflection curves (averages) nominal sealer size $2\frac{1}{2}$ $(W_n) \times 2\frac{3}{4}$.

Essentially, the "Tests for Identification Requirements" in the specification (Appendix) summarize material requirements, while the "Tests for Qualification Requirements" represent simulated service tests.

With addition of pressure-deflection testing and the development of the relationship between the limit of safe compressibility and the percentage of deflection during the high-temperature recovery test, the recovery tests become definitely more meaningful because they can, and I believe they will, be accepted as simulated service tests, rather than tests of material.

The development of pressure-deflection tests as well as the limit of safe compressibility are the offshoot of a program first presented to the ASTM at its January 1968 meeting. They remain a part of the New Jersey pilot research program on this subject.

What is the "limit of safe compressibility" and what is the "pressure-deflection test"? The specifications (Appendix) explain it in paragraphs 4 and 5; Figures 1 and 2 clarify it further. The pressure-decay graph (Fig. 1) is illustrative only, since the lack of equipment capable of adequate accuracy (such as a Universal Testing Machine) does not permit the extension of this test far enough to establish sufficiently acceptable pressure-decay values of Y.

Figure 2 illustrates the limit of safe compressibility and the minimum contact pressure. The solid lines indicate the pressure-deflection values of products presently in existence; the dashed line represents the minimum required pressure-deflection values of a desirable product and this indicates the way a producer can develop such a product. In reference to the minimum contact pressure X, the same difficulty exists as in the case of Y.

Hall, Ritzi, and Brown (3) are presently improving the testing device mentioned in their article for the purpose of obtaining equipment that will permit the determination of sufficiently accurate values of X.

Some time ago I stated that in the high-temperature recovery test the percentage of deflection should be 60 percent. At present this value is Z percent and is the limit of safe compressibility. The previous statement read in substance that this is being done to facilitate the requirements of design (Z_{min} = 40 percent), installation, and material.

[Values X, Y, and Z here are "efficiency coefficients" as explained in my earlier article (1).] In the same test, the 70 hours/212 F requirement seems to eliminate more efficiently the inadequate material.

These changes, with some other minor ones, have only one purpose—to reduce the sealer service inadequacies observed in the field. The fact is that to date, in New Jersey, sealers in bridges under observation have failed in various degrees—joints are leaking. This situation necessitates tightening of the material requirements, and seeking constructive cooperation on the part of the sealer manufacturers.

The degree of failure may be argued, although it is beside the point in this discussion. At the present time the observed inefficacy cannot always be attributed directly to an inadequacy of the sealer material. But one thing has been established: almost all sealers were installed at higher than 60 percent Y compression and many relaxed in winter months to more than 80 percent X.

For the present, considering the methods of joint construction used in New Jersey, the sealers should be compressed during installation to about Y = 55 percent and should never relax to more than X = 70 percent (Table 1).

Further, as indicated in the cost analysis example, this type of material is expensive; therefore, inefficient utilization of the sealers may not justify their cost. This can very easily happen if efforts are not made to meet the suggested requirements. I believe they can be met, provided all concerned endeavor to improve quality. This type of seal should and can solve the problem of joints in a large percentage of bridges.

In reference to the "lubricant-adhesive" material, as presently used to facilitate the application of these seals, it is useful as a lubricant. But during prolonged periods of high temperature (above 90 F) it has the tendency to set rather quickly while being applied. For all practical purposes, it is admittedly an adhesive by name only, as observed in the field.

All told, expanded research on better bridge joints is a growing need. This is why New Jersey is already proceeding with the implementation of an improved program along these lines:

1. Thorough testing of all sealers to be utilized on actual construction in accordance with the accepted specifications;
2. The same kind of testing of all sealers removed from joints for reasons of failure or otherwise; and
3. Testing for the purpose of research.

The direction of this research will be toward further development of the idea of positive retention of contact pressure in conjunction with minimum compressed width and sealer recovery.

The ultimate goal of all this measuring, recording, and correlating will be to relate the material and the simulated service tests to actual field application and to the specific period of useful life in a joint.

An explanation for the deflection value Z has already been offered; the simulated service tests are presented and explained in the proposed tentative specifications in the Appendix. As to the present implementation of the research program, the material submitted for approval, while being tested officially, is being tested completely in accordance with the tentative specifications, but for research purposes only. This obviously covers the first and third points. Regretfully, point 2 cannot as yet be implemented because no "used" sealers are available.

Some data already available are very encouraging. These data allow much better judgment of the quality of the material; so much so, in fact, that I would not hesitate to pass some material that may fail numerically in some of the tests (mainly in the material part of the specifications), while on the other hand I would fail some of the material previously considered adequate. The data already indicate possible values for Y and X in the pressure-deflection tests. If nothing else, this clearly indicates the correctness of the direction in which the study is proceeding.

TABLE 3

45-DEGREE SKEW ANGLE JOINT TEST

Load	P						1.41P						P_2			P_1 1.41P - P_2 = P_1						P	P_2	P_1
% Run	1	2	3	4	5	6	1	2	3	4	5	6	1	2	3	1	2	3	4	5	6	Avg.	Avg.	Avg.
20	160	150	145	156	160	156	225	211	204	220	225	220	80	70	70	145	141	134	140	155	150	154	73	144
25	200	175	177	187	190	187	282	247	250	264	268	264	82	72	70	200	175	180	182	196	194	186	74	187
30	235	220	212	225	228	222	331	310	299	317	321	313	100	87	85	231	223	214	217	234	228	223	90	224
35	268	252	250	257	260	259	378	355	352	362	367	365	160	140	135	218	215	217	202	227	230	257	145	218
40	310	287	290	305	304	305	437	405	409	430	428	430	235	200	205	202	205	204	195	226	225	306	213	209
45	400	370	370	375	382	380	564	522	522	529	539	536	380	330	335	184	192	187	149	209	201	379	348	187
50	530	520	510	500	520	505	747	733	719	705	733	712	625	---	---	122	---	---	80	---	---	514	625	101
45	295	305	310	305	320	320	416	430	437	430	451	451	210	---	---	206	---	---	220	---	---	309	210	213
40	235	235	240	240	250	252	331	331	338	338	352	355	132	147	155	199	184	183	206	205	200	242	145	196
35	192	197	200	200	211	213	271	278	282	282	298	300	85	92	95	186	186	187	197	206	205	202	91	194
30	165	170	165	170	180	180	232	240	233	240	254	254	60	60	60	172	180	173	180	194	194	171	60	182
25	145	140	140	140	150	149	205	197	197	197	211	210	55	55	55	150	142	142	142	156	155	144	55	148
20	105	110	120	115	125	124	148	155	169	162	176	175	52	55	52	96	100	117	110	121	123	116	53	111

THE SKEWED JOINT TEST

Table 3 and Figure 3 represent data on the skewed joint effect on a sealer, in this case a nominal sealer size of $2\frac{1}{2}$ by $2\frac{3}{4}$ in. This test was performed experimentally for the purpose of acquiring tangible data. Basically it is a success, but the relationship of some numerical values is dubious, the reason being the test procedure.

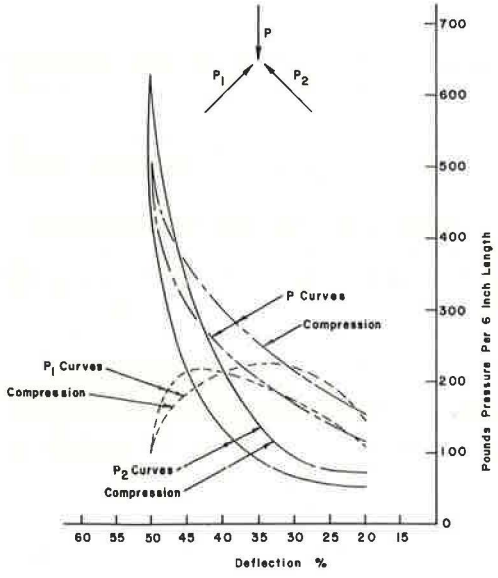

Figure 3. Pressure-deflection curves for 45-deg skew angle (averages): Graphs of forces P, P_1, P_2 for nominal sealer size $2\frac{1}{2}$ (W_n) x $2\frac{3}{4}$.

To determine the P_2 force, i.e., the force perpendicular to the width of the sealer, a usual pressure-deflection procedure was used. This force is correct when measured by itself in this manner. The skew force P was measured also in accordance with the regular pressure-deflection procedure, and by itself, is correct. The force P_1 is calculated as shown in Table 3.

The fallacy lies in the separate measuring of forces P_2 and P. I believe that if both of these forces could be measured during the skewed test, the numerical relationship of all three forces P, P_1, and P_2 would be different, although the graphs in Figure 3 would look very similar.

The value of this test is multiple. First, the basic relationship is as shown in the graph. Second, the minimum contact pressure of a sealer located in a skewed joint is larger whereas the peak of pressure is smaller than in a joint that is perpendicular to the span. Third, the force parallel to the joint is declining after a while and its peak is far below the other forces.

One very important question is not being answered and further testing is needed for

that: Do we need a larger sealer for a skewed joint and, if so, at what degree of the skewed angle does the increase in size begin and, finally, what changes of sealer sizes are needed as the skew angle increases?

Sealer sizes are being enlarged presently with the skew, but it is not certain that the enlargement is necessary. It is hoped that research will find the answer to this question.

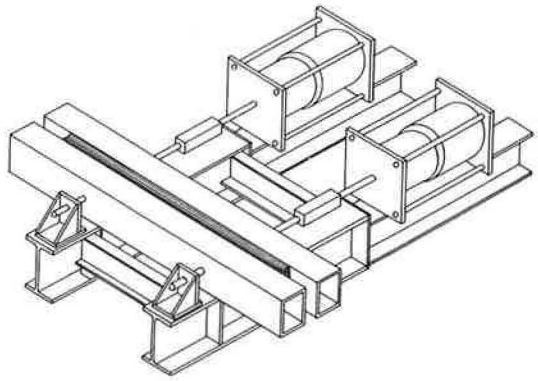

Figure 4. Schematic of model joint machine.

TESTING PROGRAM

Before going into the description of the testing phase of the research, it is important to realize the necessity of it. E. I. du Pont de Nemours and Co., among others, has amassed a considerable amount of data. In the brochure, "Elastomers Notebook" (4), for example, they discuss long-term (20 years) outdoor exposure tests of some polychloroprene compounds, but only under static service or unstressed conditions. In the application of rubber products anywhere in construction and specifically as joint sealers, the outdoor dynamic service conditions of exposure are predominant.

Outdoor weathering exposure is the condition where the similarity ends. A 50-year life span on an outdoor rack might, but also might not, represent a sealer in actual application. Therefore, the material properties and their physical requirements, if based on these tests, would not necessarily ensure quality material for use in products such as sealers, regardless of their application. Only if tested for outdoor dynamic service could such knowledge be claimed. The present program represents such a condition test for outdoor dynamic service exposure.

Methods of Procedure

Testing will be accomplished under existing field exposure conditions using "model joint" machines to simulate most of the bridge behavior patterns except for traffic. Such a machine is already developed. Its basic capability will be to compress a sealer within a range of minimum to maximum compressed widths, while being exposed to outdoor conditions and activated by environmental variations such as temperature change.

It has been recognized that adequate simulation of the outdoor exposure conditions is impossible and therefore the time period required for this test is governed by the time factor of daily (24 hours) and yearly cycles.

The principle of the model joint machine is based on the fact that some materials have an expansion coefficient many times higher than concrete, making it possible to simulate, for bridges, thermal movements of considerable magnitude, without resorting to large-size models or mechanical means of motoring.

The model joint machine is illustrated in Figure 4. In this apparatus, a sealer product is placed between a stationary and a movable jaw. The movable jaw is activated by a set of bellows. The bellows in turn are powered by a thermo-sensitive liquid. Thus, the bellows are in this case thermostatic motors and fit the purpose mostly because they will function regardless of the pressure they must overcome. In the case of minimum pressure, the internal spring with a nominal rate of 500 lb/in. will suffice. The machine will have a considerable range and the design approach was thorough.

CONCLUSIONS

In this paper a more complete attempt is made not only to describe the material but also to provide the best available tentative qualification and identification specifications (Appendix). These specifications are as realistic and as closely related to the actual field applications as combined knowledge of the subject permits. To build the bridge

between these specifications and reality, the simulated service tests and a section on "quality control of material" were added.

To substantiate these specifications, to make them realistic in as complete a sense of the word as possible, the correlation between subject specifications and the functional application of the product is needed. Because I had to conclude that field data for such a correlation are neither available nor reliable, I propose the research program mentioned in this paper. The results will be presented in the final paper of this series.

REFERENCES

1. Kozlov, George S. Preformed Elastomeric Bridge Joint Sealers. Highway Research Record 200, pp. 36-52, 1967.
2. ASTM Compression-Deflection Test, Designation D 575-67, Method A. 1967 Book of ASTM Standards, Part 28.
3. Hall, F. K., Ritzi, J. H., and Brown, D. D. Study of Factors Governing Contact Pressure Generation in Neoprene Preformed Compression Seals. Highway Research Record 200, pp. 53-74, 1967.
4. E. I. du Pont de Nemours and Co. Elastomers Notebook, April 1961.

Appendix

PROPOSED TENTATIVE SPECIFICATION FOR PREFORMED ELASTOMERIC JOINT SEALERS FOR BRIDGES

1. Scope

1.1 This specification covers the material qualification and identification requirements for preformed elastomeric compression joint sealers, to be utilized in bridge construction, the base polymer being in accordance with 2.1.

2. Materials and Manufacture

2.1 Sealers shall be preformed and manufactured from vulcanized elastomeric compound, using polychloroprene as the only base polymer.

2.2 If other base polymers are shown to be suitable in this application, the requirements of this specification shall be amended by alternate requirements, which shall be developed to define adequate quality of the new composition.

3. Physical Requirements

3.1 The material shall conform to the physical properties prescribed in Tables A1 and A2.

4. Dimensions and Permissible Variations

4.1 The size, shape, and dimensional tolerances of the sealers are subject to design and/or shall be guided as outlined in paragraphs 4.1.1 and 4.1.2.

4.1.1 The accepted width and height of a sealer shall be not less than nominal; the height of a sealer can be in excess of nominal but by not more than one quarter (+1/4") of an inch.

4.1.2 The dimensional tolerances shall be determined on the basis of the limit of safe compressibility of the sealers.

4.1.3 The limit of safe compressibility of sealers is the border line between closure of essentially all of the air voids and the beginning of solids compression and is clearly defined on the pressure deflection curve by rapid and considerable increase of pressure.

4.1.4 The limit of safe compressibility of sealers shall be at not less than "Z"% deflection from sealers nominal width, where "Z" in per cent shall be the maximum deflection contemplated in the joint sealing design, and shall be specified as stipulated in the paragraph 4.1.5.

4.1.5 The value of "Z" (in per cent) shall be agreed upon between purchaser

TABLE A1

TESTS FOR IDENTIFICATION REQUIREMENTS

TEST NO.	PROPERTIES DETERMINED ON ACTUAL SEALS	[a] TEST PROCEDURE	PHYSICAL REQUIREMENTS
Group I			
1	Tensile Strength, min. psi (kg/cm^2)	D-412	[c] 2000 (141)
2	Elongation at break, min. per cent	D-412	250
3	Hardness, Type A, Durometer	[b] D-2240	55+5 -5
4	Permanent Set at Break, max. per cent	D-412	10
Group II			
5	Oven or heat aging 70 hrs./212°F	D-573	
	a. Tensile strength, change, max. %		+10 to -20
	b. Elongation, change, max. per cent		-20
	c. Hardness, Type A, points change		0 to +10
6	Ozone resistance 20% strain, 300 pphm in air, 70 hrs./104°F(40°C) (Wipe with solvent to remove surface contamination)	D-1149	No cracks
7	Oil Swell, ASTM Oil #3, 70 hrs./212°F Weight Change, max. per cent	D-471	+45

[a] These designations refer to the following methods of the American Society for Testing and Materials:

D-412, Test for Tension Testing of Vulcanized Rubber

D-395, Test for Compression Set of Vulcanized Rubber

D-573, Test for Accelerated Aging of Vulcanized Rubber by the Oven Method

D-471, Test for Change in Properties of Elastomeric Vulcanizates Resulting from Immersion in Liquids

D-1149, Test for Accelerated Ozone Cracking of Vulcanized Rubber

D-2240, Test for Indentation Hardness of Rubber and Plastics by Means of a Durometer

D-575-67, Test for Compression-Deflection Characteristics of Vulcanized Rubber

E-4-64, Verification of Testing Machines

[b] The hardness test shall be made with the durometer in a durometer stand.

[c] For sealer sizes larger than four (4) inches in width the "Minimum Tensile Strength" of 1800 psi is required.

TABLE A2

TESTS FOR QUALIFICATION REQUIREMENTS
(simulated service tests)

Group III			
8	High Temperature Recovery	[d] Subsection 8.1 to 8.1.1.3	
	70 hrs./212° under [e] "Z"% deflection		85% min.[f] (no cracking or sticking)
9	Low Temperature Recovery	[d] Subsection 8.1 to 8.1.1.3	
	72 hrs./+14°F under 50% deflection		88% min.[f] (no cracking or sticking)
10	Low Temperature Recovery	[d] Subsection 8.1 to 8.1.1.3	
	22 hrs./-20°F under 50% deflection		83% min.[f] (no cracking or sticking)
11	Pressure-deflection	[d] Subsection 8.1.2	
	20% deflection at 73°F ± 2°F		
	a. Min. contact pressure, psi		"X"
	b. Max. Pressure-decay, percent "Z"% deflection @ 73°F ± 2°F		"Y"
	c. Max. contact pressure, psi		200

[d] The reference Subsections are those of this specification.

[e] "Z"% deflection is defined and numerically specified in Subsections 4.1.4 and 4.1.5.

[f] Cracking or splitting and/or sticking of specimen during recovery shall mean that specimen has failed the test.

and the manufacturer as stipulated in paragraph 4.1.4 and so specified in the purchaser's specification and/or drawings.

5. Quality Control of Material

5.1 The amount of Initial Contact Pressure which sealers shall be capable of exerting uniformly when compressed is stipulated in paragraphs 5.1.1, 5.1.2 and 5.1.3.

5.1.1 The minimal Initial Contact Pressure at 20% deflection for any size of bridge sealer shall be "X" pounds per square inch (lbs/in ^{2}) on the third successive test-run or cycle, at which time the pressure-decay shall not exceed "Y" per cent (%) from the first test run. ("X & Y" values must be established by tests.) Calculate pressure-decay at 20% deflection as follows:

$$\% \text{ Pressure-decay} = \frac{\text{Pressure at 1st test run - Pressure at 3rd test run}}{\text{Pressure at 1st test run}} \times 100$$

5.1.2 The maximum Initial Contact Pressure at "Z"% deflection for any size of bridge sealer shall not exceed 200 pounds per square inch (lbs/in ^{2}) on the first test run or cycle.

5.1.3 The amounts of Initial Contact Pressure (lbs/in^2) are based on the actually measured length (6 in) and height (H_a) of the sealer's test sample; they shall be established on the basis of three successive test runs or cycles, performed on the Compression Testing Machine (ASTM Designation: E4). Calculate Initial Contact Pressure as follows:

$$\text{lbs/in}^2 \text{ Pressure} = \frac{\text{Total Pressure}}{\text{Actual Contact Area}} = \frac{P}{6.0 \times H_a}$$

6. Sampling

6.1 A lot shall consist of a quantity for each cross section agreed upon by the purchaser and manufacturer.

6.2 The schedule of minimum lengths of samples for testing purposes, graduated by sealer sizes, is prescribed in Table A3.

6.3 In all tests, the material to be tested shall be furnished from standard production.

6.4 The specimens shall be taken at random from each new shipment of the preformed sealer.

TABLE A3

Minimum Lengths of Samples for Testing Purposes

Properties \ Sealer size widths	6"	5"	4"	3" to 3-1/2"	2" to 2-1/2"	1-1/2" to 1-3/4"
	Lengths of samples (inches)					
Tensile Strength, Elongation, Hardness, Permanent Set	6	6	6	6	6	18
Oven Aging, Tensile Strength, Elongation, Hardness	0*	0	0	6	6	18
Ozone Resistance	0	0	0	0	6	0
Oil Swell	0	0	0	0	0	0
High Temp. Rec.	6	6	6	6	6	6
Low Temp. Rec.	6	6	6	6	6	6
Low Temp. Rec.	6	6	6	6	6	6
Pressure-deflection	6	6	6	6	6	6
Total	30	30	30	36	42	60
Reserve for duplicate testing	6	6	6	6	12	12
Min. length of sealer sample	36	36	36	42	54	72

*"0" means that for the specific test no additional sample length is required.

7. Specimen Preparation

7.1 Compliance with the requirements of this specification shall be determined by tests conducted in accordance with the methods specified, using specimens cut or buffed from the actual extruded compression joint sealers.

7.2 Specimens for the high and low-temperature recovery tests shall consist of six-inch lengths of the preformed sealers.

7.2.1 In the high-temperature test the internal surfaces shall remain as received from production while the outside surfaces only may be dusted off with talc to prevent them from sticking to the steel compression plates.

7.2.2 For the low-temperature tests, to prevent adhesion, talcing of outside and internal surfaces is desirable.

7.3 Specimens for pressure-deflection test shall consist of six-inch lengths of preformed sealers.

7.3.1 In the pressure-deflection test, to prevent adhesion, talcing of outside and internal surfaces is desirable.

8. Methods of Testing

8.1 Perform the high and low-temperature recovery test and the pressure-deflection test, using specimens prepared in accordance with 7.2, 7.2.1, 7.2.2, 7.3 and 7.3.1 respectively. Use a new specimen for each test.

8.1.1 Deflect the specimens between parallel plates to 50 percent (%) or "Z" percent (%) of the nominal width in accordance with the schedule shown in Table A2 using the compression set clamp assembly described in ASTM D395, Method B. Each width measurement shall be taken in the center of a six-inch length using a dial caliper graduated in thousandths of an inch.

If a gauge is used, it shall have a 1/4 inch diameter foot and shall be mounted on a platform. The dial caliper, made of stainless steel hardened throughout, shall be carefully calibrated. The width measurements shall be made at both the top and bottom longitudinal edges of the specimen. For this purpose, each edge shall be placed at the center of the foot of the gauge or at the measuring tips of the caliper jaws. The position of the foot or jaw shall be carefully marked on the specimen before the first reading is made.

Prior to compression, the specimen shall be placed in such a horizontal position that the plane, through both edges of the top surface of the sealer, is perpendicular to the compression plates. As the specimen is being compressed, the top surface of the joint sealer shall fold inward toward the center of the specimen. The compressed width shall be measured on the centers of all four (4) sides of the clamp assembly, with a carefully calibrated internal-dial caliper.

8.1.1.1 Low Temperature Tests: Expose the clamp assembly with the compressed specimen in a frost-free refrigerated box for the time and at the temperature specified in Table A2. To achieve the frost-free condition, a sufficient amount of a disiccant such as calcium chloride shall be placed into the box. When the cold aging period is completed, unclamp the test specimen at the test temperature, allow it to recover for two (2) hours in a free state at the test temperature. At this point, measure the recovery width at the test temperature. The measurements shall be made at the locations at which the original widths were determined.

Calculate the recovery as in 8.1.1.3.

8.1.1.2 High Temperature Tests: Expose the clamp assembly with the compressed specimen for 70 hours in an oven maintained at 212°F± 2°F. Do not preheat the clamp assembly. When the aging period in the oven is completed, remove the clamp assembly and immediately unclamp the test specimen. Cool the test specimen at room temperature (73°F ±4°F) on a wooden surface for one hour before measuring the heat-aged recovery width; this measurement is to be made at the same location as the original width. Calculate the recovery as in 8.1.1.3.

8.1.1.3 Calculations: Calculate the recovery-expressed as a percentage of the original width and in relation to the corresponding recovered width-separately for the top and the bottom measurements. For the determination of physical requirements, use the smallest of the two recovery percentages. Calculate recovery as follows:

$$\% \text{ Recovery} = \frac{\text{Recovered Width}}{\text{Original Width}} \times 100$$

8.1.2 Pressure-Deflection. The pressure-deflection test shall be performed in accordance with the ASTM Compression-Deflection Test Designation: D-575-67, Method A. The speed that must be used in this test shall be at the rate of approximately 0.2 inch/minute. The test shall be performed in a reasonably dust-free enclosure at the constant room temperature (73°F ±4°F).
The specimen shall be placed between the platens of the testing machine in the horizontal position in such a way that a plane through both edges of the top surface of the sealer shall be perpendicular to the platens, which must be larger than the specimen.

The test limits are: "from zero percent (0.0%) deflection until the limit of safe compressibility is established", as described in paragraphs 4.1.2, 4.1.3 and 4.1.4; after this the specimen shall be immediately released at the same rate. This pressure-deflection cycle or test run shall be successively repeated three times as before, and up to the limits of pressure-deflection established in the first run.

The zero percent (0.0%) deflection corresponds to a pressure of zero pounds (0.0 lbs). The pressure exerted by the sample, its deflection, and the time-

schedule of test run, shall be continuously read and recorded from the beginning till the end of the test.

For the purpose of graphing the pressure-decay, the time at the beginning and the end of a cycle, and the rate of speed, shall be read and recorded.

9. Certification and Acceptance

9.1 The acceptance of the preformed elastomeric joint sealer shall be based upon one of the following procedures as specified by the purchaser:

9.1.1 A certification indicating conformance to the test requirements, including the value of "Z" (in per cent).

Each lot of the joint sealer shall be identified with the manufacturer's name or trade mark and shall be accompanied by the manufacturer's affidavit attesting his conformance with the test requirements as well as a copy of the manufacturer's test report. Each certification so furnished shall be signed by an authorized agent of the manufacturer.

9.1.2 A certification by an independent testing agency of test results indicating the material has been sampled, tested, and inspected in accordance with the provisions of the specification. Each certification so furnished shall be signed by an authorized agent of the testing agency.

9.1.3 Testing by the purchaser of any or all properties in accordance with the provisions of the specification.

9.1.4 Any alternative method agreed upon by the purchaser and manufacturer.

New Developments in Joint Sealing Practice for Longer Spans

STEWART C. WATSON, Acme Highway Products Corporation

ABRIDGMENT

Refinements in structural analysis; improved knowledge of material properties; wider use of prestressed concrete, composite construction, all-welded structures and battle decks; as well as radical changes in aesthetic tastes resulting in slender lines have operated to place increased emphasis on the need for improvements in jointing and joint sealing practices for our modern bridges and structures (see Figs. 1 and 2).

It is the intent of this discussion to redefine the magnitude of this developing problem, to survey what has been accomplished both here and abroad and to suggest what can be done in the light of present knowledge.

PERFORMANCE CHECKLIST FOR SEALING SYSTEMS

Based on a world study of premature bridge distress related to joints, a 17-point performance checklist has now been developed to assist bridge design engineers in determining the ability of a candidate sealing system to perform in the bridge environment.

SAWED BRIDGE EXPANSION JOINTS

The present state of the art for tandem blade sawing of bridge expansion joints is graphically portrayed and the method justified since it offers advantages in service life and the opportunity to attain temperature-width controls in as-constructed joint geometrics.

Figure 1. Rhine Harp Bridge is a 1706-ft continuous span supported by 161-ft twin pylons with steel hawsers.

Figure 2. Needle-thin prestressed concrete design.

Paper sponsored by Committee on Sealants and Fillers for Joints and Cracks in Pavements and presented at the 48th Annual Meeting.

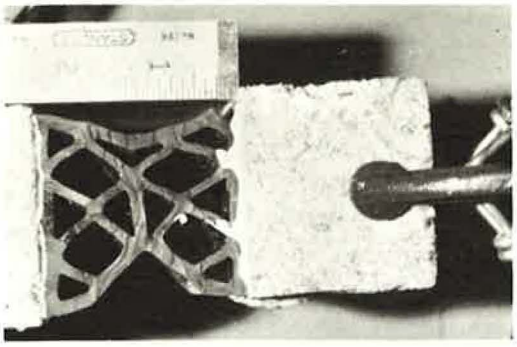

Figure 3. New adhesive system can stretch compression seal 25 percent beyond original width before peel occurs.

LUBRICANT-ADHESIVES WITH RUBBER TEARING BONDS

Improved lubricant-adhesives offering rubber tearing bonds (Fig. 3) have been developed and are available which markedly improve on compression seal performance, more positive leakproofing, skew-rack eccentrics and enhanced stroke of movement capability under unforeseen dynamic movement conditions. Aqueous epoxy lubricant-adhesives are now being used in underwater environments and for inclement weather compression sealing

Categorically stated, the mission of the lubricant-adhesive in compression sealing is threefold: to lubricate the joint interfaces and permit ease of installation, to prime the joint interfaces with a high solids filler, and to produce a rubber tearing bond. It is now considered essential that an impervious continuity be achieved between both sides of the seal configuration and both faces of the joint walls.

SKEWED BRIDGE JOINTS

Since most bridge joints are constructed on some varying angle of skew, special consideration should be given to determining the magnitude of racking movement that occurs when these longitudinal and angular movements take place at the interfaces of joints concurrently (Fig. 4).

There are definite limitations in the amount of racking movement that typical sealing systems can handle under certain conditions. When a sealing system's ability to absorb racking is exceeded, consideration should be given to bonding or fixing one side of the sealing element while arranging for the opposite side to be free sliding, possibly utilizing a surface of fluorocarbon.

PRECOMPRESSED SEALS IN ARMOR-PLATED JOINTS

The desire for perfection in joint sealing on the part of European engineer-contractor firms, who must guarantee performance for long periods of time, has led to the practice of precompressing seals in armor-plated joints in factories, and then taking them to the bridge site to be integrally cast into the decks.

Ideal conditions for leakproofing, bonding of seals in place, neatness, workmanlike and precision adjustment to temperature width can be assured under these circumstances. Obviously, to achieve a completely leakproof joint, this practice would offer a most desirable set of conditions (Figs. 5 and 6).

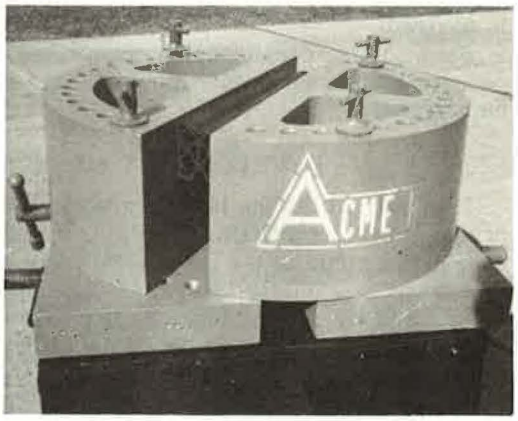

Figure 4. Variable skew testing machine programs both longitudinal and skew movements concurrently.

RUBBER CUSHION JOINTS

European experience has been relatively short-lived, since rubber exposed to traffic, abrasives and snowplows is highly subject to attrition for the same reason that rubber tires and shoe heels sustain wear. Because the rubber is

Figure 5. Factory prefabricated compression seal for a skewed bridge joint.

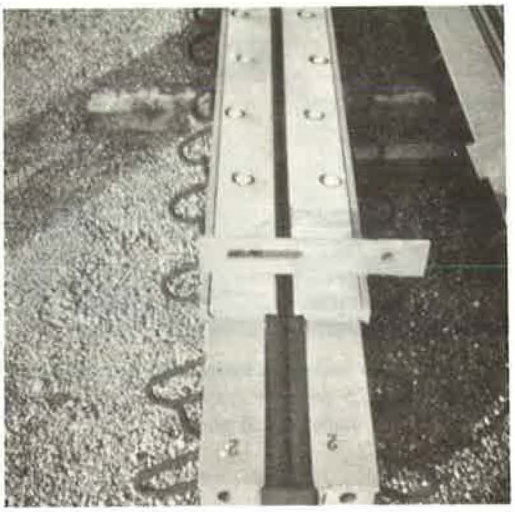

Figure 6. Prestressed prefabricated seal with cantilevered armor to lessen joint gap.

subjected to severe tension during the colder portion of the temperature cycle, its serviceable life is markedly reduced as a function of this prolonged stretching. Plastic flow occurs during the stretch cycle of weather, and in the second and successive cycles, its direction of traffic dimension becomes progressively longer resulting in buckling and a resultant banging under traffic as the device responds to the opposite pole of the temperature gap. These rubber cushions must be carefully caulked with high solids adhesives or sealers along the underside as well as their periphery and the short lengths in which they are fabricated (normally 4- to 6-ft long moldings) present a challenge to workmen because careful end-to-end bonding must be accomplished in the field.

In Europe, they have not normally been taken through curb lines since it is not practical for rubber producers to produce specially contoured moldings to match individual bridge and curb configurations; however, this is the critical area of a bridge insofar as the sealing problems are concerned. Field vulcanizing of these rubber sections into one length transversely across a bridge, up, and through the curbs is now being accomplished in one country and is an absolute necessity if a leakproof joint is desired.

Skew joints, creep-shrink, progressively opening or closing joints and deck-to-curb-to-balustrade transition problems have operated to complicate their application on bridges.

DEVELOPMENT OF MODULAR SEALING CONCEPT

It is only within the last decade that the development of a modular concept of compression sealing utilizing multiples of monolithic compartmented extruded neoprene shapes has come to the fore. The trend to longer and longer spans, the realization that there is a definite causal relationship between costly premature bridge distress and ineffective sealing practices, plus the European practice of placing legal responsibility for maintenance on the engineer-contractor, has led to the rapid development of multi-seal or modular systems (Figs. 7 and 8).

A number of variations of modular systems have been in use for the past ten years, the most popular being the RUB System. It is in wide use throughout practically every country in Europe, as well as South Africa, Asia and the Far East, with a record of service approximating thousands of bridges, most of them being longer spans.

Figure 7. Four-tube modular system in transit to joint area.

Although it is technically possible to seal joints on bridges with monolithic seals in joint openings up to 6 in., tolerable width considerations have resulted in a "sandwiching up" of smaller configurations.

Figure 9 illustrates a new North American modular sealing system covering a range of movement from 3 to 12 in. with each compartmented tube being responsible for 1½ in. of movement separately. It is actually adapted from standard monolithic bridge seal configurations now in wide use on short- to medium-length spans with the exception that the standard cross-braced shape has been redesigned to be functionally isotropic from top to bottom in an attempt to equalize sealing pressure generation along the steel separation plates.

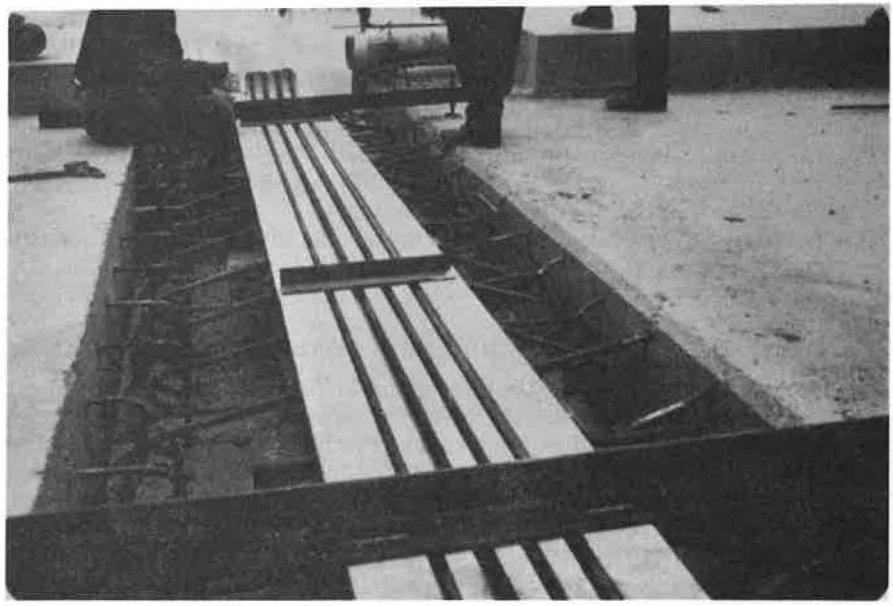

Figure 8. Modular system for 6-in. movement being adjusted to deck temperature.

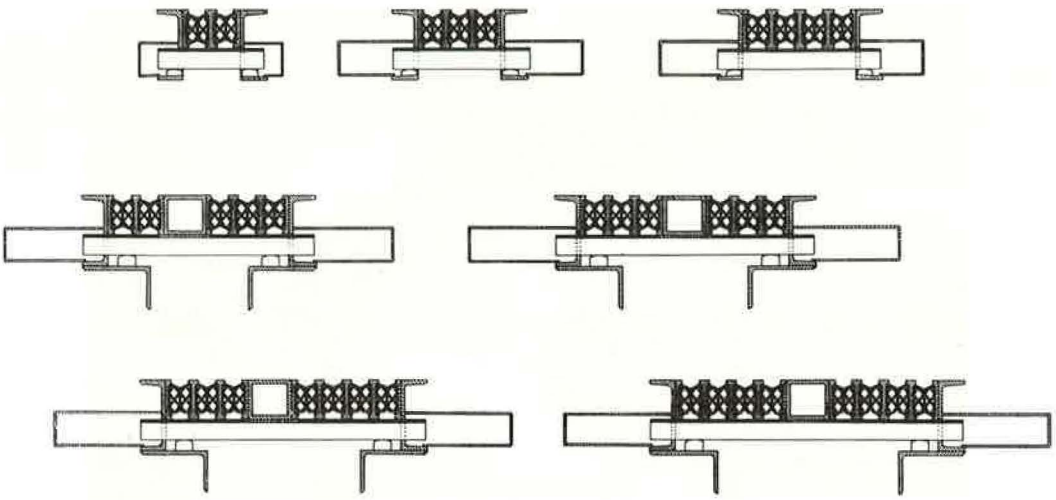

Figure 9. Typical North American modular sealing systems for 3 to 12 in. of movement, each tube individually responsible for 1½ in.

Since modular systems are factory prefabricated, they are preset to the anticipated temperature width and then taken to the bridge site for placement in the deck. After the concrete is placed and before excess drying shrinkage or any movement takes place, the system is activated.

The time-dependent eccentricities of movement associated with long-span bridges have been fully documented and must be accounted for in the design of a sealing system. Suffice it to say, it is not unusual to sustain permanent changes in joint width, in addition to regular thermal change, resulting in either progressively increasing or progressively decreasing joint openings. The modular sealing systems take this into account and individual seal cross sections or separator plates can be added or taken out to either relieve compressive stress or increase the movement capability as the case may be.

An example of this design versatility being used on the new Florenceville Bridge in New Brunswick is shown in Figures 6 and 7. This system was engineered to accommodate 6 in. of movement.

While there is virtually unlimited movement potential in a modular system, the largest displacements being attempted today in North America are on the Halifax-Narrows Bridge in Nova Scotia (18 in. of movement) and the West Lynn Bridge across the Willamette River in Oregon (12 in. of movement).

Modular sealing systems are tailor made to suit the dictates of each specific bridge. However, standardization of parts has been the rule being restricted to the six basic components as shown in Figure 9.

HEAVY DUTY BRIDGE COMPRESSION SEALS NOW IN WIDE USE

Compression sealing techniques are now being employed in an attempt to stretch out the maintenance free life of Verrazano-Narrows Bridge, Golden Gate Bridge, George Washington Bridge, Narraganset Bay approaches to Newport Bridge, Delaware Memorial original structure and approaches, Triborough Bridge, Burlington Skyway (Canada) and a number of long-span European bridges.

Development of Effective Poured-in-Place Systems for Concrete Pavement Joints

JOHN M. PACHUTA and DANIEL J. SMITH, Thiokol Chemical Corporation, Trenton, New Jersey

Four years ago Thiokol began to investigate actively the problems involved in sealing transverse highway joints. A series of highway joints were sealed with a number of first-generation highway sealants and periodically investigated for failures. A study of the failures and attempts to duplicate them in the laboratory resulted in new or improved tests of adhesion, cohesion, stress relaxation, and dynamic cycling resistance. Sealant and slab temperature gradients, joint movement, and the relationship of these variables were also investigated, as were nonthermal joint movements in shear and vertical displacement. The results of these studies led to a new testing device and technique that defined and artificially reconstructed an ideal national year in terms of temperature and joint movement.

The study of four second-generation systems in this device resulted in one final sealant system, which was then commercially installed under actual field conditions. After one year of use this sealant's good performance to date reaffirms the validity of the new test method.

•SOME years ago, Thiokol began an active program to determine the physical properties and aging characteristics needed for an effective poured-in-place joint sealant system. Initial investigations were carried out in the field to determine the types of problems that occurred. The ultimate goal was a series of laboratory tests that would screen sealants. Economics dictated this approach, provided laboratory data were a relative measure of field performance. Periodic photographs of both the commercial and laboratory sealants, which were installed in the field, comprised an accurate record of the types of sealant failures that developed. Four major types of sealant failures were identified.

1. The most prevalent and quickest to appear were failures due to lack of sealant adhesion to the sides of the concrete joint. Considering that highway joints are continuously moving, it is important that the sealant adhere to the sides of the joint almost instantaneously, under the following conditions or combinations thereof: high or low temperatures, dry or damp joint surface, expanding or contracting slab, and with or without movement of vehicular traffic.
2. Another prevalent failure was cohesive rupturing of the joint sealant within itself, while subjected to extension and compression after months of exposure to environmental conditions. The majority of these sealant failures were caused by the dynamic stresses imposed by thermal expansion and contraction of the concrete.
3. Failures caused by improper mixing of the two sealant components were identified. Striations of improperly mixed sealant were dispersed throughout the sealant

Paper sponsored by Committee on Sealants and Fillers for Joints and Cracks in Pavements and presented at the 48th Annual Meeting.

within the joint. Eventually they appeared, seemingly as cohesive failures, whereas similar striations at the sealant concrete joint interface appeared as adhesive failures. Obviously, disproportionate mixing of sealant component viscosities and/or volume ratios increased the magnitude of this problem and the frequency of its occurrence, whereas color-coded component differentials decreased them.

4. Sealants that were of sufficient quality to resist adhesive, cohesive, and mixing failures eventually began to crack or tear wherever localized stress concentrations in the sealant occurred, causing points or planes of weaknesses. These would eventually progress, over the years, through the sealant until failure occurred.

As development work progressed, three sets of laboratory tests were developed to simulate the field conditions and screen prospective sealant systems. The adhesion series of laboratory tests consisted of both destructive testing and sealant extension durability testing during artificial aging simulation. In the former case, sealants of a ½- by ½- by 2-in. geometry were extended to failure as a uniform rate on a tensile test under the following conditions: after aging at room temperature and after aging at 158 F and in H_2O (each individually for one week). Lack of any adhesive failure was a prime requisite for selection of a sealant system. In the latter case, sealant test samples were extended 100 percent and then subjected to water, heat, and cold conditions to simulate the adverse environmental conditions in the field.

In addition to adhesion testing of the original laboratory-made sealant specimens, tests on aged sealants were also recognized as important. This resulted in a series of screening tests which measured a sealant's change in hardness and percent weight loss, after aging at elevated temperatures. Such tests tended to eliminate sealant systems containing quantities of volatile plasticizers or solvent components. The loss of volatile materials from the sealant imposes a volume shrinkage that induces internal stresses and makes the sealant susceptible to cohesive failures.

A Bostic cycling machine (Fig. 1) was used to extend and compress repeatedly sealant samples at room temperature, thereby simulating years of dynamic cyclic movement which sealants must withstand—compressing years into days. As dynamic testing of the sealants progressed, it was deemed necessary and desirable to vary the temperature during the cycling test, since the sealant's physical properties will change over a range of temperatures as witnessed by seasonal conditions in the field. The cycling machine was housed in an environmental chamber, and the test cycling fixture compressed the sealant as the temperature rose from 55 to 130 F and extended the sealant while the temperature dropped from 55 to -20 F, thus versus time giving a sinusoidal curve. This expressed sealant movement versus temperature change as shown in Figure 2. A complete cycle was adjusted to a 24-hr period that was postulated to simulate the movement over a year's period.

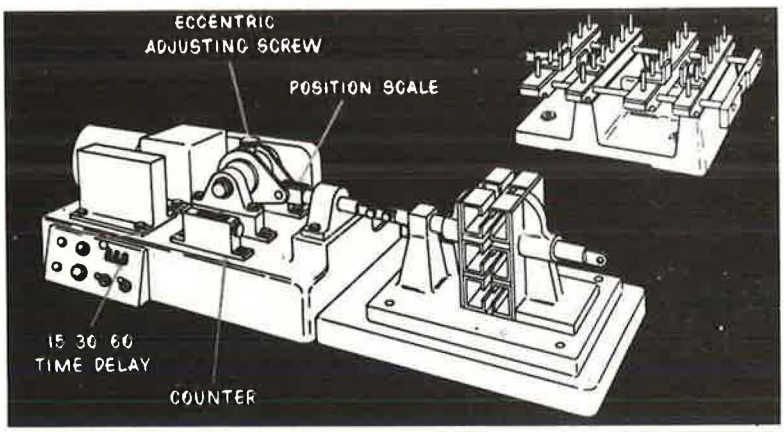

Figure 1. Bostic cycling machine.

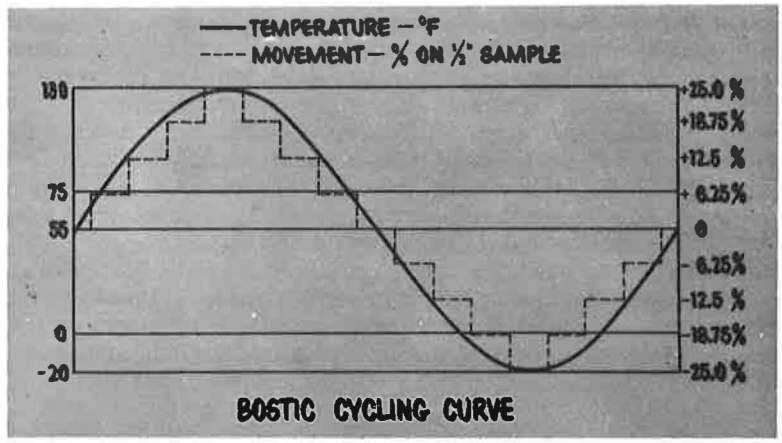

Figure 2. Temperature vs movement.

The development program encompassed three generations of sealants. The sealant extension durability tests provided the ability to overcome adhesive and cohesive failures, whereas heat aging at elevated temperature provided information on how to avoid high weight loss, thereby decreasing the sealant's volume shrinkage on aging. The use of the dynamic cycling tester provided the necessary information to tailor the third generation sealant. It was found that this material could withstand repeated cycles of 25 percent compression and extension over a temperature range of -20 to 130 F. The third generation sealant was chosen for promotion and is now commercially available.

A major contributing factor on the life expectancy of a sealant in the field is the dynamic condition imposed by the movement of the joint due to thermal expansion and contraction of the concrete. Analyzing F. C. Lang's experimental work (1) at Worthington, Minnesota, it can be concluded that the joint movement correlates with the average temperature of the concrete rather than average air temperature. On sunny days, the average concrete temperature is significantly higher than the average air temperature, producing movements greater than would be anticipated from air temperatures. This is due to the absorption of solar heat by the concrete slab.

In Lang's experiment, concrete slabs with lengths ranging from 25 to 60 ft were used. Thermocouples were embedded within the slab 1 in. apart starting ½ in. below the sur-

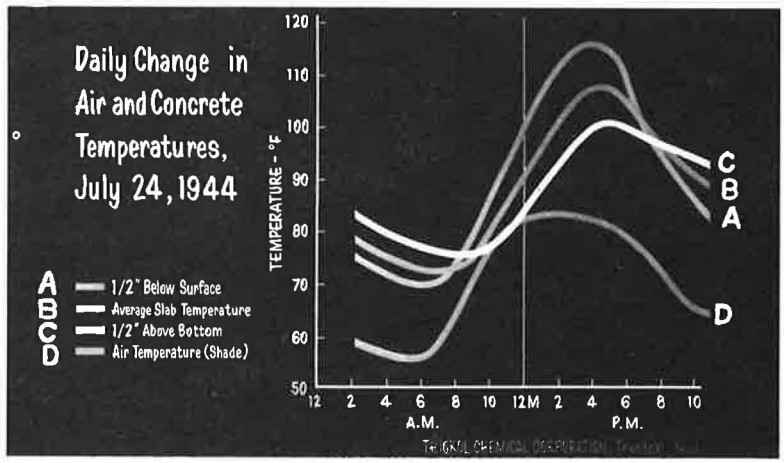

Figure 3.

face and down through the concrete to within ½ in. of the bottom. When hourly temperature and joint movements were made under typical climatic conditions, which included a sunny day, an excellent correlation prevailed between the average slab temperature and joint movement. It is significant to note that the average slab temperature had reached a temperature about 20 F higher than the air temperature (see curves for the air temperature and the average temperature, Fig. 3). However, during cloudy winter days the average slab temperature was essentially the same as the average high temperature. Thus, in utilizing this information with the temperature extremes attained during a typical year, it can be established that the average slab temperature will vary in Minnesota from -20 F in winter, to approximately 130 F during summer, giving a total differential of 150 F. This differential causes joint movements significantly larger than those anticipated only from average air temperature.

To continuously measure joint movement, Thiokol utilized an inexpensive device consisting of a rectilinear potentiometer and a simple, rugged, inexpensive transducer. The mounting of the transducer device across a joint is shown in Figure 4. A concrete highway bridge was instrumented for slab temperature and joint movement. Thermocouples were installed at several points and at varying depths at each of the location points. Figure 5 shows joint movement with changes in temperature at the surface and at the center of the depth of the slab during a 5-day period in the summer. An excellent correlation is shown for the joint movement with the temperature at the center of the slab. As in Lang's work, the peak temperature at the center of the slab was 20 to 25 F above the ambient air temperature.

Based on a paper by Barber (2), we computed the seasonal temperature differential which affected slab movement based on the air temperatures. We then developed a temperature differential map for the continental United States (Fig. 6). In general, the temperature differential areas fall into three groupings: (a) higher differentials in the North and Northwest, (b) middle differentials in the Northeast and Central, and (c) lower differentials in the Southeast. The average differential is 154 F.

Using an average temperature differential of 150 F and the ability of the sealant to withstand continuous cycling of 25 percent compression and extension, the recommended joint widths were then computed for the various slab lengths (Table 1). The depth of the sealant is controlled to give a rectangular profile where the sealant width is twice

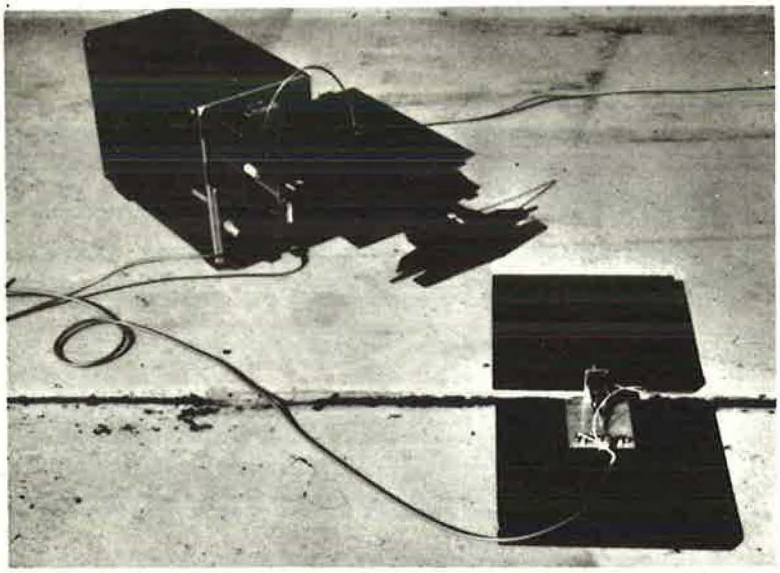

Figure 4. Joint movement measuring device.

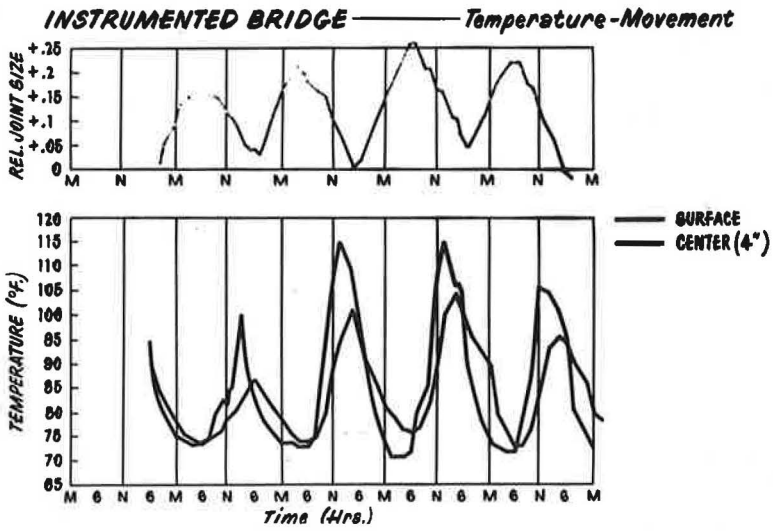

Figure 5. Joint movement and slab temperature.

the height. However, above a 1¼-in. joint width, the sealant depth is retained at ⅝ in. because increase in sealant depth only induces additional strains on the sealant. The optimum condition for cycling would be to have a sealant depth as thin as possible. Any increase in sealant depth imposes higher strains on the sealant. However, a minimum sealant depth must be maintained to prevent intrusion of incompressibles in the sealant.

The use of a poured-in-place sealant must be considered from a systems standpoint. Proper design, material, and application methods are required to make the sealant

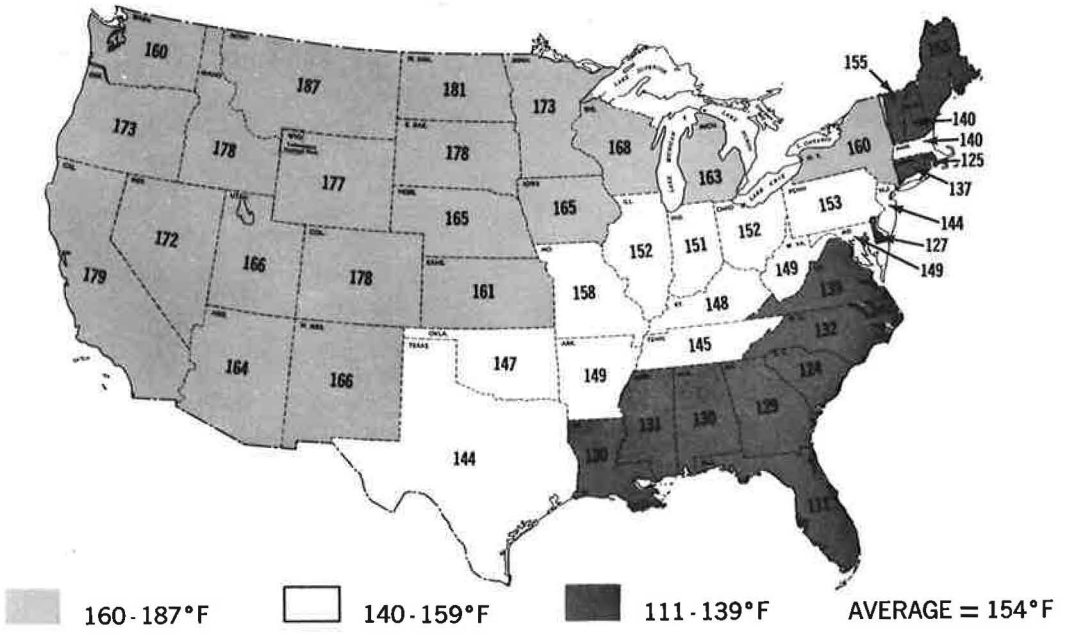

Figure 6. Differential pavement temperatures.

TABLE 1

RECOMMENDED TRANSVERSE CONTRACTION JOINTS

Spacing of Joint (ft)	Joint Width (in.)	Joint Depth (in.)
20	½	⅜
30	½	⅜
40	⅝	⅜
50	1	½
60	1¼	⅝

perform satisfactorily. With our LP® polysulfide base sealant system we recommend:

1. Cleaned joints, preferably by sawing,
2. Use of the proper joint dimensions for slab length,
3. Use of a nonbituminous back-up material to control the sealant depth,
4. Repair of all joint spalls, and
5. Use of a primer and proper mixing and application of sealant.

By utilizing this system's approach, effective sealing of concrete pavement joints can be achieved. By using these criteria it is expected that a life of eight years or more can be obtained in a joint sealed with an LP® polysulfide base sealant.

In conclusion, it is possible to formulate and provide effective, long-lasting, poured-in-place joint sealant systems for highway joints. To date, our experimental program has allowed us to quickly screen and evaluate LP® polysulfide polymer joint sealant systems in the laboratory, with a high level of confidence in regard to their field performance ability. Consequently, better LP® polysulfide base sealants have been developed and better performance will result if the right material is selected, the right joint design is specified and used, and if proper application techniques are followed.

REFERENCES

1. Lang, F. C. Investigational Concrete Pavement in Minnesota. Highway Research Board, Research Report No. 3B, p. 58-72, 1945.
2. Barber, Edward S. Calculation of Maximum Pavement Temperatures from Weather Reports. HRB Bull. 168, p. 1-8, 1957.

Fabrication and Erection of Poplar Street Orthotropic-Plate Deck Girder Bridge

E. J. SHIELDS and A. E. SCHMIDT, Sverdrup & Parcel and Associates, Inc.

This paper describes design concepts concerning construction, and the fabrication and erection techniques employed on the first major orthotropic-plate deck girder bridge undertaken in the United States. The bridge was completed in November 1967.

Except for a small amount of structural shapes, the bridge is composed of plates of various types of steel. The article describes the jigs and special handling equipment used to fabricate and assemble large orthotropic-plate deck sections and large welded box girders. It illustrates the special mounting of welding equipment used to perform the miles of automatic submerged-arc welding, and it describes the shop-assembly procedures. Erection sequences, erection equipment, and suspended trolley platforms are described and illustrated.

It was learned that precise and accurate fabrication methods, coupled with good supporting equipment, permitted extensive use of automatic welding equipment for the miles of welding required on the bridge. Another conclusion was that large units of deck sections and girder sections could be economically fabricated and erected.

•THE Poplar Street Bridge, crossing the Mississippi River at St. Louis, is the first major orthotropic-plate deck girder bridge in the United States. This bridge type (Fig. 1) was recommended in a preliminary engineering report completed in 1961 by Sverdrup & Parcel and Associates for the States of Illinois and Missouri as being aesthetically satisfying, as providing motorists a clear view of the St. Louis waterfront, and as being economically attractive. Final design was completed in 1964 and construction was finished in November 1967.

Dravo Corporation was the substructure contractor and, under a prime contract, Bethlehem Steel Corporation fabricated and erected the structural steel. A separate contract included the concrete curbs, parapets, and the wearing surface. Field painting was done under another contract. The total cost of all construction was $13,260,000.

The 2,165-ft bridge is composed of five spans; the 600-ft central span is the longest. Since the three main spans and parts of each of the end spans are over water during normal river stages, the design plans were based on water shipment to permit fabricating larger units in the shop, thus leaving fewer pieces to be erected and joined in the field.

The eight-lane roadway is divided into two separate four-lane structures supported by common substructure units. Each four-lane deck is supported on two box girders (Fig. 2). The deck is thus divided into a center deck section of about 27-ft width between the girders, and about 9-ft wide cantilever sections outside each girder. The deck units were field-bolted to the girders at the floorbeams, which are spaced 15 ft apart and are connected by continuous welds in the deck plate.

Paper sponsored by Committee on Construction Practices—Structures and presented at the 48th Annual Meeting.

Figure 1. General view of the completed bridge.

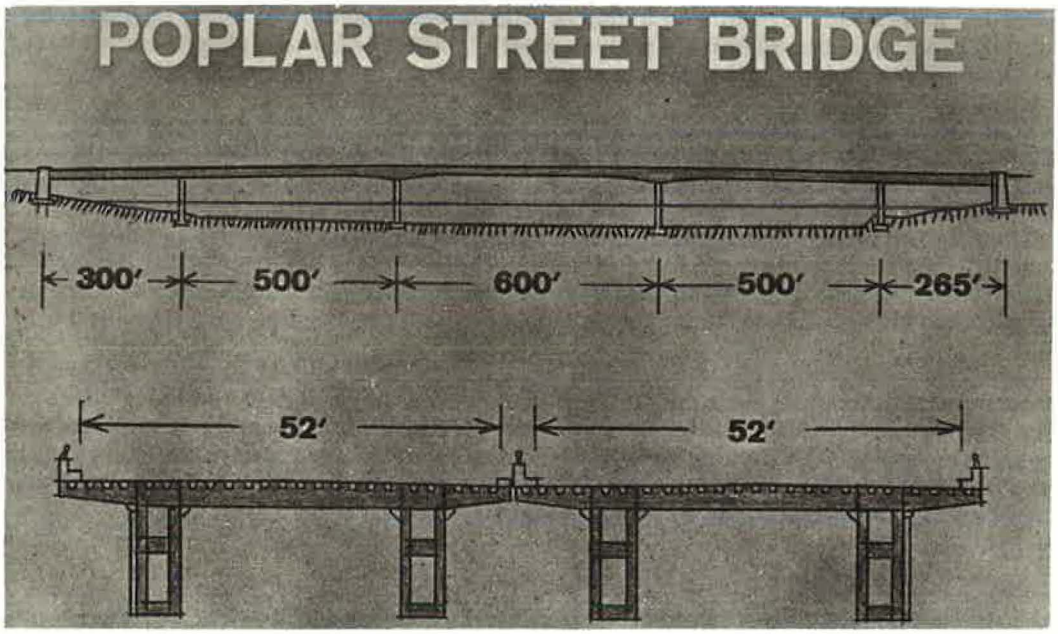

Figure 2. Spans and bridge cross section.

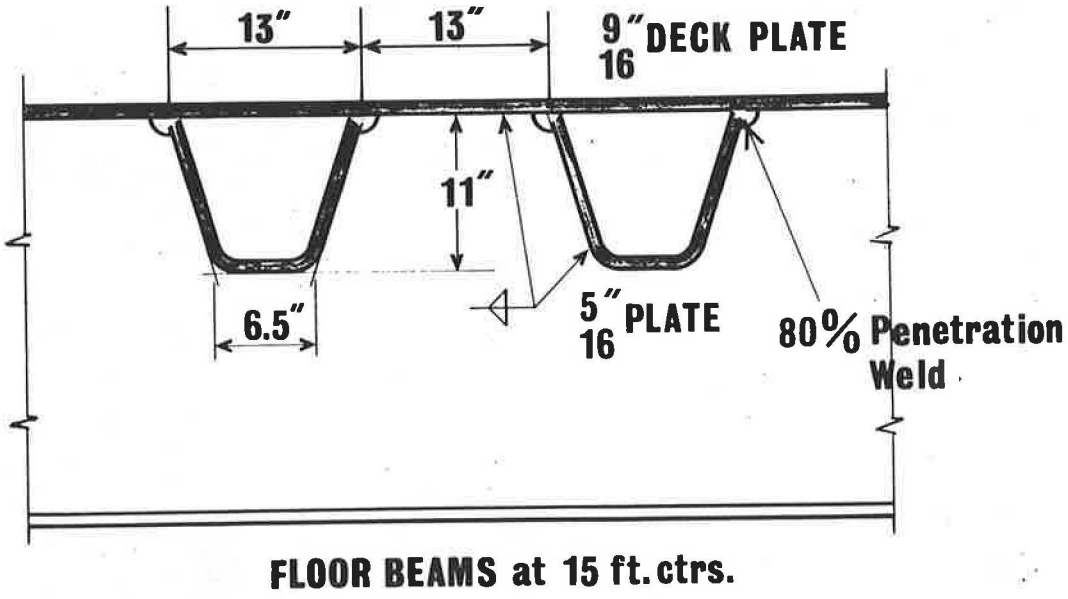

Figure 3. Selected orthotropic deck elements.

DECK UNIT FABRICATION

The main elements of the orthotropic plate are shown in Figure 3 along with the dimensions and spacing of the trapezoidal stiffening ribs. The stiffeners and deck plate are A-242 atmospheric-corrosion-resistant steel; the floorbeams are A-441 steel. Beginning with flat plates a little wider than required, the stiffeners were automatically

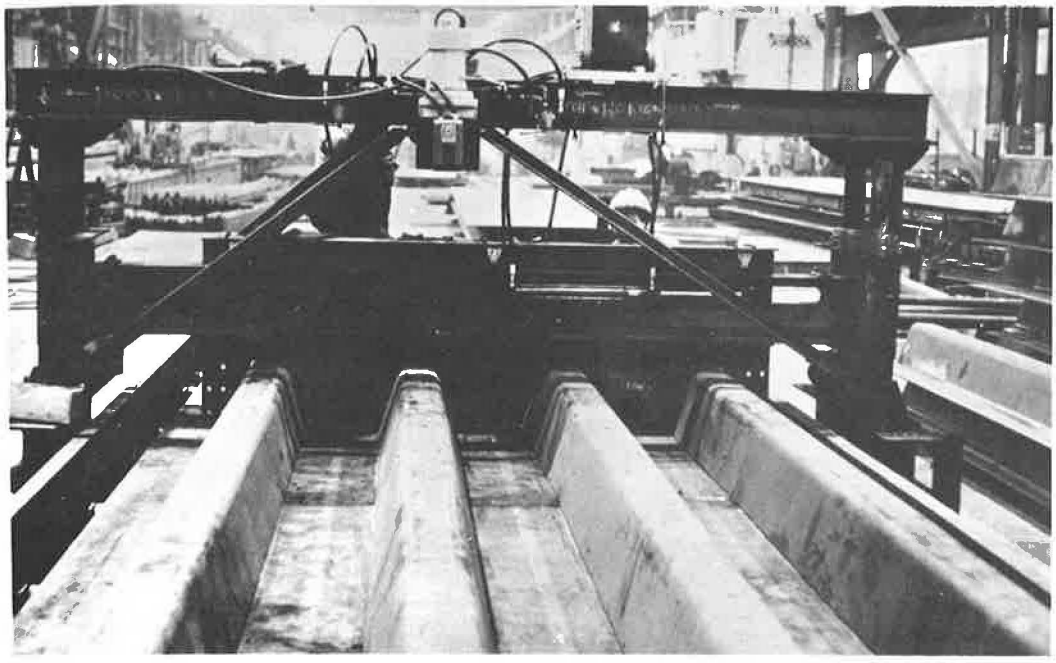

Figure 4. Gantry positioning ribs on deck plate.

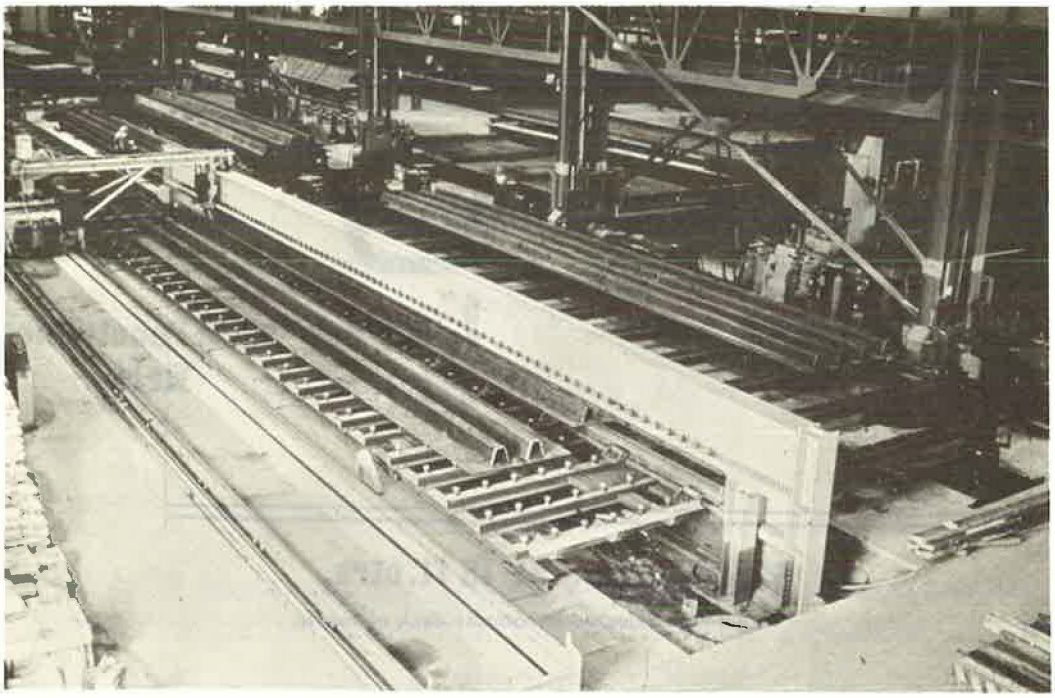

Figure 5. Strongback in operation.

Figure 6. Cutting floor beams to fit the deck ribs.

flame-cut to the exact width and edge-bevel to suit the welding procedure and then cold-rolled into the trapezoidal-shaped ribs in a Yoder mill.

A gaging-gantry positioned four ribs on a 9-ft wide deck plate and also held the ribs in position while short lengths of submerged-arc welds were made (Fig. 4).

A strongback (Fig. 5) was developed to facilitate welding the ribs to the deck plate. This equipment has a template adjustment that was set to counteract welding distortion in the unsymmetrical section. One rib at a time was placed under the strongback, and pressure applied from the underside of the plate forced the assembly to the desired configuration. Submerged-arc, 80 percent penetration welds were deposited on both edges of the rib at the same time. The subassembly was shifted under the strongback as each rib was, in turn, welded to the deck plate.

Three deck plate and rib subassemblies were butt-welded along the bottom side of the deck plate to form a 27-ft wide centerdeck section. These units were later turned over for second-side welding after the floorbeams were fitted.

The floorbeams were made up as three-plate welded girders, and then cut to form two floorbeams. The formed beam was automatically flame-cut near the center of the web with a tape-controlled, multi-torch machine to obtain a good fit around the deck stiffeners (Fig. 6). The two halves were held together to control distortion.

The floorbeams were next fitted to the underside of the deck units, and manually welded to the deck plate and stiffeners (Fig. 7).

The fabrication procedures for the deck sections between the girders were also used for the 9-ft wide cantilever deck units and the 6-ft wide sections attached to the girders.

BOX GIRDER FABRICATION

The box girders are 5 ft 6 in. between webs and vary from 16 to 25 ft in depth. The bottom flange is 7 ft wide and varies from $\frac{3}{4}$ to $3\frac{1}{4}$ in. in thickness. During the fabrication and erection periods a 6-ft width of orthotropic deck formed the top flange of the

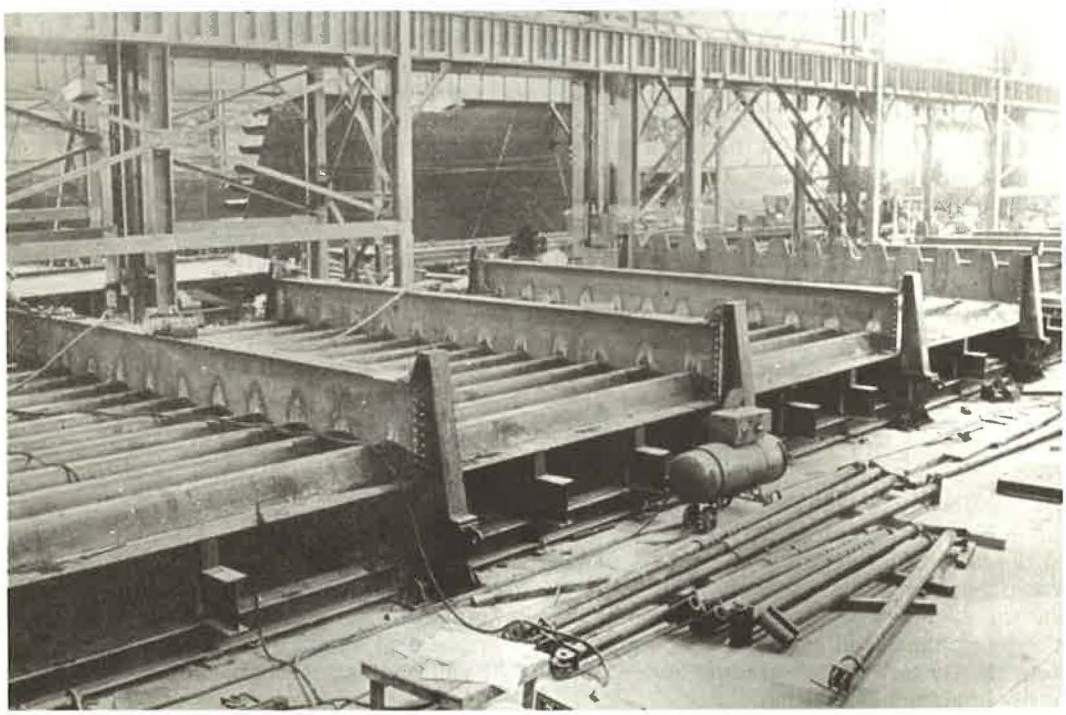

Figure 7. Assembling the floor beams and the deck units.

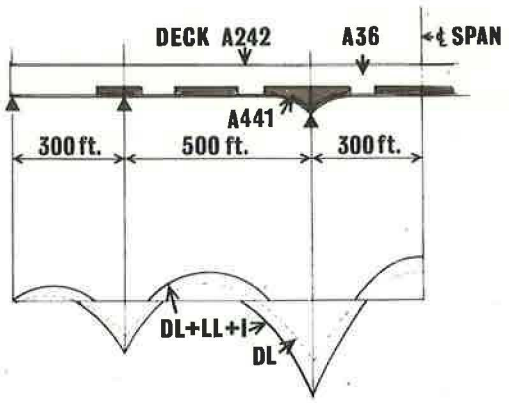

Figure 8. Types of metal in girders.

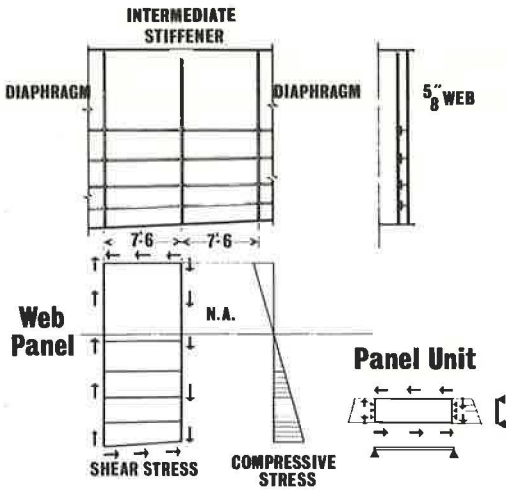

Figure 9. Web plate stiffening members.

girder, and welded connections to the adjacent deck sections completed the girder top flange.

The girder webs and bottom flanges are A-36 and A-441 steel (Fig. 8). The top flange of the girder, comprised of the deck plate and stiffening ribs, is A-242 steel. In addition to providing greater protection against atmospheric corrosion, this metal type was specified to provide for the high stress resulting from girder moments and the stress caused by wheel loads. However, the girder is proportioned so the stress at the top of the web plate is within A-36 steel limitations.

The 2,165-ft girders were each divided into 35 sections, ranging between 56 and 80 ft in length. Items controlling the unit lengths included section weight, change of type of metal in the bottom flange, and change of bottom-flange plate thickness. The deck sections were made the same length as the corresponding girder sections. The heaviest girders were the 113-ton, 70-ft long haunched sections over the piers. The lightest girder sections were each 56 ft long and weighed 56 tons.

The 7-ft wide girder bottom-flange plate was butt-welded, where required, to make up the full length of a girder section. A table jig was used to permit welding on one side and inverting to weld the second side. The submerged arc-welds were ground smooth and fully X-rayed.

The same table was used for laying out the longitudinal plates making up the girder webs. The $\frac{5}{8}$-in. web plates were butt-welded with automatic submerged-arc equipment. After welding on one side, a lifting rig was used to turn the assemblies for second-side welding. The welds on the exterior faces of the outside girders were then ground smooth. After the web plates were welded and inspected, the plates were flame-cut along the edges to the cambered dimensions and shape.

The diaphragms within the box girders were spaced at 15-ft centers, and an intermediate vertical T-stiffener was placed halfway between the diaphragms. The horizontal T-stiffeners were fitted between the vertical elements (Fig. 9). The number and spacing of the horizontal T's varied according to the stability requirements of the webs. The T's were tack-welded into position and, with a specially mounted submerged-arc welder, two fillet welds were simultaneously applied.

A boxing jig clamped the elements of a girder together for tack-and-finish-welding on the horizontal seams (Fig. 10). A sequence was established in which the bottom flange was pressed against one web plate and tack-welded; the diaphragms were then set in place, and the second web-plate was placed and tack-welded to the bottom flange and diaphragms; the top flange (deck section) was next positioned, pressed against the webs, and tack-welded. By turning the girders twice, nearly all longitudinal strength-welds were made in the horizontal position.

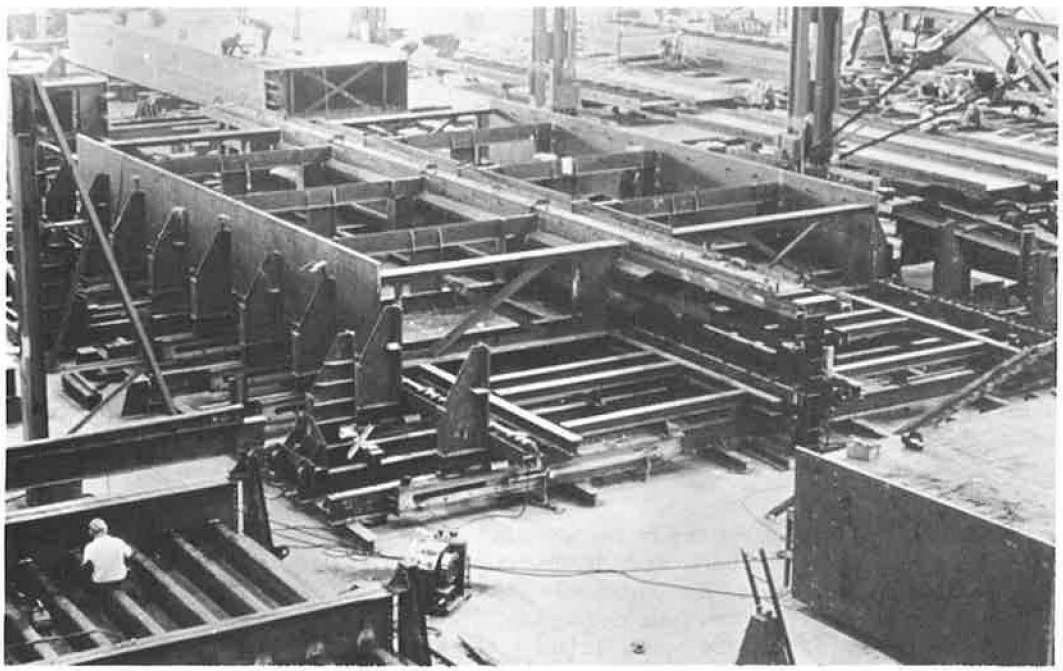

Figure 10. Boxing jig.

After the girders were boxed and welded, they were fitted with exterior stiffeners at floorbeam locations, bolt holes were subdrilled for end-connections, and miscellaneous items such as bracing connections and floorbeam supports were added.

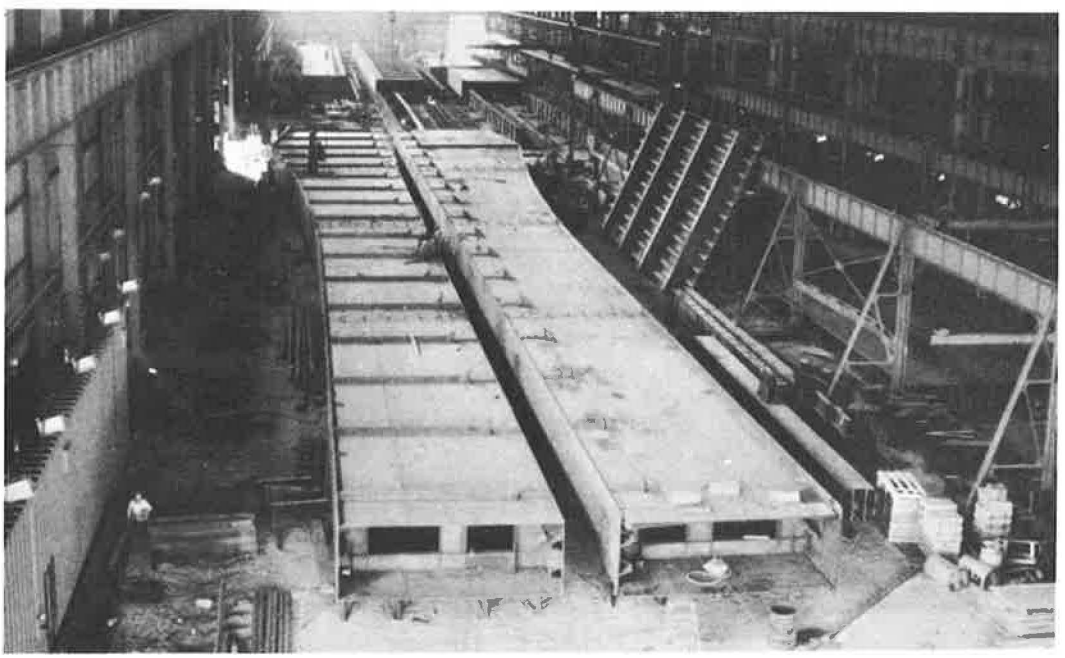

Figure 11. Assembling girder units in the shop.

SHOP ASSEMBLY

Three continuous girder sections were assembled to cambered shape in the shop (Fig. 11), and after reaming the end-connections to full size, two additional girder units were added to the last unit. This assembly procedure was followed for the full length of the girders.

Selected sections were check-assembled with the girders and all the deck units in place. These were then disassembled, cleaned, and spray-painted with three coats on the inside of the girders and one on the outside of all surfaces. The top surface of the deck was not painted.

BRIDGE SHOES

The bridge shoes are high-strength cast-steel units having a 48-in. radius spherical bearing surface which permits slight rotations of the superstructure. The expansion shoes are similar; however, they are supported on a nest of rollers that permit longitudinal motion.

ERECTION

Scheduled shipping operations began when sufficient bridge elements were fabricated, cleaned, and painted. The units were loaded into barges at Bethlehem's Leetsdale Plant near Pittsburgh, and reached the bridge site about two weeks later.

A barge-mounted tower derrick, consisting of a 95-ft tower, an 85-ft boom, and a 20-ft jib was used to erect the steel. It had a 115-ton capacity at the boom hitch.

The steel erection began at Pier 3, which is the fixed pier in the five-span continuous unit. The first girder section (70 ft long, 113 tons) was set in September 1965. The girder was guyed to the pier by a triangular brace. All four girder strings were carried forward at the same time.

The sequence of erection is shown in Figure 12. The first erection phase centered about Pier 3 and required two erection bents. Following this, erection progressed

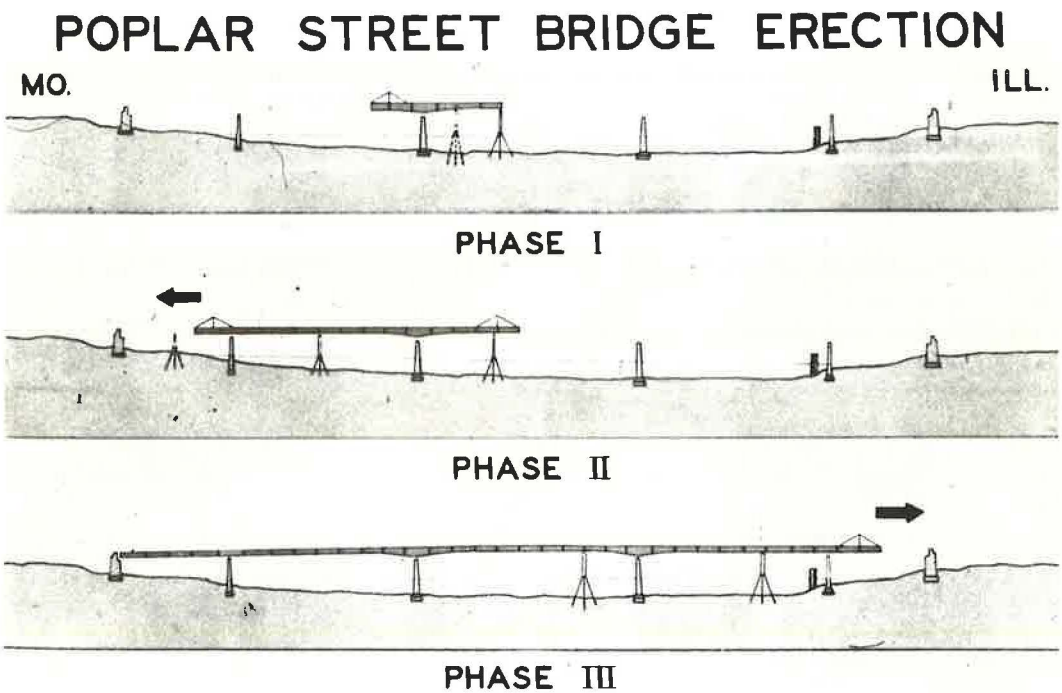

Figure 12. Erection sequence.

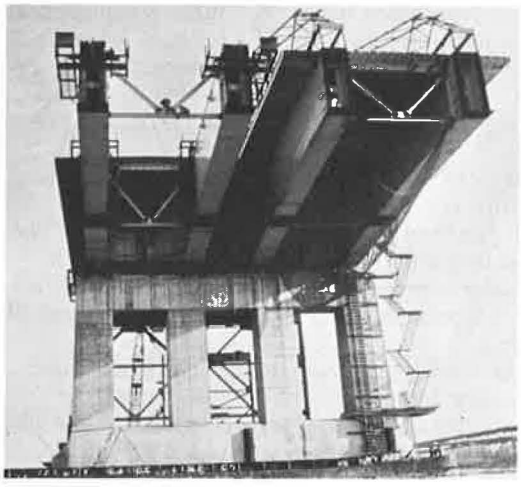

Figure 13. Girders and cross bracing.

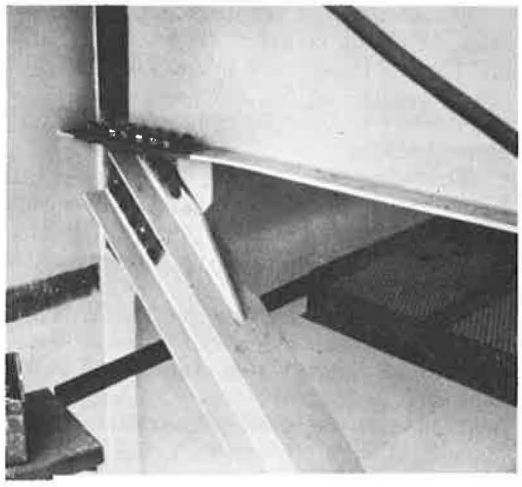

Figure 14. Bolted floor beam and bracing connection.

toward the Missouri shore only to allow more time for completion of concreting operations on Piers 4, 5, and 6. The third phase included erecting the remainder of the steel toward the Illinois shore.

Only six erection bents were used (Fig. 12). Erection bent locations and their removal had to be planned to keep a 300-ft navigation channel open at all times during construction. Jacking was necessary at the erection bents to obtain the desired configuration and to control stress. At each pier, the steel girders were landed directly on the shoes without a jacking assembly.

Figure 13 shows a typical scene during erection. The first step was to make the bolted splice in the girder web and the bottom flange, which was sufficient to support the cantilevered girder. The deck sections were installed and welded before setting the next girder section.

After a pair of girders were erected, K-bracing was placed near the free ends of the girders. This was the only bracing used between girders, except for the plate diaphragms over the interior piers which were designed to resist torsional forces and to transmit lateral forces to the substructure.

Figure 15. Traveling trusses.

Floorbeam and bracing connections to the girders were made with high-strength bolts (Fig. 14). The contract drawings permitted shims in both the floorbeam seat connections and the floorbeam web connections to the girder connection plate. The deck units were set to suit the welded connections, after which the holes were reamed-assembled and the joints bolted. The connection for the bracing was also field-reamed for the high-strength bolts.

Traveling trusses (Fig. 15) were positioned to relieve the stress in connections between the girder and deck plate connections while the welding was done.

The end of the central deck unit is shown in position in Figure 16. At this end of the deck plate, welding back-up strips were tacked in place on the underside of the deck plate in the shop. Back-up plates were also placed on the inner edges of the stiffener ribs to be placed with the next unit. The 3-in. projection of the stiffener ribs beyond the deck plate permitted easy setting of the next unit.

Both longitudinal and transverse welds in the deck plate were made with automatic submerged-arc machines. The ends of the girders were supported by the traveling trusses until the welding operations above and below the deck were completed. The deck plate back-up strip was tack-welded to the newly placed unit before the top side automatic welding was begun.

Manual welding was used in making the butt welds in the stiffeners. The shop welding of the ribs to the deck plate was stopped 12 in. from the end of the ribs to provide some flexibility in fitting-up the butt-welded joint. The rib was manually welded to the deck plate to complete all strength field-welding. The manual welds were inspected by magnetic-particle testing.

The edges of the deck plate joint were wedged into proper relationship prior to tack-welding. A continuous back-up strip of A-242 metal was tack-welded to both plates on the underside prior to beginning the deckside welding.

Figure 17 shows the procedure for making the automatic submerged-arc longitudinal welds on the deck plate. A guiderail was tacked to the deck to control the position of the welding machine, and a flux recovery unit was attached to the welder. Preheating was required for welding the low-alloy high-strength steel in the deck plate. The deck plate thickness varied from $^{9}/_{16}$ to $^{3}/_{4}$ in., requiring multiple passes to complete the weld. Similar procedures were used in making the transverse welds.

The transverse deck welds were radiographically inspected between ribs, and 10 percent of the longitudinal deck welds were radiographed.

By midwinter the superstructure erection from Pier 3 had progressed 270 ft toward midriver and 150 ft toward the Missouri shore. The steel was supported on Pier 3 and on one erection bent. An accident occurred at this point that seriously upset erection progress. A string of river barges traveling upstream went out of control and hit the erection bent, removing the pile support under one leg of the bent. Figure 18 shows that one-half of the superstructure was supported only at one girder. Fortunately, the meshing of the cantilever end of the units on the other side of the pier prevented the steel work from rotating further and falling into the river.

The first emergency move was to tie the two bridge roadways together to prevent further movement. To reestablish support and to get the steel back to its proper position, the contractor drove supporting piling beyond the edges of the structure and inserted a needle beam so the rotated bent could be moved back into proper position. This also was a temporary measure until further girder construction on the other side of the pier could relieve the load on this bent to facilitate placing a stable support directly under the bent column.

This accident clearly demonstrates the torsional rigidity of the orthotropic structure, and it was just this element which prevented a complete structural collapse. A thorough check of the structure after return to its proper position showed no structural damage in either the metal or the welds, except at areas of local contact.

The steel erection was completed in May 1967, just 21 months from its start, including delays caused by the barge accident, substructure completion, and labor disputes. Figure 19 is a view of the underside of the completed structure.

A separate contract was let for the metal railing, signing, the electrical work including lighting, the concrete curbs and parapets, and the wearing surfacing.

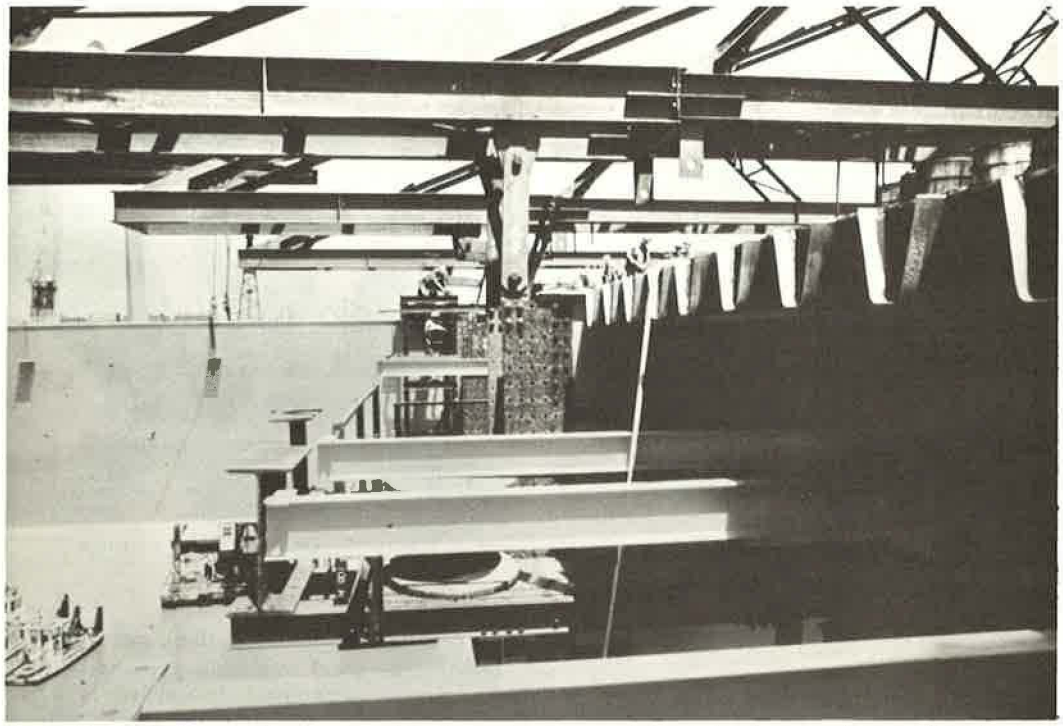

Figure 16. End of central unit—the wide-flange beams are the rails for the traveling scaffold (a traveling truss is in the background).

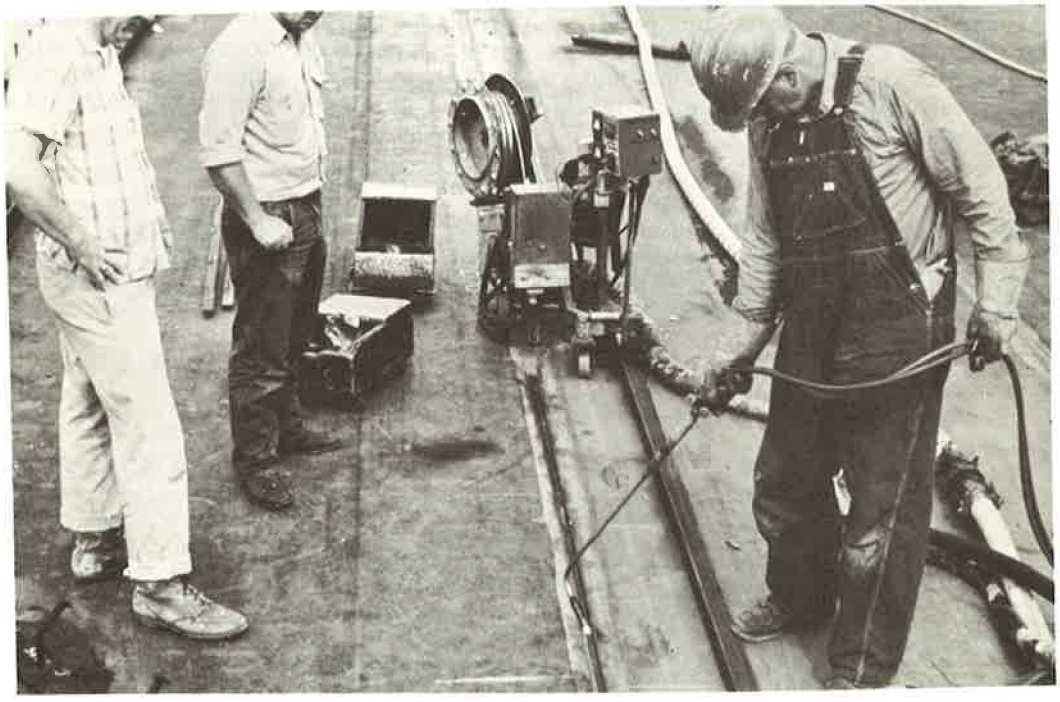

Figure 17. Welding a longitudinal deck joint.

Figure 18. Damage caused by the barge accident that knocked one support from under a construction bent.

Figure 19. Underside of the bridge.

A layered system of deck surfacing was used. The steel was blast-cleaned and coated with inorganic zinc. Two coats of coal-tar epoxy were applied, and two layers of asphaltic concrete with latex rubber additive were placed.

The wearing surface placement was completed, traffic markers were added, and the bridge was opened to traffic on November 9, 1967. Field painting was completed with the bridge under traffic.

In conclusion, this project again proved that accurate fabrication methods and good supporting equipment are required for successfully accomplishing the many miles of shop and field automatic welding required to build such a bridge. It was also apparent that the large orthotropic deck sections and large box girder sections could be readily handled both in the shop and in the field. The fabrication and erection techniques used by the contractor contributed to the low bid price of about $0.31 per pound for the 13,200 tons of metal.

ACKNOWLEDGMENTS

Most of the photographs used in this paper were furnished by the Bethlehem Steel Corporation; Kurt A. Keller, Project Engineer, Missouri State Highway Commission; and Carl Thunman, Jr., Engineer of Bridge and Traffic Structures, Division of Highways, Department of Public Works and Building.